2020-11-27

Four-Dimensional Computed Tomography to Determine Normal Syndesmotic Motion and to Compare Motion after Rigid and Flexible Fixation of Syndesmotic Injuries

Wong, Murray T

UNIVERSITY OF CALGARY

Four-Dimensional Computed Tomography to Determine Normal Syndesmotic Motion and to Compare Motion after Rigid and Flexible Fixation of Syndesmotic Injuries

by

Murray Thomas Wong

A THESIS

SUBMITTED TO THE FACULTY OF GRADUATE STUDIES

IN PARTIAL FULFILMENT OF THE REQUIREMENTS FOR THE

DEGREE OF MASTER OF SCIENCE

GRADUATE PROGRAM IN BIOMEDICAL ENGINEERING

CALGARY, ALBERTA

NOVEMBER, 2020

Abstract

Syndesmotic injuries occur in up to one-quarter of all ankle fractures. Despite mitigating efforts, malreduction of the syndesmosis is common after both rigid and flexible fixation methods, causing inferior patient function. Conventional assessments of syndesmotic reduction do not account for normal syndesmotic motion with ankle range-of-motion (ROM). The aims of this thesis were to use four-dimensional computed tomography (4DCT) to determine normal syndesmotic motion and to investigate the impact of rigid and flexible fixation on postoperative syndesmotic kinematics.

Fifty-eight uninjured ankles were imaged to quantify normal syndesmotic kinematics. Thirteen patients after rigid or flexible fixation underwent bilateral ankle 4DCT to evaluate postoperative syndesmotic kinematics. Measures of syndesmotic width including anterior, middle, and posterior syndesmosis distances as well as tibiofibular clear space and tibiofibular overlap were automatically extracted from 4DCT data. Sagittal translation and fibular rotation were also recorded. Linear mixed effects models were used to determine the position of the syndesmosis at neutral dorsiflexion as well as syndesmotic motion, defined as the change in syndesmotic measurements with ankle ROM.

In uninjured ankles, various measures of syndesmotic width decreased by 0.7-1.1 mm as ankles moved from dorsiflexion to plantarflexion ($p < 0.001$). The fibula externally rotated by 1.2° with plantarflexion ($p < 0.001$). There was no significant motion in the sagittal plane ($p = 0.43$). Rigid fixation increased syndesmotic width compared to uninjured ankles when measured by middle syndesmotic distance and tibiofibular clear space only ($p = 0.039$ and 0.032 respectively). Rigid fixation demonstrated reduced motion compared to uninjured ankles in middle and posterior syndesmotic distance, tibiofibular clear

space, and tibiofibular overlap ($p < 0.01$). There were no differences in syndesmotic position or motion between flexible fixation and uninjured ankles.

Ankle plantarflexion leads to decreased syndesmotic width and fibular external rotation in uninjured ankles, indicating ankle position must be accounted for when performing syndesmotic imaging and fixation. Flexible fixation better restores syndesmotic position and motion compared to rigid fixation. These findings may be used to decrease the rate of syndesmotic malreduction and, consequently, improve post-surgical outcomes.

Preface

Chapters 1, 2, 4, 6, and 7 of this thesis are original and unpublished work by the author, M. Wong. Chapter 3 of this thesis has been submitted for publication with the co-authors C. Wiens, S. Manske, and P. Schneider. M. Wong was responsible for performing the review and writing the manuscript. The co-authors reviewed the manuscript and provided revisions. Chapter 5 of this thesis has been prepared for submission for publication with the co-authors C. Wiens, J. LaMothe, W.B. Edwards, and P. Schneider. The study was designed by M. Wong and P Schneider with input from C. Wiens and W.B. Edwards. M. Wong performed the study, analysed and interpreted the data, and prepared the manuscript. C. Wiens, J. LaMothe, W.B. Edwards, and P. Schneider reviewed the manuscript and provided revisions. The experiments reported in chapters 5 and 6 were covered by Ethics Certificate numbers REB14-1142 for the study "Static versus Dynamic Fixation in Syndesmotic injuries – Tightrope", effective April 16, 2015, and REB18-2146 for the study "Dynamic CT Syndesmosis", effective August 27, 2019, issued by the Conjoint Health Research Ethics Board at the University of Calgary.

Acknowledgements

I would like to first thank Dr. Prism Schneider for her support and mentorship since my first year of residency. I'm grateful not only for the guidance related to my studies, but also for her commitment to my professional development and seeking out every opportunity she could for my benefit. The Orthopaedic Trauma research team was also instrumental to the successful completion of our projects and are responsible for building a research infrastructure that can continue to improve patient outcomes with 4DCT. Thank you, Leah, Aftab, Karin, Steph, and Maria. I appreciate Dr. Charmaine Wiens, Dr. W. Brent Edwards, and Dr. Sarah Manske for each lending their expertise and being cheerleaders to help keep the project on track.

Thank you to Dr. John Bertram and the Biomedical Engineering Graduate Program for their enthusiastic support which allowed me to pursue graduate studies during residency training. I appreciate their willingness to work with my residency timeline and their financial support, as well. I'd also like to thank my coresidents for their camaraderie and willingness to pitch in wherever they could, especially Dan and Joe for helping me navigate the year of dedicated research.

My family deserves a tremendous thank you for their unwavering support and belief in me. Finally, thank you to Karrie for everything, whether it was feedback and advice, encouragement, or planning an adventure together. I couldn't have done it without you.

Table of Contents

List of Tables

List of Figures

List of Abbreviations

3D: three-dimensional

4D: four-dimensional

4DCT: four-dimensional computed tomography

AITFL: anterior inferior tibiofibular ligament

AOFAS: American Orthopaedic Foot and Ankle Hindfoot Score

AP: anteroposterior

ASD: anterior syndesmosis distance

CT: computed tomography

FAAM: foot and ankle ability measure

HU: Hounsfield units

IML: intermalleolar ligament

IOL: interosseous ligament

MCS: medial clear space

MRI: magnetic resonance imaging

MSD: middle syndesmosis distance

MDCT: multi-row detector computed tomography

MSK: musculoskeletal

OM: Olerud and Molander Score

OTA: Orthopaedic Trauma Association

PER: pronation-external rotation

PITFL: posterior inferior tibiofibular ligament

PSD: posterior syndesmosis distance

RMSE: root mean square error

ROM: range-of-motion

SER: supination-external rotation

SFMA: Short Form Musculoskeletal Function Assessment

STL: stereolithography

TTO: tibial tubercle osteotomy

TTTG: tibial tubercle trochlear groove distance

TFCS: tibiofibular clear space

TFO: tibiofibular overlap

TTFL: transverse tibiofibular ligament

VAS: visual analog pain scale

1. Introduction

1.1. Background

The syndesmosis is a group of ligaments that stabilizes the distal tibiofibular joint while allowing small but significant motion. Injuries to the syndesmosis are common, occurring in up to 18% of all ankle sprains[1,2] and up to one-quarter of all ankle fractures.[3,4] When injured, malreduction of the syndesmosis after surgical or nonsurgical treatment has been found to be the most important factor contributing to inferior outcomes including pain, instability, stiffness, and ankle arthritis.[5–7] These can have a debilitating impact on quality of life, leading to reduced function, time away from work, and need for future surgery.[8] However, syndesmotic reduction is both challenging to achieve and measure. Malreduction is common,[9–12] with reported malreduction rates as high as 52% post-operatively.[9] Rigid screw fixation of syndesmotic injuries can lead to a higher risk of symptomatic malreduction compared to flexible fixation with heavy suture and an endobutton spanning the distal tibiofibular joint.[13–15] Syndesmotic kinematics are altered after either method, though flexible fixation is more physiologic.[16]

The syndesmotic complex is a dynamic structure, therefore conventional computed tomography (CT) does not provide a complete picture of changes in syndesmotic position, giving potentially inaccurate results. This may also explain the high rates of malreduction reported if motion is not accounted for during surgery or with imaging assessment of reduction. Four-dimensional CT (4DCT) is an emerging technology which can be used to image joints in real-time, as they move through a range-of-motion (ROM).[17]

1.2. Study Rationale and Contributions

Despite injuries to the syndesmosis being a common orthopaedic problem, significant variability in treatment remains. A poor understanding of normal syndesmotic motion and the resultant impact of rigid and flexible fixation on post-injury kinematics contributes to this variability. Given the importance of accurate syndesmotic reduction, we proposed a novel application of 4DCT to determine the relative position of the distal tibiofibular joint throughout full ankle ROM, rather than the single, non-standardized position, as is evaluated by conventional CT. This study is the first to define normal syndesmotic motion *in vivo* throughout a full ankle ROM and compare syndesmotic motion and reduction quality following rigid and flexible fixation throughout ankle ROM. Knowledge gained from this study may be used to optimize reduction methods, improve patient outcomes, and guide the further development of 4DCT techniques.

1.3. Research Aims and Hypotheses

By shifting the paradigm of syndesmotic reduction from a single, constant measurement to a dynamic variable which changes with ankle motion, the aim of this study is to reduce functional impairment after syndesmotic injury. This will be achieved by first understanding normal syndesmotic motion, followed by quantifying the impact of fixation methods on post-injury motion.

1.3.1. Specific Objectives

1) To quantify normal syndesmotic kinematics through ankle ROM.
2) To quantify side-to-side variability in syndesmotic kinematics in healthy participants.

3) To compare syndesmotic kinematics following rigid and flexible syndesmotic fixation to normal, uninjured motion.

1.3.2. Hypotheses

1) The relative position of the distal tibia and fibula will change significantly throughout ankle range of motion in uninjured ankles.
2) There will be minimal side-to-side variability within participants with bilateral uninjured ankles.
3) Flexible fixation for the treatment of syndesmotic injury will more accurately reproduce normal, uninjured motion, compared to rigid fixation.

1.4. Organization

In this thesis, Chapter 2 will review the existing literature around syndesmotic injuries. Different treatment options will be discussed, along with the functional consequences of malreduction, and strategies to improve reduction. Chapter 3 discusses 4DCT imaging developments and its utility in evaluating musculoskeletal (MSK) pathology. Chapter 4 describes our methodology for 4DCT image acquisition and processing. This includes development of a novel computer program to automatically register bone positions between 4DCT timepoints. Chapter 5 is a study of normal syndesmotic kinematics, as measured in healthy volunteers using 4DCT. This addresses Objectives 1 and 2. Chapter 6 analyses a pilot cohort of 13 patients one year after treatment of syndesmotic injury with rigid or flexible fixation. With this pilot study, we investigate Objective 3 and lay the groundwork for a larger prospective study to further address the objective. Chapter 7 is a general discussion of the findings related to this thesis.

1.5. References

1. Boytim, MJ, Fischer, DA, Neumann, L: Syndesmotic ankle sprains. *Am J Sports Med* 1991;19:294–298.

2. Lin, CF, Gross, MT, Weinhold, P: Ankle syndesmosis injuries: Anatomy, biomechanics, mechanism of injury, and clinical guidelines for diagnosis and intervention. *J Orthop Sports Phys Ther* 2006;36:372–384.

3. Purvis, GD: Displaced, unstable ankle fractures. Classification, incidence, and management of a consecutive series. *Clin Orthop Relat Res* 1982;No. 165:91–98.

4. Zalavras, C, Thordarson, D: Ankle syndesmotic injury. *J Am Acad Orthop Surg* 2007;15:330–339.

5. Naqvi, GA, Cunningham, P, Lynch, B, Galvin, R, Awan, N: Fixation of ankle syndesmotic injuries: Comparison of tightrope fixation and syndesmotic screw fixation for accuracy of syndesmotic reduction. *Am J Sports Med* 2012;40:2828–2835.

6. Weening, B, Bhandari, M: Predictors of functional outcome following transsyndesmotic screw fixation of ankle fractures. *J Orthop Trauma* 2005;19:102–108.

7. Sagi, HC, Shah, AR, Sanders, RW: The Functional Consequence of Syndesmotic Joint Malreduction at a Minimum 2-Year Follow-Up. *J Orthop Trauma* 2012;26:439–443.

8. Slobogean, GP, Younger, A, Apostle, KL, Marra, CA, Wing, K, Penner, M, Daniels, T, Glazebrook, M: Preference-based quality of life of end-stage ankle arthritis treated with arthroplasty or arthrodesis. *Foot Ankle Int* 2010;31:563–566.

9. Gardner, MJ, Demetrakopoulos, D, Briggs, SM, Helfet, DL, Lorich, DG: Malreduction of the Tibiofibular Syndesmosis in Ankle Fractures. *Foot Ankle Int* 2006;27:788–792.

10. Phisitkul, P, Ebinger, T, Goetz, J, Vaseenon, T, Marsh, JL: Forceps reduction of the syndesmosis in rotational ankle fractures: A cadaveric study. *J Bone Jt Surg - Ser A* 2012;94:2256–2261.

11. Futamura, K, Baba, T, Mogami, A, Morohashi, I, Kanda, A, Obayashi, O, Sato, K, Ueda, Y, Kurata, Y, Tsuji, H, *et al.*: Malreduction of syndesmosis injury associated with malleolar ankle fracture can be avoided using Weber's three indexes in the mortise view. *Injury* 2017;48:

12. Rammelt, S, Obruba, P: An update on the evaluation and treatment of syndesmotic injuries. *Eur J Trauma Emerg Surg* 2015;41:601–614.

13. Andersen, MR, Frihagen, F, Hellund, JC, Madsen, JE, Figved, W: Randomized trial comparing suture button with single syndesmotic screw for syndesmosis injury. *J Bone Jt Surg - Am Vol* 2018;100:2–12.

14. Sanders, D, Schneider, P, Taylor, M, Tieszer, C, Lawendy, A-R: Improved Reduction of the Tibiofibular Syndesmosis with Tightrope Compared to Screw Fixation: Results of a Randomized Controlled Study. *J Orthop Trauma* 2019;3:2473011418S0012.

15. Liu, G, Chen, L, Gong, M, Xing, F, Xiang, Z: Clinical Evidence for Treatment of Distal Tibiofibular Syndesmosis Injury: A Systematic Review of Clinical Studies. *J Foot Ankle Surg* 2019;58:1245–1250.

16. Lamothe, JM, Baxter, JR, Murphy, C, Gilbert, S, Desandis, B, Drakos, MC: Three-Dimensional Analysis of Fibular Motion after Fixation of Syndesmotic Injuries with a Screw or Suture-Button Construct. *Foot Ankle Int* 2016;37:1350–1356.

17. Kwong, Y, Mel, AO, Wheeler, G, Troupis, JM: Four-dimensional computed tomography (4DCT): A review of the current status and applications. *J Med Imaging Radiat Oncol* 2015;59:545–554.

2. Syndesmotic Injuries

2.1. Normal Anatomy

2.1.1. Ligamentous Anatomy

The syndesmosis is a complex of ligaments which stabilize the distal tibiofibular joint. These ligaments resist rotation and translation of the fibula relative to the tibia, facilitate fibular load transfer, and help maintain congruity of the ankle joint.[1–5] The syndesmosis is comprised of the anterior inferior tibiofibular ligament (AITFL), posterior inferior tibiofibular ligament (PITFL), transverse tibiofibular ligament (TTFL), also referred to as the inferior transverse ligament, and the interosseous ligament (IOL) which is a distal continuation of the interosseus membrane (Figure 2.1).

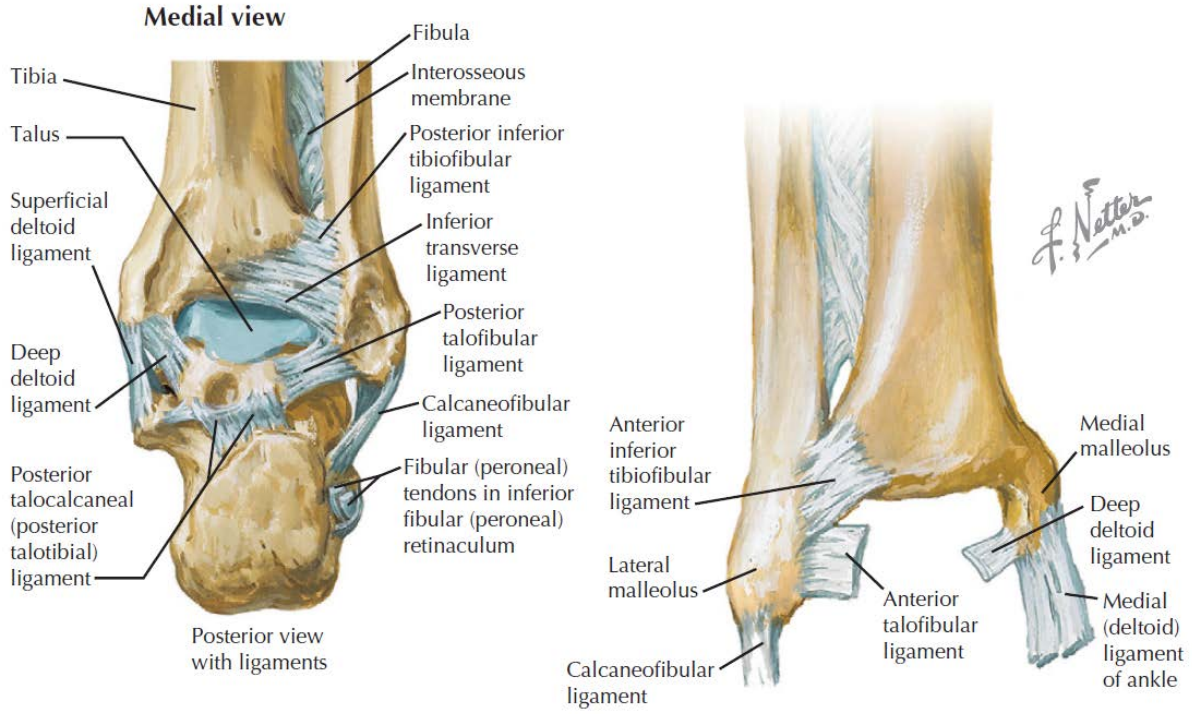

Figure 2.1: Ligamentous anatomy of the distal tibiofibular joint and ankle. Reprinted from Netter's Concise Orthopaedic Anatomy (p. 349), by J. C. Thompson, 2016, Philadelphia, Elsevier. Copyright 2016 by Saunders, Elsevier.[6]

The AITFL is a trapezoidal ligament which extends from the anterior tibial (Tillaux-Chaput) tubercle to the anterior (Wagstaffe) tubercle on the fibula.[2,7] Three fascicles run from a broad tibial origin to converge on the fibula, oriented 35°inferiorly and 25°posteriorly.[2,7,8] The most distal fascicle of the AITFL, Bassett's ligament, runs intraarticularly through the anterolateral tibiotalar joint and abuts the lateral talus during dorsiflexion.[7,9] The AITFL length is 9 mm superiorly and 20 mm distally with a total intrasubstance width of all three fascicles of 17mm.[2,8] The thickness varies from 2-4 mm.[8,10] The AITFL provides the primary restraint to external rotation of the fibula.[11]

The PITFL originates on the posterior malleolus (Volkmann tubercle) of the tibia and inserts on the posteromedial aspect of the lateral malleolus behind the articular facet.[2,7] The PITFL also has multiple fascicles making up both a deep and superficial component, but these are more variable and less distinct than the AITFL.[2,9] Similar to the AITFL, the PITFL has a trapezoidal shape with a broader tibial origin which narrows slightly at the fibular insertion.[7,12] The course of the PITFL is mostly in the coronal plane, travelling 20° inferiorly and only 5° anteriorly.[2] The inferior margin abuts the trochlea of the talus and the superior margin is in close proximity to the IOL, making distinction difficult.[2,12] Superiorly, the PITFL is 13 mm in length compared to 24 mm distally. The width is 18 mm and the thickness is 6 mm. The PITFL primarily resists internal and external rotation and lateral translation of the distal fibula.[8,11,13–15]

The TTFL is a fibrocartilaginous structure which lies distal to the PITFL and travels from the tibial plafond dorsally to the lateral malleolar fossa.[2,7,16] It is still debated whether this ligament should be considered a separate entity rather than a component of the PITFL or thickening of the synovial capsule.[2,7,8,13,15] Those who view it as a continuation of the PITFL argue that it is oriented parallel to the remainder of PITFL fibres and performs the same function.[8,9] Others have demonstrated that the PITFL and TTFL are distinct structures via dissection, arthroscopy, or magnetic resonance arthrography, that the TTFL has a more horizontal orientation, and that the two ligaments are separated by fibro-fatty connective tissue.[2,7,17,18] The TTFL varies in shape and size.[13,19] In most cases, it originates on the posteroinferior corner of the posterior tibial tubercle, but may reach the medial malleolar fossa in some cadaveric specimens.[2,7] It inserts on the fibula just inferior to the PITFL at the proximal fibular malleolar fossa.[7] Length of the TTFL is 36 mm on average with a width of 4 mm and 2 mm thickness.[2] The TTFL appears to perform a meniscal or labrum-like role, increasing joint contact area between the distal tibia and talus.[2,7,20]

The interosseous membrane gradually transitions distally to the thicker IOL which spans approximately 3-4 cm, ending 1 cm above the ankle joint.[2,7] The tibial origin begins on the fibular ridge proximally and follows the anterior edge of the incisura distally.[2,8] The insertion is on the medial aspect of the distal fibula.[2,8] Fibres are oriented in the lateral, distal, and anterior direction.[2] In an unstressed configuration, these fibres have redundancy and are folded within the interosseous space.[2,7,21] The IOL length ranges from 6-10 mm with a width of 2-4 mm and a thickness of 2-5 mm.[2,21] The IOL contributes to ankle stability by allowing slight diastasis of the tibia and fibula during ankle motion or loading, neutralizing forces and preventing fibular bowing during foot impact, and has also been found to transmit axial loads from the tibia to the fibula to varying extents throughout the gait cycle.[2,7,13,22]

Though not considered part of the syndesmotic complex and variably present, the intermalleolar ligament (IML) also contributes to ankle stability.[23] The IML has been identified in 50-80% of uninjured ankles based on magnetic resonance imaging (MRI), varying from a thin fibrous band to a thicker, cord-like structure.[12,23] Situated between the TTFL and PITFL, the IML runs parallel to the TTFL and likely serves a similar purpose.[7,12,23] In addition to these ligaments, the deltoid ligament has also been shown to restrict fibular external rotation and lateral translation by constraining talar motion.[13,14,24]. Situated on the medial side of the ankle, the superficial deltoid attaches to the tibial anterior colliculus with fibres to the navicular, calcaneus, and talus, while the deep deltoid inserts on the posterior colliculus and intercollicular groove and attaches to the talus.[25]

2.1.2. Bony Anatomy

Bony congruency of the distal tibiofibular joint also contributes to stability of the syndesmosis. On the tibial side, the syndesmosis begins superiorly where the crista interossei tibiae, or lateral ridge, bifurcates into anterior and posterior ridges at 6-8 cm above the plafond.[7] These ridges become the anterior and posterior tubercles that enclose the syndesmosis.[7] The area between these tubercles, the incisura, is generally concave to accommodate the distal fibula (Figure 2.2).[16,26,27] Mean incisural width is 22 mm, but the morphology varies greatly between cadaveric specimens, and therefore the depth ranges from 0-7.5 mm.[16,26,28,29] While 60-75% of incisurae are concave, others are classified as flat or irregular.[26,27,30]

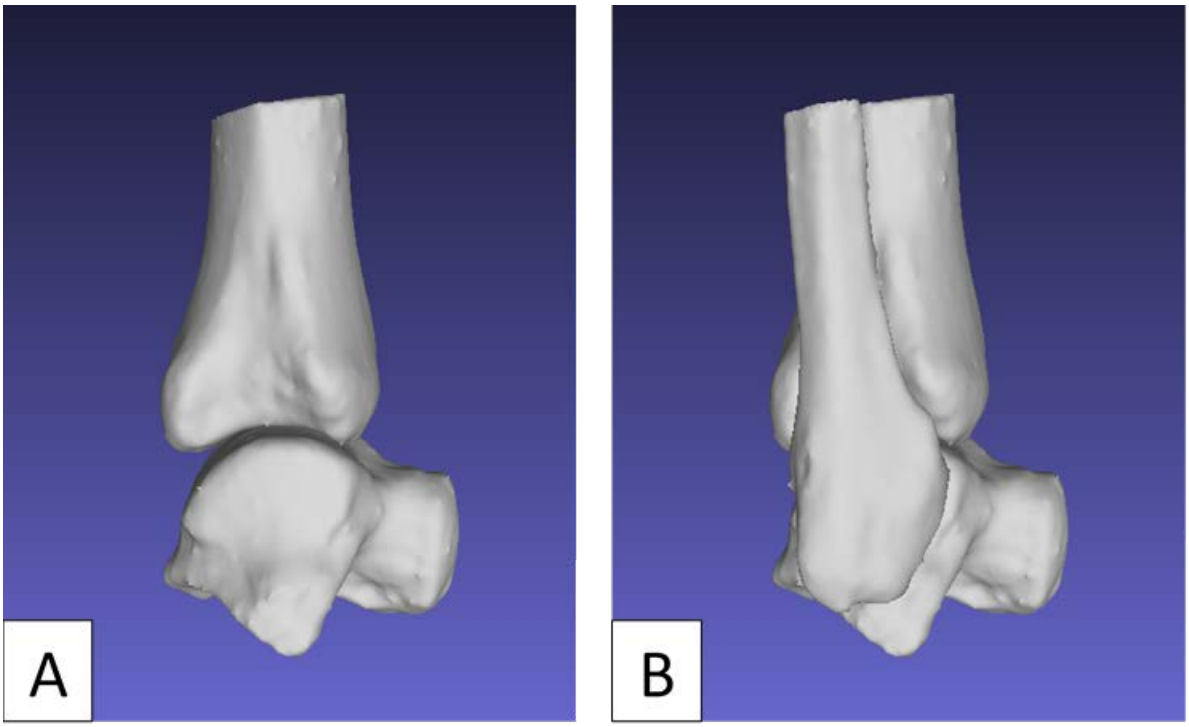

Figure 2.2: Lateral view of the tibial incisura, enclosed by the anterior and posterior tubercles, which improves bony congruity between the distal tibia and fibula. Fibula removed in (A) and present in (B).

Cross-sectional osseous anatomy of the fibula also shows considerable variability at the level of the syndesmosis.[27] Four borders are described, the anterior, medial, posterior, and lateral borders, but are inconsistent in size and prominence.[7,19,31] In general, the fibula has an oval cross-section to match the incisura, with a more prominent anterior tubercle than posteriorly and a best defined lateral border.[2,7,10]

There is a small area of articulation between the distal tibia and fibula that is covered in cartilage and spans 2-5 mm from the plafond, which is present in upwards of 88% of specimens.[2,7–9] Above this, the syndesmotic recess is a synovial-lined plica which extends 4-25 mm into the syndesmosis from the tibiotalar joint, ending just distal to the IOL.[7–9,19]

2.2. Normal Motion

Cadaveric and *in vivo* imaging studies have quantified syndesmotic motion at the distal tibiofibular joint both throughout ankle ROM and in response to stress. Physiologic motion serves to provide ankle stability, while allowing for increased motion of the irregularly shaped talus which is broader anteriorly.[8,32–34] This adaptation maintains joint congruity and consequently lowers joint contact stresses.[33,35–41] In addition, fibular motion can serve to adjust the load transmitted from the tibia to the fibula during loading and gait by 6-30%.[4,42–45]

During ROM, as the ankle moves from dorsiflexion to plantarflexion, there is up to 1.3 mm of anterior fibular translation, 3.0 mm of medial translation, and 3.7°of internal rotation relative to the tibia.[16,33,46,47] Many studies have shown up to 5°of fibula internal rotation although motion in the opposite direction has been demonstrated as well.[33,46,48–50] Reporting of translation and rotation in other planes is inconsistent or insignificant.[33,46]

Weightbearing may also induce changes in syndesmotic position. Under a 600 N axial load, Hu et al.[48] showed significant changes in cadaveric fibular position compared to the unloaded state, with 0.8 mm of lateral translation, 0.5 mm of posterior translation, and 1.2°of external rotation. However, other studies have failed to find significant changes between loaded and unloaded conditions in both *in vitro* and *in vivo* experiments.[11,51]

There is a corresponding change in syndesmotic position that occurs with varying foot position, given the function of the syndesmosis in preventing excessive external rotation of the distal fibula. Under external rotation stresses due to foot position, the fibula translates up to 2.8 mm posteriorly, 1.5 mm laterally, and externally rotates up to 3.9°.[11,32,51,52] Similarly, during the gait cycle, incorporating ankle ROM and loading, the syndesmosis exhibits 2.6 mm of translation in the medial-lateral direction, 3.8 mm in the anterior-posterior directions,[53] Internal-external rotation of 6.0°,[53,54] and the distal fibula translates up to 2.4 mm distally.[16,50]

2.3. Incidence of Injury to the Syndesmosis

Syndesmotic injuries have become a more common orthopaedic diagnosis due to both increased incidence and improved recognition. Injuries to the syndesmosis can be isolated ligamentous injuries but are more commonly associated with ankle fractures. Incidence is increasing due to both growing participation in sports and the increasing incidence of elderly ankle fractures.[55–58] Ankle sprains occur between 215 and 696 times per 100,000 person-years in the general population, with half of these being associated with sporting injuries.[59] Purely ligamentous syndesmotic injuries are commonly referred to as high ankle sprains and occur in 1-18% of all ankle sprains.[13,55,60–62]

Eighty percent of diagnosed syndesmotic injuries have an associated ankle or proximal fibula (Maisonneuve) fracture.[13] Ankle fractures make up 10% of all fractures, with an estimated frequency of 187 fractures per 100,000 person-years.[63,64] Approximately 20-25% of these fractures have a recognized injury to the syndesmosis.[20,24,58,65,66] The diagnosis of syndesmotic instability is dramatically higher when arthroscopy is used routinely during fracture fixation.[67] Based on fracture pattern, 17-45% of Lauge-Hansen supination-external rotation (SER) IV fractures and 57-95% of pronation-external rotation (PER)

have syndesmotic injuries (Table 2.1).[65,68–72] Under the AO Foundation/Orthopaedic Trauma Association (OTA)/Danis-Weber classification, upwards of 18% of unstable Weber B fractures and 72-90% of Weber C have syndesmotic injuries.[65,73–75]

Table 2.1: Lauge-Hansen and AO/OTA/Danis-Weber classification systems for describing ankle fractures.

Classification Scheme	Subtype	Findings
Lauge-Hansen[72]	**Supination-Adduction**	1. Transverse low fibular fracture or lateral ligament injury 2. Vertical medial malleolus fracture
	Supination-External Rotation	1. AITFL sprain 2. Oblique trans-syndesmotic fibula fracture 3. PITFL rupture or coronal posterior malleolus fracture 4. Transverse medial malleolus fracture or deltoid ligament injury
	Pronation-Abduction	1. Transverse medial malleolus fracture or deltoid ligament injury 2. AITFL sprain 3. Transverse comminuted supra-syndesmotic fibular fracture
	Pronation-External Rotation	1. Transverse medial malleolus fracture or deltoid ligament injury 2. AITFL rupture 3. Oblique supra-syndesmotic fibula fracture 4. PITFL rupture or coronal posterior malleolus fracture
AO /OTA/Danis-Weber[75]	**A**	Infra-syndesmotic fibula fracture
	B	Trans-syndesmotic fibula fracture
	C	Supra-syndesmotic fibula fracture

2.4. Mechanism of Injury

The majority of syndesmotic injuries occur from low-energy falls, followed by sport-related injuries.[76] Most isolated ligamentous injuries occur during sports participation[55,77] Injury to the syndesmosis most often occurs from an external rotation moment to the ankle with a pronated foot, or a Lauge-Hansen PER pattern.[13] Injuries can also be associated with external rotation when the foot is supinated (Lauge-Hansen SER), with forceful eversion of the talus (Lauge-Hansen pronation-abduction), or hyper-dorsiflexion.[13,16,62,68,72,78] In external rotation, the AITFL is generally the first syndesmotic ligament to tear, followed by the IOL and PITFL sequentially.[7,72] Bony avulsions occur with 50% of syndesmotic injuries and the PITFL is more likely to cause a posterior malleolus fracture, rather than an intra-substance ligament rupture, due to its strength.[7,79] Deltoid ligament injuries are also commonly associated with syndesmotic injuries, which leads to further instability.[60,80–82]

Multiple classification systems exist to categorize syndesmotic injuries and inform treatment. These are similar in nature and most commonly applied to isolated syndesmotic injuries.[82] Gerber et al.[61] developed the West Point Ankle Grading System in which grade 1 injuries are isolated AITFL sprains or tears, without instability or radiographic diastasis. Grade 2 injuries involve injury to the AITFL and partial tear of the IOL, leading to mild instability, while grade 3 injuries require complete disruption of all ligaments and frank instability and/or diastasis.[61]

2.5. Instability

Injury to the syndesmosis can lead to significant instability and altered biomechanics of the tibio-fibular and ankle joints, compared to normal motion. Some studies suggest AITFL injuries may require a second syndesmotic ligament injury or deltoid ligament injury before significant alterations to syndesmotic biomechanics are detected,[11,83,84] whereas others demonstrate instability after isolated AITFL injury.[14,85–87] Based on cadaveric work by Ogilvie-Harris et al.,[15] the AITLF, PITFL, TTFL, and IOL contribute 35%, 33%, 9%, and 22% of resistance to syndesmotic diastasis, respectively. During cadaveric ankle ROM, sectioning of all syndesmotic ligaments leads to a 207% increase in sagittal translation and 252% increase in posterior translation.[33,49,78] Axial rotation increases by 316%.[33,49]

Under external rotation stress, a complete syndesmotic injury leads to lateral translation of 2.0 mm, increasing 1.2 mm from the intact condition, and posterior translation is 7.7 mm, an increase of 5.1 mm in cadaveric studies.[11,87,88] Under the same conditions there are 6.5° of external rotation, with a mean increase of 3.7°compared to the intact state.[11,14,49,85,87] When sectioning the distal interosseous membrane in addition to the syndesmosis, diastasis increases an additional 7.4 mm and rotation increases 10.2°.[86] Sectioning of the deltoid ligament further decreases stability.[83,87]

Disruption of the syndesmosis leads to instability in multiple planes.[89] An 80 N laterally directed force serves to increase diastasis by up to 5 mm, while the same magnitude directed posteriorly induces 10 mm of posterior translation.[90,91]

2.6. Clinical Presentation

Diagnosis of syndesmotic injuries can be challenging, especially in subtle injuries or those without bony involvement. The accepted gold standard for diagnosis of syndesmotic injuries is direct visualization of the syndesmosis with open dissection or ankle arthroscopy, but diagnosis is most commonly made based on clinical and imaging findings.[13,16,60,81]

2.6.1. History

Patients should be questioned about classic mechanisms including external rotation, eversion, or forceful dorsiflexion.[13] Athletic syndesmotic injuries commonly occur in football, soccer, hockey, skiing and basketball and are often related to contact with another player.[56,77] In cases of milder injury, patients present with lateral ankle pain, swelling, a sensation of instability, or difficulty walking on uneven surfaces or pushing off.[13,92]

2.6.2. Physical Exam

Numerous clinical exam maneuvers exist to detect syndesmotic injury, however diagnostic accuracy of physical exam alone is poor. Twenty percent of syndesmotic injuries can go undetected.[93] Basic provocative maneuvers for syndesmotic injuries includes palpation over the syndesmotic ligaments,[43] passive external rotation,[94] or dorsiflexion[95,96] of the foot. A squeeze test where the fibula and tibia are compressed proximal to the syndesmosis may elicit pain in the syndesmotic region.[62,84] Similar tests include lunging or squatting, with and without external compression at the syndesmosis by the examiner, or with bandaging, to determine if symptoms abate with compression.[16,97] A heel thump test involves a forceful impact to a dorsiflexed foot and is considered positive if it causes pain.[13] The crossed-leg test where the subject crosses the affected leg over the contralateral knee and compression is caused by

gravity.[98] Inability to perform a single leg hop on the affected side is also predictive of a syndesmotic injury.[97] When compared to gold-standard arthroscopy (Table 2.2) or MRI (Table 2.4) sensitivity and specificity are poor.[84,93,97,99] Chronic injuries are even more difficult to detect with physical exam and only 15% of patients had a positive external rotation test and 10% had a positive squeeze test.[100] Instability is gauged with either the rarely-performed clinical Cotton test[93], where the examiner applies a lateral distracting force to the foot and gauges lateral translation of the talus and fibula from the tibia, or the fibular translation test[94], where anterior-posterior force is applied to the fibula to assess relative motion. Beumer et al.[80] performed a biomechanical study that found instability testing to be insensitive unless both a complete injury of the syndesmosis and anterior deltoid ligament injury were present, and that degree of instability did not predict the injury severity. Clinically, sensitivity ranges from 0.29-0.64 with specificity of 0.43-0.71.[93] On assessment of gait, patients may ambulate with a decreased stride length and limited dorsiflexion.[43] Given the poor performance of physical exam, imaging is recommended when syndesmotic injuries are suspected.

Table 2.2: Clinical test sensitivity and specificity compared to arthroscopy.

Test	Sensitivity	Specificity
External rotation[93]	0.50	0.00
Dorsiflexion[93]	0.50	0.57
Squeeze test[93]	0.26-0.57	0.14-0.88

Table 2.3: Clinical test sensitivity and specificity compared to MRI.

Test	Sensitivity	Specificity
Direct palpation[97]	0.92	0.29
External rotation[84]	0.20	0.85
External rotation and dorsiflexion[97]	0.71	0.63
Squeeze test[84,97]	0.26-0.30	0.88-0.94
Lunge compression test[97]	0.69	0.41
Inability to hop[97]	0.89	0.29

2.7. Imaging

2.7.1. Standard Radiography

To detect syndesmotic injuries, an ankle x-ray series should include an anteroposterior (AP), lateral, and mortise view which is taken in 15-20°of internal rotation.[16,82] However, numerous studies have shown that standard x-rays lack the detail required to detect syndesmotic injury with adequate sensitivity.[19,69,81,86,101–107] Anatomic variability, overlap of reference points, and changes with ankle rotation limit the utility of reference measurements to diagnose injury.[19,102,106,108] In addition, the level of a fibular fracture, when present, or increased medial clear space (MCS) between the talus and medial malleolus, do not reliably predict the extent of syndesmotic injury as previously believed.[69,74,104] Measured 1 cm proximal to the plafond, tibiofibular clear space (TFCS) is the horizontal distance between the medial border of the incisura and the medial border of the fibula. At the same level, tibiofibular overlap (TFO) is the most lateral point of the tibial tubercles to the medial border of the fibula.[101] Increase in the TFCS greater than 6 mm on AP or mortise view, decrease in TFO less than 6 mm on the AP view or 1-2 mm on the mortise view, or tibiofibular overlap less than 42% of the fibular width are generally accepted markers of syndesmotic injuries (Figure 2.3).[92,101] Bony avulsions from the anterior and posterior tibia are also

highly suggestive of injury.[79] Of these accepted measurements, TFCS on the AP view is recommended as it is the least affected by rotation of the foot, which can lead to false positives and negatives with other measurements.[104,106,109,110] Ankle plantarflexion has also been shown to affect these measurements.[111] Despite high specificities reaching 1.00 in some studies, sensitivity is reportedly 0.36-0.58 compared to MRI and arthroscopy.[60,81,112,113] When Nielsen et al.[104] compared x-ray measures with MRI diagnosis of syndesmotic injury, using more liberal injury thresholds, they found poor correlation as well. Specificities ranged from 0.00 to 0.65 and sensitivities from 0.22 to 1.00 for the various measurements.[104] Given the low utility of applying reference values in most cases, authors have advocated using bilateral ankle imaging.[102,114–116] Minimal side-to-side variability is present and asymmetry can be predictive of injury.[102,114] With low sensitivity overall, standard x-rays cannot be relied on to diagnose syndesmotic injury.

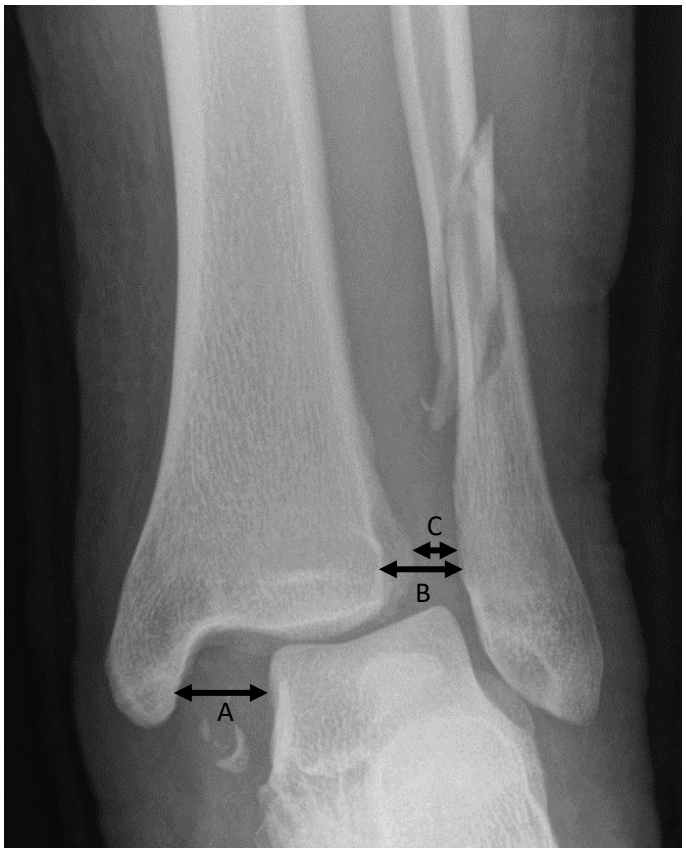

Figure 2.3: X-ray of a Weber C ankle fracture with increased medial clear space (A) from deltoid ligament avulsion and disruption of the syndesmosis, leading to increased tibiofibular clear space (B) and loss of tibiofibular overlap (C).

2.7.2. Stress Imaging

Stress view x-rays are used to improve the detection of latent syndesmotic instability, where a stress applied to incompetent or torn syndesmotic ligaments induces radiographic changes including increase in the TFCS, TFO, or MCS. Change in these measurements of 2 mm or greater is generally considered positive.[3] Stress can be applied in the form of weightbearing, an external rotation stress, or by gravity, where the patient is positioned laterally with the affected side down, such that the weight of the foot creates an external rotation stress.[60,70,86,117] In a nonoperative setting, a single leg weightbearing series is

most accurate, but is rarely tolerated.[13,118] No superior method between double leg weightbearing, external rotation, or gravity stress views have been found.[117,119,120] Intraoperative diagnosis of syndesmotic instability can be made with external rotation stress views or a hook test, also referred to as the Cotton test, which uses a surgical instrument to distract the fibula from the tibia to detect diastasis under fluroscopy.[70,90,121,122] Traditional stress views are not always reliable either, especially in chronic injury.[51,60,90,122,123] LaMothe et al.[90] compared complete syndesmotic and deltoid injuries to intact cadavers and found that a 2 mm increase in TFCS under lateral stress had a sensitivity of 0.63 and specificity of 1.00 compared to external rotation stress sensitivity of 0.23 and specificity of 1.00. Increases in medial clear space have limited specificity due to possible deltoid ligament injuries causing false positives.[122,123] To address these limitations, many authors have explored lateral imaging to assess instability. Given that instability is greater in the AP direction, lateral imaging shows improved sensitivity to detect even partial injuries with a posteriorly directed stress.[86,90,124]

2.7.3. Computed Tomography (CT)

CT can more accurately detect syndesmotic injury compared to x-ray due to lack of osseous overlap and 3D reconstruction of the distal tibiofibular joint.[31,103,125] CT can detect diastasis of 1 mm compared to the 3 mm required before diastasis may be apparent on x-ray.[19] CT also allows for assessment of fibular rotation within the incisura, which is difficult, if not impossible, using x-ray.[110,126,127] Conventional CT is a static, unloaded, and unstressed modality and thus is more suited to assessing fibular position and syndesmotic malreduction than instability.[121] When conventional CT is used to diagnose syndesmotic injury, malreduction must be present consistently and not just under stressed conditions.

Numerous measurements are available based on absolute values or relative change compared to the contralateral ankle.[27,28,31,126,128–133] As with plain x-rays, absolute reference values have low yield due to anatomic variability as well as fibular motion.[10,28,33,53,103,134] Intra-subject anatomy has demonstrated consistency and therefore performing CT imaging of bilateral ankles to assess for side-to-side variation is recommended.[27,28,126,130,132,135,136] However, the impact of ankle position on side-to-side symmetry has not been investigated. Commonly used measurements such as the direct distances between the tibia and fibula at the anterior and posterior aspects of the syndesmosis,[27,130] fibular rotation,[130] and sagittal translation of the fibula demonstrate reliability.[130] Additionally, parameters analogous to x-ray measurements, such as TFCS and TFO can be measured,[126,135] as can more complex measurements from 3D datasets including syndesmotic area or volume.[10,129]

Weightbearing CT can increase the detection of syndesmotic injuries by stressing the syndesmotic ligaments during imaging.[137] Additional external rotation stress is also possible.[32] Using weightbearing CT, side-to-side differences in syndesmotic area can accurately predict syndesmotic instability.[138] However, this modality is not always practical or available for routine use.

2.7.4. Magnetic Resonance Imaging (MRI)

MRI allows for direct assessment of ligament integrity and is especially accurate in diagnosing injury to the AITFL and PITFL.[139] Though, it is sometimes unclear if ligamentous injury found is significant enough to cause instability.[60] MRI also has the ability to detect secondary signs of injury such as edema, bony bruising, and osteochondral lesions.[82,140] Standard 3.0 T protocols with oblique planes have been developed to assess the syndesmotic ligaments in continuity and reduce false positive exams.[141–143] MRI studies show a sensitivity of 0.90 or greater and a specificity of 0.84 or greater to detect injury compared

408 to arthroscopy.[81,100,113,142,143] MRI has excellent diagnostic accuracy, however it is generally performed
409 unilaterally, and it's use is also limited by availability, high cost, and the inability to perform dynamic or
410 stress examinations.[24,60]

411

412 ### 2.7.5. Ultrasound

413 Given the limitations of other modalities, ultrasound is being used to evaluate patients with suspected
414 syndesmotic injuries more frequently.[82] Ultrasound has the advantage of being inexpensive, more readily
415 available, without ionizing radiation, and has the capability to perform stress examinations.[144,145] In
416 dynamic ultrasound, the examiner is able to directly visualize the AITFL as well as visualize the interval
417 between the anterior tibial tubercle and anterior border of the fibula.[144] In unstable cases, this interval
418 will increase with external rotation of the foot.[144] Due to variability in diagnostic criteria, cohorts
419 examined, and differing reference standards, there is a wide variety in published accuracies. Sensitivity
420 ranges from 0.66-1.00 and specificity of 0.33-1.00.[145–148] In the largest study, Van Niekerk et al.[148]
421 examined 114 patients with acute ankle injuries requiring surgery and lateral ankle pain. Dynamic
422 ultrasound had a sensitivity of 0.86 and a specificity of 0.97 compared to arthroscopic findings.[148]

423

424 Bilateral examination is more accurate as well. In a small series, Mei-Dan et al.[147] analyzed their receiver
425 operator characteristic to achieve 1.00 sensitivity and specificity when comparing bilateral ankles under
426 external rotation stress, with 0.89 sensitivity and specificity when examining only the affected ankle. A
427 cadaveric study by Fisher et al.[149] demonstrated a difference in motion between the intact state and
428 isolated complete AITFL rupture, but not between intact and a 75% AITFL tear. Given that the clinical
429 importance of isolated AITFL injuries remains unclear,[11,83,84] appropriate thresholds must be developed to
430 help interpret the results of dynamic ultrasound.

431

432 2.8. Arthroscopy

433 Arthroscopy is the established reference standard for diagnosis of injury to the syndesmotic
434 ligaments.[13,16,60,81] Ligaments can be directly visualized for discontinuity or irregularity, along with
435 assessment of instability using arthroscopic probes.[81,94,121] Other benefits include the ability to assess for
436 loose bodies or osteochondral defects, and there is the option to perform treatment at the same time as
437 the diagnostic assessment.[115,150] Obvious drawbacks are the high cost, availability, subspecialized training
438 required, and potential for surgical complications.[115,133] In addition, the IOL is poorly visualized
439 arthroscopically.[121]

440

441 2.9. Treatment

442 When injured, treatment of syndesmotic injuries should be aimed at anatomic reduction and restoring
443 stability to the distal tibiofibular joint.[58,151,152]

444

445 2.9.1. Stable Injuries

446 In patients with a congruent ankle joint and without diastasis of the syndesmosis under stress, the injury
447 to the syndesmosis may be incomplete and conservative management is recommended.[7,16,152] These
448 patients have grade 1 sprains and should be immobilized and prevented from weightbearing for two to
449 six weeks, followed by functional rehabilitation.[16,43,152] In ankle fractures without pre- or intra-operative
450 evidence of syndesmotic instability, the fracture should be managed with stable fixation, but without
451 syndesmotic-specific fixation.[117,152]

452

2.9.2. Rigid Screw Fixation

When syndesmotic injury with frank or latent diastasis is present, stabilization of the syndesmosis is required to restore a congruent, stable ankle and minimize functional consequences.[103,153–155] Multiple techniques including ligament repair or reconstruction, augmentation with synthetic materials, bolts, staples, and hooks have been investigated.[88,151,156–167] The historic gold standard has been rigid fixation with one or more syndesmotic screws, which fix the fibula directly to the tibia.[58,168] Extensive study into the technical details of screw fixation has been performed, though the majority of these studies are biomechanical investigations or underpowered clinical studies.

One versus two syndesmotic screws have been compared. Two screws provide a biomechanically stronger construct with higher yield strength.[86] Clinically this has not translated into any difference in functional outcomes.[169–172] Conflicting conclusions have come from biomechanical studies investigating the optimal position for syndesmotic screws. One study found less syndesmotic diastasis in screws placed 2 cm above the plafond compared to 3.5 cm above,[173] while another determined that screws at 5 cm had less syndesmotic diastasis and greater strength compared to screws placed at 2 cm.[174] A third study performed finite element analysis and reported that fixation at 3-4 cm above the plafond is optimal to minimize displacement and implant failure.[175] Prior recommendations suggested screws below 2 cm risked direct injury to remaining intact syndesmotic ligaments or placement into the intraarticular syndesmotic recess.[176,177] In a clinical studies however, no differences between trans-syndesmotic and supra-syndesmotic fixation were found.[178,179] Screw diameter has also shown not to impact outcomes after syndesmotic fixation. Some biomechanical studies have found a significant increase in fixation strength using 4.5 mm diameter screws compared to 3.5 mm,[86] while others have not.[180–182] Screws larger than 4.5 mm carry a higher risk of iatrogenic fibular fracture.[183] Clinically, Stuart and Panchbhavi[179] found that while

3.5 mm screws were more likely to break, this had no effect on radiographic reduction or functional outcomes. When determining whether to engage three or four cortices (lateral fibula, medial fibula, lateral tibia, and medial tibia), no biomechanical difference has been detected.[182,184] Again, no difference in clinical outcomes has been reported either.[171,172,185,186] Some authors are of the opinion that three cortex screws are more likely to loosen while four cortex screws are more prone to break, however this assertion is not supported by the literature.[155,187–190] Proponents of four cortex fixation argue that implant removal is easier in the case of implant failure.[174,187] Most syndesmotic screws are stainless steel but titanium, as well as bioabsorbable screws, have been investigated. No biomechanical differences have been found between stainless steel and titanium screws.[191] Bioabsorbable screws were introduced to avoid secondary surgery for screw removal and allow for gradual loading of the syndesmosis during resorption.[192] Early screws made of polyglycolide acid hydrolyzed approximately four weeks post-operatively, while newer screws made of polylactide acid and polylevolactic acid degrade over 3-12 months.[193,194] Metallic and bioabsorbable screws are biomechanically similar.[195] Randomized trials comparing screw materials are limited in that metallic screws were removed routinely, however clinical results are not significantly different.[187,196–198] In addition to higher implant cost, bioabsorbable screw complication rates are high, predominantly related for foreign body reaction and wound complications.[196,199,200] In the largest clinical study, Sun et al.[196] found that 24/86 patients with bioabsorbable fixation suffered a post-operative complication compared to 4/82 patients with metallic fixation. Given the high complication rate and lack of clinical benefit with bioabsorbable fixation, stainless steel remains the gold standard material for rigid syndesmotic fixation.

2.9.3. Flexible Fixation

More recently, flexible devices have been developed which are made up of a heavy, nonabsorbable suture secured in a tract through the fibula and tibia with a suture button construct (Figure 2.4). These are often referred to as their brand names such as the Tightrope® (Arthex, Naples, USA), ZipTight™ (Zimmer Biomet, Warsaw, USA), or INVISIKNOT™ (Smith+Nephew, Watford, UK). Suture button devices attempt to improve functional outcomes and syndesmotic reduction by biomechanically mimicking the intact syndesmosis and allowing subtle motion at the distal tibiofibular joint.[47,201]

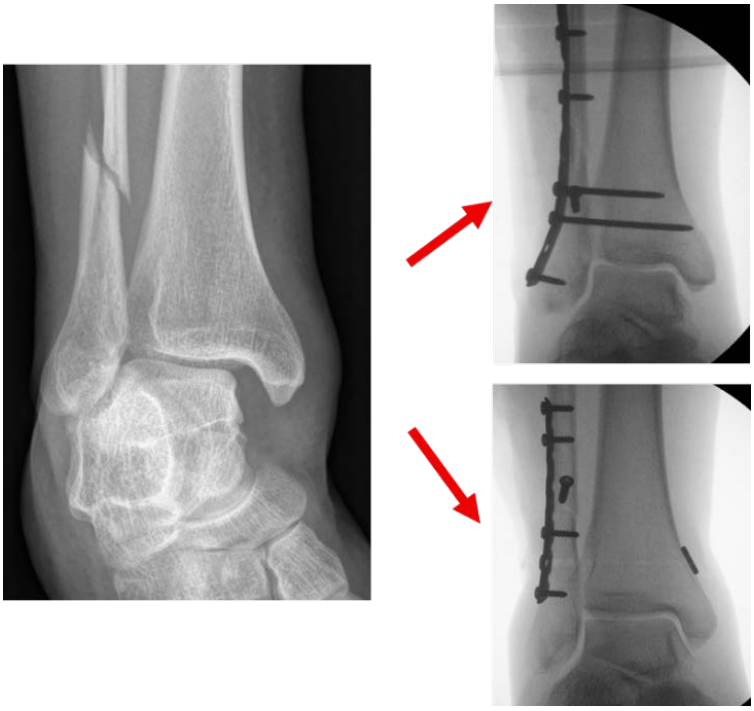

Figure 2.4: Treatment of a syndesmotic injury with traditional rigid fixation with screws (top) compared to flexible fixation with a suture button (bottom).

Cadaveric and modelling studies have shown that motion after flexible fixation is more physiologic than rigid fixation. Results vary, but the overall trend is that rigid fixation results in reduced motion, whereas motion after flexible fixation is supraphysiologic, especially in sagittal translation, but still more accurately recreates normal motion compared to rigid fixation.[33,51,52,83,88,161,201–204] More physiologic motion appears to have a positive impact on ligament healing, creating more organized structure with improved strength.[205–207] Despite this, some authors have speculated that flexible fixation does not adequately constrain fibular motion, which could lead to chronic instability and functional impairment.[88,208,209]

Clinical outcomes for flexible fixation are equivalent or improved compared to rigid fixation. Multiple randomized controlled trials have been performed addressing reduction, functional outcomes, and complications rates.[29,210–215] Individually, only some studies showed improvement in functional outcomes,[210,213] ROM,[214,216] reduction,[212] or complication rates.[215] When these randomized control trials are pooled, significant improvements in functional outcomes, ROM, reduction, complication rates, and unplanned reoperation rates are all found for dynamic fixation.[187,217–219] Though statistically significant, the clinical importance of these functional outcome improvements is unclear.[187,213]

Another benefit of flexible fixation is apparent compensation for malreduction, as the suture button allows the fibula to self-centre within the incisura to a degree.[29,160,220] Flexible fixation can also allow for earlier recovery through permissible early weightbearing.[215,221,222]

2.9.4. Posterior Malleolus Fixation

While previously reserved for restoring articular congruity with large fracture fragments, fixation of a smaller posterior malleolar fracture, when present, is an increasingly popular technique to restore syndesmotic stability.[223,224] In external rotation type injuries, a posterior malleolus fracture may be produced as an avulsion fragment of the PITFL and TTFL.[225] In these instances, the PITFL and TTFL are intact and reduction of the bony fragment can restore syndesmotic stability by re-tensioning these ligaments (Figure 2.5).[225] As the PITFL and TTFL combined contribute most to syndesmotic stability, this method has been shown to provide greater stiffness than rigid screw fixation in response to external rotation stress.[225] Posterior malleolus fixation leads to equivalent functional outcomes to conventional screw fixation and arguably avoids the challenges of malreduction since an anatomic bony reduction can be perfomed.[161,223,226]

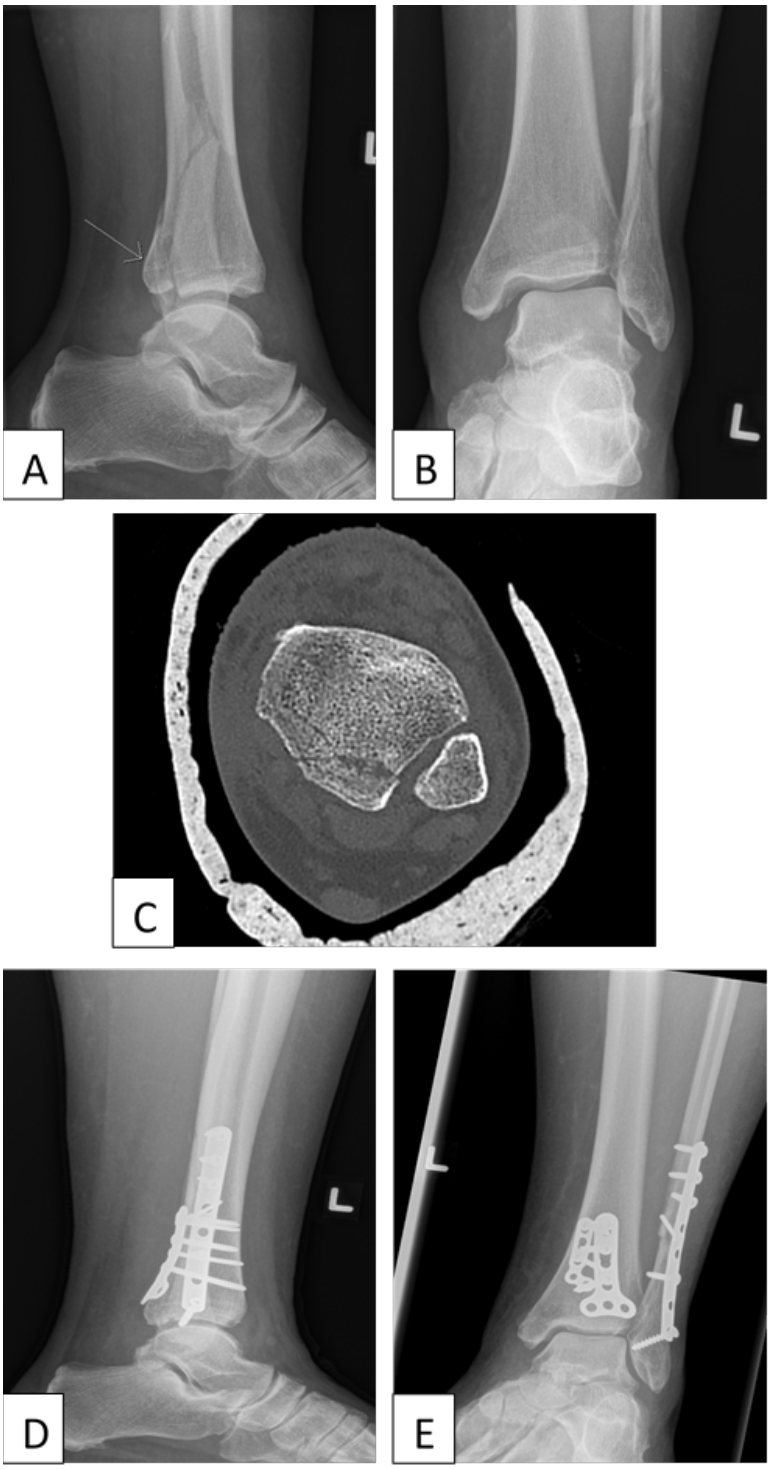

Figure 2.5: Lateral (A) and AP (B), and axial CT (C) images of a high fibular fracture and a posterior malleolus fracture (arrow). Though there is a probable syndesmotic injury with this fracture pattern, syndesmotic stability has been restored with fixation of the posterior malleolus fracture (D, E).

2.10. Complications

2.10.1. Implant Failure and Removal

Due to normal, physiologic motion at the distal tibiofibular joint, rigid screws are prone to breakage, loosening, or planned removal which necessitates secondary surgery.[160,179] Routine removal was previously recommended 6-12 weeks post-operatively due to alterations in normal syndesmotic motion and contact area with rigid fixation.[35,37,227] However, studies have challenged this practice by showing that screw removal may not significantly affect outcomes.[71,73,155] When left intact, screw breakage occurs in 7-29% of patients and screw loosening with radiographic osteolysis around the implant occurs 68-91% of the time.[16,73,155,172,189,228–230] Risk of breakage is up to 12 times higher in obese patients.[231] Studies in favour of screw removal cite spontaneous reduction of malreduced tibiofibular joints[232] and improved ROM[154]. In contrast, other authors have found loss of reduction following routine removal and no change in clinical parameters compared to screws left in situ.[155,185,189,233,234] In studies comparing between removed screws, intact screws, and broken or loosened screws, the cases with radiographic implant failure fared better clinically, whereas those with intact screws had the worst outcomes.[155,189,230] Presumably, rigid fixation leads to inferior patient-reported outcomes, which improve with restoration of motion following implant failure or removal.[155] Screw removal is not a benign procedure and infection-related complications range from 5-9%.[234,235] Estimated cost of implant removal ranges from $1700-3600 USD.[236,237] Understandably, implant removal rates are decreasing and newer recommendations advocate selective removal only in symptomatic patients with intact hardware.[188,230,236] In series where selective implant removal was performed, unplanned removal rates ranged from 13-22%.[212,217,238,239]

567 Suture button devices are less prone to require implant removal, as they do not limit normal
568 motion[212,215,217,221] Early studies reported removal rates as high as 10-25%, primarily attributed to irritation
569 and wound breakdown over the suture knot.[16,160,221,234] However, surgical techniques to reduce knot
570 prominence and newer generation knotless suture buttons have reduced the need for
571 reoperation.[215,240,241] Current estimates of suture button revision rates are 4-6%.[217,238,239,242] Lower
572 reoperation rates reduce complications including loss of reduction, but also limit costs.[29,210,238,239] Despite
573 higher initial implant costs, flexible fixation is cost effective, except when the implant removal rate for
574 rigid fixation is less than 10-13.7%.[238,239]

575

576 ### 2.10.2. Infection

577 Superficial and deep infection have been reported in both rigid and flexible fixation.[243–247] Meta-analysis
578 shows no difference in infection rates, though this also incorporates older generation suture buttons with
579 increased rates of wound complications, including infection.[217–219] Conversely, some studies have shown
580 insignificant increases in infection in flexible fixation, hypothesizing that braided suture can act as a nidus
581 for infection.[243]

582

583 ### 2.10.3. Synostosis

584 Synostosis is an abnormal bony connection between two bones. Synostosis between the distal tibia and
585 fibula can occur after syndesmotic injury with or without associated fractures.[62,176,248] In ankle fractures,
586 published rates based on radiographic assessment are 2% in Weber B fractures and 12% in Weber C
587 fractures.[176] In these fractures, rigid fixation of a syndesmotic injury has a 2.46 odds ratio for developing
588 synostosis.[249] However, when comparing radiographs to CT, Wikerøy et al.[171] found that radiographs
589 overestimated true bony bridging on CT by 200%. This may explain why studies based on plain x-rays

found that synostosis did not impair function, while when using CT to judge synostosis, patients with synostosis had worse ROM and clinical outcomes.[171,176] A single case of synostosis was found after flexible fixation, but overall rates are much lower than in rigid fixation.[160]

2.10.4. Rare Complications

Rare cases of fracture around suture-button tracts and following screw removal have been reported.[250–252] Both rigid and flexible fixation place peroneal and tibial tendons at risk without careful drilling and implant placement.[253,254]

2.11. Outcomes

2.11.1. Stable Injuries

Multiple studies describe successful results treating low grade syndesmotic sprains nonoperatively.[20,43,248,255] Good to excellent results are reported in 86-100% of cases.[16] Management is variable in terms of immobilization and protected weightbearing.[13,92,181,256] Despite good eventual outcomes, recovery and time off sport are substantially higher than other lateral ankle ligamentous injuries.[62,113] In cases of syndesmotic injury, recovery was six times longer than lateral ankle sprains, on average, and twice as long compared to the most severe ankle spains.[55,62] Gerber et al.[61] described persistent symptoms at six months following syndesmotic injury, though other studies show that permanent dysfunction is rare and that return to sport is nearly universal.[16,62] Injuries are reported to recur in 6% of patients.[248,255]

2.11.2. Unstable Injuries

Left untreated, unstable syndesmotic injuries fare poorly. Prior to intervention for chronic syndesmotic injury, mean patient American Orthopaedic Foot and Ankle Hindfoot Scores (AOFAS) were 48 and 56 in two separate studies.[257,258] While not part of the original description, scores less than 60 can be considered poor results, 60-79 fair, 80-89 good, and 90-100 excellent.[259,260] Patients scored 6.1 out of 10 on a visual analog pain scale, where higher scores indicate more severe pain.[257]

When considering all operative ankle fractures, with and without syndesmotic injury, results vary. Some studies describe good outcomes at 1 year with 90% of patients describing no limitations or only with recreational activities, and 88% of patients reporting no or mild ankle discomfort.[261] At longer term follow-up, outcomes suffer. Only 52-79% of patients report good or excellent function at 5-14 years.[262–264] Twenty-four percent of patients have poor outcomes.[264] In these fractures, syndesmotic injuries, even when treated, are poor prognostic factors for pain and functional impairment in the early and late post-operative period.[71,73,265] Maximal recovery is thought to occur by one year.[261]

Reasons for worse outcomes include arthritis, instability, pain, and impingement. High rates of secondary arthritis are reported. Syndesmotic injury leads to reduction in joint contact area and increased contact stresses, predisposing patients to secondary arthritis.[87,153,266–268] Even after rigid or flexible fixation, contact stresses do not normalize, though flexible fixation better approximates physiologic stresses.[36,37,269] Ray et al.[270] found 11% of syndesmotic injuries treated with rigid fixation had radiographic and clinical ankle arthritis at 7 years, and Lambers et al.[169] found radiographic evidence of arthritis in 49% of patients at 18 years. Of these patients, 5% required eventual arthrodesis for their symptoms.[169,270] Patients may also complain of ongoing multidirectional instability.[89] This instability accelerates degenerative change

through joint incongruity as well as motion itself.[271,272] Lastly, impingement may be another cause of pain after injury and arthroscopic studies after injury have found impacted hypertrophic remnants of the AITFL and scar tissue in the anterior incisura to be pain generators and causes of impingement.[94,100]

Overall, poor outcomes after syndesmotic injury despite treatment can be related to malreduction and inadequate restoration of normal biomechanics. Anatomic reduction has been shown to limit degenerative changes and instability of the syndesmosis.[71,105,107,211,273,274]

2.12. Malreduction

2.12.1. Diagnosis

Syndesmotic malreduction is a common problem in both rigid and flexible fixation, reported in up to 52% of cases.[16,103,275,276] Due to the low sensitivity of x-rays in detecting subtle translational and rotational abnormalities, this modality underestimates the incidence of malreduction.[19,106,110] X-ray malreduction rates are approximately 16%[71,210,215,277,278] In comparison, malreduction is found on CT 20-52% of the time.[103,105,128,171,211,275,279] One fundamental issue is how to best define reduction. Highest estimates of malreduction come from a landmark study by Gardner et al.,[103] where a 2 mm difference between the anterior and posterior syndesmosis widths was considered a malreduction. This criterion has been heavily cited and used,[135,280] but subsequently has been shown to be a common normal finding.[28] When performing CT in uninjured ankles, normal differences between the anterior and posterior syndesmotic widths are between 2-4 mm.[27,126,130,279,281,282] In one series, twelve of nineteen uninjured ankles would have been considered malreduced according to Gardner's criteria.[28] These normative studies have shown substantial anatomic variability between subjects,[28,102,126,131,133,135] but minimal side-to-side variation within subjects.[27,28,126,130,135,136,283] Thus, more recent consensus is to perform side-to-side assessment with

657 bilateral ankle CT to assess reduction based on the contralateral ankle.[27–29,105,126,130,131,138,282,284] Still, ankle
658 position during CT assessment is not standardized, potentially affecting measures of reduction. Numerous
659 different measurements have been proposed, most often assessing the syndesmotic width, sagittal
660 translation, and fibular rotation.[126,130,135] Based on bilateral ankle post-operative CT scans, post-operative
661 malreduction rates continue to be as high 44%.[105,171,211,281]

662

663 Secondary malreduction, or loss of reduction, can occur over time in previously reduced ankles. Authors
664 have demonstrated syndesmotic diastasis after screw removal or even with radiographically intact rigid
665 fixation.[29,210,213,215,219,234]

666

667 ### 2.12.2. Functional Impairment

668 Syndesmotic malreduction is the primary predictor of poor outcomes after fixation. Malreduction is the
669 most important factor in predicting poor function, more so than age, ankle dislocation, open injuries, or
670 other associated fractures.[71,105,211,281] A difference in syndesmotic width of just 1.5 mm compared to the
671 contralateral, uninjured ankle is associated with clinically important and statistically significant reductions
672 in patient-reported outcome measures such as the validated Olerud and Molander Score (OM), AOFAS,
673 and Short Form Musculoskeletal Function Assessment (SFMA).[71,73,105,126,171,189,211] These patients are at risk
674 of developing chronic pain, stiffness, instability, or post-traumatic arthritis.[87,107,153,221,270,273,285] This can be
675 a severely debilitating problem, with reduced quality of life from physical and mental disability
676 comparable to end-stage hip arthritis.[286] Consequently, patients have reduced function and activity levels,
677 take time away from work and sports, and often require future surgical intervention. The clear functional
678 implications of syndesmotic reduction, coupled with the high incidence of malreduction, can explain why

679 poorer outcomes are seen in patients with syndesmotic injuries overall compared to regular ankle sprain
680 or fracture cohorts.

681

682 ### 2.12.3. Impact of Fixation Method on Reduction

683 When introduced, one of the proposed benefits of flexible fixation was the improved ability to self-centre
684 within the incisura and combat malreduction.[220] Rates of malreduction in flexible fixation are lower than
685 with rigid fixation, but the problem has not been eliminated. In trials that directly compare the two,
686 malreduction after flexible fixation can occur from 0-20% of the time, versus 16-39% for rigid fixation.[29,211–
687 213,283] A systematic review of syndesmotic treatments found a 0.34 relative risk reduction for malreduction
688 with flexible fixation compared to rigid.[187]

689

690 Flexible fixation is also less prone to secondary malreduction.[29,52,210,211,221] Even in cases where suture-
691 buttons have been removed, it appears that reduction is maintained.[221] Kortekangas et al.[29] demonstrated
692 a three-fold increase in malreduction in rigid fixation comparing two year post-operative imaging to
693 immediate post-operative imaging. Conversely, there was no change in flexible fixation malreduction.[29]
694 Despite significant improvements, flexible fixation on its own does not eliminate malreduction and the
695 associated functional impairment.

696

697 ### 2.12.4. Mitigation Efforts

698 Obtaining an anatomic syndesmotic reduction is challenging intraoperatively. Many authors have
699 attempted to address these concerns with novel measurement techniques intraoperatively or
700 implementing intraoperative CT scans. Given the poor sensitivity of standard fluoroscopy measurements

701 to detect malreduction, multiple measurement techniques have been developed. These include close
702 evaluation of specific relationships on mortise views, novel parameters measured on the lateral x-ray, and
703 the use of contralateral templating.[110,114,116,275,287,288] Yet, even with these methods, our ability to detect
704 malreduction intraoperatively is poor.[275,289] Perhaps surprisingly, intraoperative CT has failed to improve
705 reduction as well. When measured with post-operative CT, syndesmotic malreduction rates remain
706 elevated between 5-38% after intraoperative CT has been implemented.[288–295] Therefore, intraoperative
707 CT requires specialized equipment not available at many institutions and increases surgical time without
708 a clear reduction benefit.

709

710 Reduction methods have also been investigated in an attempt to improve reduction. Clamp and implant
711 (screw or suture button) placement is generally recommended parallel to the plafond at 30° off the
712 coronal plane, from posterolateral to anteromedial.[24,298] However, the trans-syndesmotic axis is variable
713 between individuals and off axis clamping and fixation can increase malreduction rates.[276,299–302] When
714 applying a reduction clamp to the syndesmosis, overcompression is common.[276,300,303,304] Both reducing
715 the force applied via reduction clamp or performing manual reduction using the surgeon's thumb to
716 centre the fibula in the incisura are described to avoid this problem, with limited success.[300,305–307]
717 Regardless, both clamp and thumb reductions fail to restore normal ankle joint contact area and stress.[36]
718 When flexible fixation is used, lower tensions are associated with higher instability, while higher tensions
719 also overcompress the syndesmosis.[308]

720

721 Authors have explored the effect of direct visualization of the anterior incisura and AITFL compared to
722 percutaneous syndesmotic reduction and found improved quality of reduction with open
723 reduction.[105,163,279,309] Even with open reduction, malreduction rates of 16% persisted.[105,279] Further efforts

to minimize malreduction are ongoing including arthroscopic visualization of the syndesmosis or computer-assisted navigation.[100,118,310] These methods are not available routinely, require surgical expertise, and increase time and cost of the procedure.

2.12.5. Limitations of Conventional Imaging

Unfortunately, malreduction remains an unresolved issue in the treatment of syndesmotic injuries despite our improved understanding of its implications and the substantial efforts to improve reduction. Syndesmotic malreduction is still the most important factor that leads to residual disability after ankle injury. Moreover, the syndesmosis is a dynamic structure, and therefore conventional CT does not provide a complete picture of syndesmotic position. Conventional imaging of the ankle in a single, non-standardized, patient-selected ankle position may give an incomplete picture of syndesmotic kinematics and misrepresent reduction. A seemingly reduced syndesmosis in one ankle position can actually be malreduced in another position and vice versa.[29,311] Emphasis on restoring normal syndesmotic motion and maintaining reduction throughout ankle ROM can reduce impairment after injury. Dynamic imaging is required to better appreciate syndesmotic kinematics in uninjured and post-fixation settings.

2.13. 4DCT

2.13.1. 4DCT Development

4DCT, also known as dynamic CT or kinematic CT, is an emerging technology that can capture image volumes in real time, as a joint is moved through ROM.[312,313] 4DCT was introduced in 1999 with multi-row detector scanners which can capture multiple image slices at once.[314] By arranging detectors in a row along the gantry axis, these machines create multiple images from a single x-ray source.[314] Initial scanners

could complete a full gantry rotation in 0.8 seconds to capture a 20 millimeter field along the gantry axis.[314] Over time, gantry speeds have increased and the number of detector rows have grown from four to 320.[315] At present, modern scanners have the ability to image a 160mm field of view along the axis of rotation in under 0.3 seconds with future improvements anticipated.[316] This ultra-fast imaging may be repeated continuously or at multiple timepoints to create a kinematic volume depicting the subject's position with time (Figure 2.6). Such improvements have led to increasing use of 4DCT for clinical and research applications over the past decade.

Figure 2.6: 4DCT imaging of the ankle joint through plantarflexion and dorsiflexion.

2.13.2. Syndesmotic 4DCT Imaging

In the musculoskeletal field, 4DCT has investigated shoulder, elbow, wrist, hip, knee, and ankle motion, providing new insight into dynamic phenomena such as instability, impingement, and joint kinematics.[317–323] Because of the subtle but important motion of the distal tibiofibular joint, it is plausible that variation in ankle position when imaging the syndesmosis statically can lead to inaccurate or misleading results. This may contribute to the relative lack of success in eliminating malreduction or explain poor outcomes seen in some patients with seemingly reduced ankles on conventional imaging.[53,282,324] 4DCT evaluation of the syndesmosis may provide a new understanding of both normal motion as well as quantification of the consequences of malreduction throughout range of motion, which may inform strategies to improve consistent syndesmotic reduction.

2.14. References

1. Snedden MH, Shea JP. 2001. Diastasis With Low Distal Fibula Fractures. Clin. Orthop. Relat. Res. 382(382):197–205.

2. Ebraheim NA, Taser F, Shafiq Q, Yeasting RA. 2006. Anatomical evaluation and clinical importance of the tibiofibular syndesmosis ligaments. Surg. Radiol. Anat. 28(2):142–149.

3. Zwipp H, Rammelt S, Grass R. 2002. Ligamentous injuries about the ankle and subtalar joints. Clin. Podiatr. Med. Surg. 19(2):195–229, v.

4. Goh JC, Mech AM, Lee EH, et al. 1992. Biomechanical study on the load-bearing characteristics of the fibula and the effects of fibular resection. Clin. Orthop. Relat. Res. (279):223–8.

5. Sarsam IM, Hughes SPF. 1988. The role of the anterior tibio-fibular ligament in talar rotation: an anatomical study. Injury 19(2):62–64.

6. Thompson JC. 2016. Netter's Concise Orthopaedic Anatomy, 2nd ed. Philadelphia: Elsevier.

7. Hermans JJ, Beumer A, De Jong TAW, Kleinrensink GJ. 2010. Anatomy of the distal tibiofibular syndesmosis in adults: A pictorial essay with a multimodality approach. J. Anat. 217(6):633–645.

8. Bartonicek J. 2003. Anatomy of the tibiofibular syndesmosis and its clinical relevance. Surg. Radiol. Anat. 25(5–6):379–386.

9. Williams BT, Ahrberg AB, Goldsmith MT, et al. 2015. Ankle syndesmosis: A qualitative and quantitative anatomic analysis. Am. J. Sports Med. 43(1):88–97.

10. Taser F, Shafiq Q, Ebraheim NA. 2006. Three-dimensional volume rendering of tibiofibular joint space and quantitative analysis of change in volume due to tibiofibular syndesmosis diastases. Skeletal Radiol. 35(12):935–941.

11. Clanton TO, Williams BT, Backus JD, et al. 2017. Biomechanical Analysis of the Individual Ligament Contributions to Syndesmotic Stability. Foot Ankle Int. 38(1):66–75.

12. Boonthathip M, Chen L, Trudell DJ, Resnick DL. 2010. Tibiofibular Syndesmotic Ligaments: MR Arthrography in Cadavers with Anatomic Correlation. Radiology 254(3):827–836.

13. Lin CF, Gross MT, Weinhold P. 2006. Ankle syndesmosis injuries: Anatomy, biomechanics, mechanism of injury, and clinical guidelines for diagnosis and intervention. J. Orthop. Sports Phys. Ther. 36(6):372–384.

14. Rasmussen O, Tovborg-Jensen I, Boe S. 1982. Distal tibiofibular ligaments: Analysis of function. Acta Orthop. 53(4):681–686.

15. Ogilvie-Harris DJ, Reed SC, Hedman TP. 1994. Disruption of the ankle syndesmosis: Biomechanical study of the ligamentous restraints. Arthroscopy 10(5):558–560.

16. Rammelt S, Obruba P. 2015. An update on the evaluation and treatment of syndesmotic injuries. Eur. J. Trauma Emerg. Surg. 41(6):601–614.

17. Lee SH, Jacobson J, Trudell D, Resnick D. 1998. Ligaments of the Ankle: Normal Anatomy with MR Arthrography. J. Comput. Assist. Tomogr. 22(5):807–813.

18. Golanò P, Mariani PP, Rodríguez-Niedenfuhr M, et al. 2002. Arthroscopic anatomy of the posterior ankle ligaments. Arthrosc. J. Arthrosc. Relat. Surg. 18(4):353–358.

19. Ebraheim NA, Lu J, Yang H, et al. 1997. Radiographic and CT Evaluation of Tibiofibular Syndesmotic Diastasis: A Cadaver Study. Foot Ankle Int. 18(11):693–698.

20. Dattani R, Patnaik S, Kantak A, et al. 2008. Injuries to the tibiofibular syndesmosis. J. Bone Joint Surg. Br. 90-B(4):405–410.

21. Nikolopoulos CE, Tsirikos AI, Sourmelis S, Papachristou G. 2004. The Accessory Anteroinferior Tibiofibular Ligament as a Cause of Talar Impingement. Am. J. Sports Med. 32(2):389–395.

22. Norkus SA, Floyd RT. 2001. The anatomy and mechanisms of syndesmotic ankle sprains. J. Athl. Train. 36(1):68–73.

23. Rosenberg ZS, Cheung YY, Beltran J, et al. 1995. Posterior intermalleolar ligament of the ankle: normal anatomy and MR imaging features. AJR. Am. J. Roentgenol. 165(2):387–90.

24. Zalavras C, Thordarson D. 2007. Ankle syndesmotic injury. J. Am. Acad. Orthop. Surg. 15(6):330–339.

25. Pankovich AM, Shivaram MS. 1979. Anatomical Basis of Variability in Injuries of the Medial Malleolus and the Deltoid Ligament: I. Anatomical Studies. Acta Orthop. Scand. 50(2):217–223.

26. Paredes-Vázquez R, Sesma-Villalpando RA, Herrera-Tenorio G, Romero-Ogawa T. [date unknown]. CT scan evaluation of the syndesmotic diastasis in AO/OTA B and C ankle fractures. Acta Ortop. Mex. 25(1):32–8.

27. Elgafy H, Semaan HB, Blessinger B, et al. 2010. Computed tomography of normal distal tibiofibular syndesmosis. Skeletal Radiol. 39(6):559–564.

28. Mukhopadhyay S, Metcalfe A, Guha AR, et al. 2011. Malreduction of syndesmosis—Are we considering the anatomical variation? Injury 42(10):1073–1076.

29. Kortekangas T, Savola O, Flinkkilä T, et al. 2015. A prospective randomised study comparing TightRope and syndesmotic screw fixation for accuracy and maintenance of syndesmotic reduction assessed with bilateral computed tomography. Injury 46(6):1119–1126.

30. Ebraheim NA, Lu J, Yang H, Rollins J. 1998. The Fibular Incisure of the Tibia on CT Scan: A Cadaver Study. Foot Ankle Int. 19(5):318–321.

31. Yeung TW, Chan CYG, Chan WCS, et al. 2015. Can pre-operative axial CT imaging predict syndesmosis instability in patients sustaining ankle fractures? Seven years' experience in a tertiary trauma center. Skeletal Radiol. 44(6).

32. Lepojärvi S, Niinimäki J, Pakarinen H, Leskelä HV. 2016. Rotational Dynamics of the Normal Distal Tibiofibular Joint With Weight-Bearing Computed Tomography. Foot Ankle Int. 37(6):627–635.

33. Huber T, Schmoelz W, Bölderl A. 2012. Motion of the fibula relative to the tibia and its alterations with syndesmosis screws: A cadaver study. Foot Ankle Surg. 18(3):203–209.

34. Gonzalez T, Egan J, Ghorbanhoseini M, et al. 2017. Overtightening of the syndesmosis revisited and the effect of syndesmotic malreduction on ankle dorsiflexion. Injury 48(6):1253–1257.

35. Needleman RL, Skrade DA, Stiehl JB. 1989. Effect of the Syndesmotic Screw on Ankle Motion. Foot Ankle 10(1):17–24.

36. LaMothe J, Baxter JR, Gilbert S, et al. 2017. Effect of Complete Syndesmotic Disruption and Deltoid Injuries and Different Reduction Methods on Ankle Joint Contact Mechanics. Foot Ankle Int. 38(6):694–700.

37. Pereira DS, Koval KJ, Resnick RB, et al. 1996. Tibiotalar Contact Area and Pressure Distribution: The Effect of Mortise Widening and Syndesmosis Fixation. Foot Ankle Int. 17(5):269–274.

38. Calhoun JH, Li F, Ledbetter BR, Viegas SF. 1994. A Comprehensive Study of Pressure Distribution in the Ankle Joint with Inversion and Eversion. Foot Ankle Int. 15(3):125–133.

39. Lundberg A. 1989. Kinematics of the ankle and foot. In vivo roentgen stereophotogrammetry. Acta Orthop. Scand. Suppl. 233:1–24.

40. Michelson JD, Helgemo SL. 1995. Kinematics of the Axially Loaded Ankle. Foot Ankle Int. 16(9):577–582.

41. Haraguchi N, Armiger RS, Myerson MS, et al. 2009. Prediction of three-dimensional contact stress and ligament tension in the ankle during stance determined from computational modeling. Foot ankle Int. 30(2):177–85.

42. Skraba JS, Greenwald AS. 1984. The role of the interosseous membrane on tibiofibular weightbearing. Foot Ankle 4(6):301–4.

43. Mulligan EP. 2011. Evaluation and management of ankle syndesmosis injuries. Phys. Ther. Sport 12(2):57–69.

44. Takebe K, Nakagawa A, Minami H, et al. 1984. Role of the fibula in weight-bearing. Clin. Orthop. Relat. Res. (184):289–92.

45. Wang Q, Whittle M, Cunningham J, Kenwright J. 1996. Fibula and Its Ligaments in Load Transmission and Ankle Joint Stability. Clin. Orthop. Relat. Res. 330(330):261–270.

46. Mousavian A, Shakoor D, Hafezi-Nejad N, et al. 2019. Tibiofibular syndesmosis in asymptomatic ankles: initial kinematic analysis using four-dimensional CT. Clin. Radiol. 74(7):571.e1-571.e8.

47. Qamar F, Kadakia A, Venkateswaran B. 2011. An Anatomical Way of Treating Ankle Syndesmotic Injuries. J. Foot Ankle Surg. 50(6):762–765.

48. Hu WK, Chen DW, Li B, et al. 2019. Motion of the distal tibiofibular syndesmosis under different loading patterns: A biomechanical study. J. Orthop. Surg. 27(2):1–6.

49. Close JR. 1956. Some applications of the functional anatomy of the ankle joint. J. Bone Joint Surg. Am. 38-A(4):761–81.

50. Svensson OK, Lundberg A, Walheirn G, Selvik G. 1989. In vivo fibular motions during various movements of the ankle. Clin. Biomech. 4(3):155–160.

51. Beumer A, Valstar ER, Garling EH, et al. 2003. Kinematics of the distal tibiofibular syndesmosis: Radiostereometry in 11 normal ankles. Acta Orthop. Scand. 74(3):337–343.

52. Klitzman R, Zhao H, Zhang L-Q, et al. 2010. Suture-Button Versus Screw Fixation of the Syndesmosis: A Biomechanical Analysis. Foot Ankle Int. 31(1):69–75.

53. Wang C, Yang J, Wang S, et al. 2015. Three-dimensional motions of distal syndesmosis during walking. J. Orthop. Surg. Res. 10(1):166.

54. Lundgren P, Nester C, Liu A, et al. 2008. Invasive in vivo measurement of rear-, mid- and forefoot motion during walking. Gait Posture 28(1):93–100.

55. Boytim MJ, Fischer DA, Neumann L. 1991. Syndesmotic ankle sprains. Am. J. Sports Med. 19(3):294–298.

56. Waterman BR, Belmont PJ, Cameron KL, et al. 2011. Risk Factors for Syndesmotic and Medial Ankle Sprain. Am. J. Sports Med. 39(5):992–998.

57. Kannus P, Palvanen M, Niemi S, et al. 2008. Stabilizing incidence of low-trauma ankle fractures in elderly people. Bone 43(2):340–342.

58. Carr JC, Werner BC, Yarboro SR. 2016. An Update on Management of Syndesmosis Injury: A National US Database Study. Am. J. Orthop. (Belle Mead. NJ). 45(7):E472–E477.

59. Waterman CBR, Owens MBD, Davey CS, et al. 2010. The Epidemiology of Ankle Sprains in the United States. J. Bone Jt. Surgery-American Vol. 92(13):2279–2284.

60. Krähenbühl N, Weinberg MW, Davidson NP, et al. 2017. Imaging in syndesmotic injury: a systematic literature review. Skeletal Radiol. 47(5):631–648.

61. Gerber JP, Williams GN, Scoville CR, et al. 1998. Persistent disability associated with ankle sprains: A prospective examination of an athletic population. Foot Ankle Int. 19(10):653–660.

62. Hopkinson WJ, St.Pierre P, Ryan JB, Wheeler JH. 1990. Syndesmosis sprains of the ankle. Foot Ankle 10(6):325–330.

63. Court-Brown C, Aitken S, Forward D, O'Toole R. 2010. The epidemiology of fractures. In: Bucholz R, Court-Brown C, Heckman J, Tornetta P, editors. Rockwood and Green's Fractures in Adults, 7th ed. Philadelphia: Lippincott, Williams, and Wilkins.

64. Daly PJ, Fitzgerald RH, Melton LJ, Llstrup DM. 1987. Epidemiology of ankle fractures in Rochester, minnesota. Acta Orthop. 58(5):539–544.

65. du Plessis G, Griesel L, Lourens D, Gräbe R. 2008. Incidence of syndesmotic injuries in all different types of ankle fractures. SA Orthop. J. 7(1):28–33.

66. Purvis GD. 1982. Displaced, unstable ankle fractures. Classification, incidence, and management of a consecutive series. Clin. Orthop. Relat. Res. No. 165(165):91–98.

67. TH L, K I, HT C. 2005. Comparison of radiologic and arthroscopic diagnoses of distal tibiofibular syndesmosis disruption in acute ankle fracture. Arthroscopy 21(11):1370–1370.

68. Pakarinen HJ, Flinkkilä TE, Ohtonen PP, et al. 2011. Syndesmotic fixation in supination-external rotation ankle fractures: a prospective randomized study. Foot ankle Int. 32(12):1103–9.

69. Jenkinson RJ, Sanders DW, Macleod MD, et al. 2005. Intraoperative diagnosis of syndesmosis injuries in external rotation ankle fractures. J. Orthop. Trauma 19(9):604–609.

70. Tornetta P, Axelrad TW, Sibai TA, Creevy WR. 2012. Treatment of the Stress Positive Ligamentous SE4 Ankle Fracture: Incidence of Syndesmotic Injury and Clinical Decision Making. J. Orthop. Trauma 26(11):659–661.

71. Weening B, Bhandari M. 2005. Predictors of functional outcome following transsyndesmotic screw fixation of ankle fractures. J. Orthop. Trauma 19(2):102–108.

72. Lauge-Hansen N. 1950. Fractures of The Ankle: II. Combined Experimental-Surgical and Experimental-Roentgenologic Investigations. Arch. Surg. 60(5):957.

73. Egol KA, Pahk B, Walsh M, et al. 2010. Outcome after unstable ankle fracture: Effect of syndesmotic stabilization. J. Orthop. Trauma 24(1):7–11.

74. Ebraheim NA, Elgafy H, Padanilam T. 2003. Syndesmotic disruption in low fibular fractures associated with deltoid ligament injury. Clin. Orthop. Relat. Res. (409):260–267.

75. Meinberg E, Agel J, Roberts C, et al. 2018. Fracture and Dislocation Classification Compendium—2018. J. Orthop. Trauma 32:S1–S10.

76. Elsoe R, Ostgaard SE, Larsen P. 2018. Population-based epidemiology of 9767 ankle fractures. Foot Ankle Surg. 24(1):34–39.

77. Hunt KJ, George E, Harris AHS, Dragoo JL. 2013. Epidemiology of Syndesmosis Injuries in Intercollegiate Football. Clin. J. Sport Med. 23(4):278–282.

78. Markolf KL, Jackson S, McAllister DR. 2012. Force and displacement measurements of the distal fibula during simulated ankle loading tests for high ankle sprains. Foot ankle Int. 33(9):779–86.

79. Sclafani SJA. 1985. Ligamentous injury of the lower tibiofibular syndesmosis: Radiographic evidence. Radiology 156(1):21–27.

935 80. Beumer A, Van Hemert WLW, Swierstra BA, et al. 2003. A biomechanical evaluation of clinical
936 stress tests for syndesmotic ankle instability. Foot Ankle Int. 24(4):358–363.

937 81. Takao M, Ochi M, Oae K, et al. 2003. Diagnosis of a tear of the tibiofibular syndesmosis. The role
938 of arthroscopy of the ankle. J. Bone Jt. Surg. - Ser. B 85(3):324–329.

939 82. van Dijk CN, Longo UG, Loppini M, et al. 2016. Classification and diagnosis of acute isolated
940 syndesmotic injuries: ESSKA-AFAS consensus and guidelines. Knee Surgery, Sport. Traumatol. Arthrosc.
941 24(4):1200–1216.

942 83. Lamothe JM, Baxter JR, Murphy C, et al. 2016. Three-Dimensional Analysis of Fibular Motion after
943 Fixation of Syndesmotic Injuries with a Screw or Suture-Button Construct. Foot Ankle Int. 37(12):1350–
944 1356.

945 84. De César PC, Ávila EM, De Abreu MR. 2011. Comparison of magnetic resonance imaging to
946 physical examination for syndesmotic injury after lateral ankle sprain. Foot Ankle Int. 32(12):1110–1114.

947 85. Beumer A, R Valstar E, H Garling E, et al. 2006. Effects of ligament sectioning on the kinematics of
948 the distal tibiofibular syndesmosis: A radiostereometric study of 10 cadaveric specimens based on
949 presumed trauma mechanisms with suggestions for treatment. Acta Orthop. 77(3):531–540.

950 86. Xenos JS, Hopkinson WJ, Mulligan ME, et al. 1995. The tibiofibular syndesmosis. Evaluation of the
951 ligamentous structures, methods of fixation, and radiographic assessment. J. Bone Jt. Surg. - Ser. A
952 77(6):847–856.

953 87. Hunt KJ, Goeb Y, Behn AW, et al. 2015. Ankle Joint Contact Loads and Displacement with
954 Progressive Syndesmotic Injury. Foot Ankle Int. 36(9):1095–1103.

955 88. Goetz JE, Davidson NP, Rudert MJ, et al. 2018. Biomechanical Comparison of Syndesmotic Repair
956 Techniques During External Rotation Stress. Foot Ankle Int. 39(11):1345–1354.

957 89. Teramoto A, Kura H, Uchiyama E, et al. 2008. Three-dimensional analysis of ankle instability after
958 tibiofibular syndesmosis injuries: A biomechanical experimental study. Am. J. Sports Med. 36(2):348–352.

959 90. LaMothe JM, Baxter JR, Karnovsky SC, et al. 2018. Syndesmotic Injury Assessment With Lateral
960 Imaging During Stress Testing in a Cadaveric Model. Foot Ankle Int. 39(4):479–484.

961 91. Massri-Pugin J, Lubberts B, Vopat BG, et al. 2018. Role of the Deltoid Ligament in Syndesmotic
962 Instability. Foot Ankle Int. 39(5).

963 92. Amendola A, Williams G, Foster D. 2006. Evidence-based approach to treatment of acute
964 traumatic syndesmosis (high ankle) sprains. Sports Med. Arthrosc. 14(4):232–236.

965 93. Beumer A, Swierstra BA, Mulder PGH. 2002. Clinical diagnosis of syndesmotic ankle instability.
966 Acta Orthop. Scand. 73(6):667–669.

967 94. Ogilvie-Harris DJ, Reed SC. 1994. Disruption of the ankle syndesmosis: diagnosis and treatment by
968 arthroscopic surgery. Arthroscopy 10(5):561–8.

969 95. Alonso A, Khoury L, Adams R. 1998. Clinical Tests for Ankle Syndesmosis Injury: Reliability and
970 Prediction of Return to Function. J. Orthop. Sport. Phys. Ther. 27(4):276–284.

971 96. Taylor DC, Englehardt DL, Bassett FH. 1992. Syndesmosis sprains of the ankle. Am. J. Sports Med.
972 20(2):146–150.

973 97. Sman AD, Hiller CE, Rae K, et al. 2015. Diagnostic accuracy of clinical tests for ankle syndesmosis
974 injury. Br. J. Sports Med. 49(5):323–329.

975 98. Kiter E, Bozkurt M. 2005. The crossed-leg test for examination of ankle syndesmosis injuries. Foot
976 Ankle Int. 26(2):187–188.

977 99. Sman AD, Hiller CE, Refshauge KM. 2013. Diagnostic accuracy of clinical tests for diagnosis of ankle
978 syndesmosis injury: A systematic review. Br. J. Sports Med. 47(10):620–628.

979 100. Han SH, Lee JW, Kim S, et al. 2007. Chronic tibiofibular syndesmosis injury: The diagnostic
980 efficiency of magnetic resonance imaging and comparative analysis of operative treatment. Foot Ankle
981 Int. 28(3):336–342.

982 101. Harper MC, Keller TS. 1989. A radiographic evaluation of the tibiofibular syndesmosis. Foot Ankle
983 10(3):156–160.

984 102. Beumer A, Van Hemert WLW, Niesing R, et al. 2004. Radiographic measurement of the distal
985 tibiofibular syndesmosis has limited use. Clin. Orthop. Relat. Res. (423):227–234.

986 103. Gardner MJ, Demetrakopoulos D, Briggs SM, et al. 2006. Malreduction of the Tibiofibular
987 Syndesmosis in Ankle Fractures. Foot Ankle Int. 27(10):788–792.

988 104. Nielson JH, Gardner MJ, Peterson MGE, et al. 2005. Radiographic measurements do not predict
989 syndesmotic injury in ankle fractures: An MRI study. Clin. Orthop. Relat. Res. NA;(436):216–221.

990 105. Sagi HC, Shah AR, Sanders RW. 2012. The Functional Consequence of Syndesmotic Joint
991 Malreduction at a Minimum 2-Year Follow-Up. J. Orthop. Trauma 26(7):439–443.

992 106. Pneumaticos SG, Noble PC, Chatziioannou SN, Trevino SG. 2002. The effects of rotation on
993 radiographic evaluation of the tibiofibular syndesmosis. Foot Ankle Int. 23(2):107–111.

994 107. Mont MA, Sedlin ED, Weiner LS, Miller AR. 1992. Postoperative radiographs as predictors of
995 clinical outcome in unstable ankle fractures. J. Orthop. Trauma 6(3):352–357.

996 108. Stiehl JB. 1990. Complex ankle fracture dislocations with syndesmotic diastasis. Orthop. Rev.
997 19(6):499–507.

998 109. Beumer A, Swiestra BA. 2003. The influence of ankle positioning on the radiography of the distal
999 tibial tubercules. Surg. Radiol. Anat. 25(5–6):446–450.

1000 110. Marmor M, Hansen E, Han HK, et al. 2011. Limitations of standard fluoroscopy in detecting
1001 rotational malreduction of the syndesmosis in an ankle fracture model. Foot Ankle Int. 32(6):616–622.

1002 111. Saldua NS, Harris JF, LeClere LE, et al. 2010. Plantar flexion influences radiographic measurements
1003 of the ankle mortise. J. Bone Jt. Surg. - Ser. A 92(4):911–915.

1004 112. Takao M, Ochi M, Naito K, et al. 2001. Arthroscopic diagnosis of tibiofibular syndesmosis
1005 disruption. Arthroscopy 17(8):836–843.

1006 113. Oae K, Takao M, Naito K, et al. 2003. Injury of the Tibiofibular Syndesmosis: Value of MR Imaging
1007 for Diagnosis. Radiology 227(1):155–161.

1008 114. Summers HD, Sinclair MK, Stover MD. 2013. A reliable method for intraoperative evaluation of
1009 syndesmotic reduction. J. Orthop. Trauma 27(4):196–200.

1010 115. Gardner MJ, Graves ML, Higgins TF, Nork SE. 2015. Technical considerations in the treatment of
1011 syndesmotic injuries associated with ankle fractures. J. Am. Acad. Orthop. Surg. 23(8):510–518.

1012 116. Schreiber JJ, McLawhorn AS, Dy CJ, Goldwyn EM. 2013. Intraoperative Contralateral View for
1013 Assessing Accurate Syndesmosis Reduction. Orthopedics 36(5):360–361.

1014 117. McConnell T, Creevy W, Tornetta P. 2004. Stress examination of supination external rotation-type
1015 fibular fractures. J. Bone Jt. Surg. - Ser. A 86(10):2171–2178.

1016 118. Scranton PE. 2002. Isolated Syndesmotic Injuries: Diastasis of the Ankle in the Athlete. Tech. Foot
1017 Ankle Surg. 1(2):88–93.

1018 119. LeBa TB, Gugala Z, Morris RP, Panchbhavi VK. 2015. Gravity Versus Manual External Rotation
1019 Stress View in Evaluating Ankle Stability: A Prospective Study. Foot Ankle Spec. 8(3):175–179.

1020 120. Hoshino CM, Nomoto EK, Norheim EP, Harris TG. 2012. Correlation of Weightbearing Radiographs
1021 and Stability of Stress Positive Ankle Fractures. Foot Ankle Int. 33(2):92–98.

1022 121. van den Bekerom MPJ. 2011. Diagnosing syndesmotic instability in ankle fractures. World J.
1023 Orthop. 2(7):51–56.

1024 122. Stoffel K, Wysocki D, Baddour E, et al. 2009. Comparison of two intraoperative assessment
1025 methods for injuries to the ankle syndesmosis: A cadaveric study. J. Bone Jt. Surg. - Ser. A 91(11):2646–
1026 2652.

1027 123. Pakarinen H, Flinkkilä T, Ohtonen P, et al. 2011. Intraoperative assessment of the stability of the
1028 distal tibiofibular joint in supination-external rotation injuries of the ankle sensitivity, specificity, and
1029 reliability of two clinical tests. J. Bone Jt. Surg. - Ser. A 93(22):2057–2061.

1030 124. Candal-Couto J., Burrow D, Bromage S, Briggs P. 2004. Instability of the tibio-fibular syndesmosis:
1031 have we been pulling in the wrong direction? Injury 35(8):814–818.

1032 125. Choi Y, Kwon S-S, Chung C, et al. 2014. Preoperative radiographic and CT findings predicting
1033 syndesmotic injuries in supination-external rotation-type ankle fractures. J. Bone Jt. Surg. - Am. Vol.
1034 96(14):1161–1167.

1035 126. Dikos GD, Heisler J, Choplin RH, Weber TG. 2012. Normal Tibiofibular Relationships at the
1036 Syndesmosis on Axial CT Imaging. J. Orthop. Trauma 26(7):433–438.

1037 127. Knops SP, Kohn MA, Hansen EN, et al. 2013. Rotational malreduction of the syndesmosis:
1038 Reliability and accuracy of computed tomography measurement methods. Foot Ankle Int. 34(10):1403–
1039 1410.

1040 128. Vasarhelyi A, Lubitz J, Gierer P, et al. 2006. Detection of fibular torsional deformities after surgery
1041 for ankle fractures with a novel CT method. Foot Ankle Int. 27(12):1115–1121.

1042 129. Malhotra G, Cameron J, Toolan BC. 2014. Diagnosing chronic diastasis of the syndesmosis: A novel
1043 measurement using computed tomography. Foot Ankle Int. 35(5):483–488.

1044 130. Nault M-LL, Hébert-Davies J, Laflamme G-YY, Leduc S. 2013. CT scan assessment of the
1045 syndesmosis: A new reproducible method. J. Orthop. Trauma 27(11):638–641.

1046 131. Kotwal R, Rath N, Paringe V, et al. 2016. Targeted computerised tomography scanning of the ankle
1047 syndesmosis with low dose radiation exposure. Skeletal Radiol. 45(3):333–338.

1048 132. Mendelsohn ES, Hoshino CM, Harris TG, Zinar DM. 2014. CT Characterizing the Anatomy of
1049 Uninjured Ankle Syndesmosis. Orthopedics 37(2):e157–e160.

1050 133. Prakash AA. 2018. Syndesmotic stability: Is there a radiological normal?—A systematic review.
1051 Foot Ankle Surg. 24(3):174–184.

1052 134. Chen BH, Chen C, Yang ZT, et al. 2019. To compare the efficacy between fixation with tightrope
1053 and screw in the treatment of syndesmotic injuries: A meta-analysis. Foot Ankle Surg. 25(1):63–70.

1054 135. Lepojärvi S, Pakarinen H, Savola O, et al. 2014. Posterior translation of the fibula may indicate
1055 malreduction: CT study of normal variation in uninjured ankles. J. Orthop. Trauma 28(4):205–209.

1056 136. Shah AS, Kadakia AR, Tan GJ, et al. 2012. Radiographic Evaluation of the Normal Distal Tibiofibular
1057 Syndesmosis. Foot Ankle Int. 33(10):870–876.

1058 137. Abdelaziz ME, Hagemeijer N, Guss D, et al. 2019. Evaluation of Syndesmosis Reduction on CT Scan.
1059 Foot Ankle Int. 40(9).

1060 138. Hagemeijer NC, Chang SH, Abdelaziz ME, et al. 2019. Range of Normal and Abnormal Syndesmotic
1061 Measurements Using Weightbearing CT. Foot Ankle Int. 40(12).

1062 139. Clanton TO, Ho CP, Williams BT, et al. 2016. Magnetic resonance imaging characterization of
1063 individual ankle syndesmosis structures in asymptomatic and surgically treated cohorts. Knee Surgery,
1064 Sport. Traumatol. Arthrosc. 24(7):2089–2102.

1065 140. Calder J, Mitchell A, Lomax A, et al. 2017. The broken “ring of fire”: A new radiological sign as
1066 predictor of syndesmosis injury? Orthop. J. Sport. Med. 5(3).

1067 141. Hermans JJ, Ginai AZ, Wentink N, et al. 2011. The additional value of an oblique image plane for
1068 MRI of the anterior and posterior distal tibiofibular syndesmosis. Skeletal Radiol. 40(1):75.

1069 142. Kim S, Huh Y-M, Song H-T, et al. 2007. Chronic Tibiofibular Syndesmosis Injury of Ankle: Evaluation
1070 with Contrast-enhanced Fat-suppressed 3D Fast Spoiled Gradient-recalled Acquisition in the Steady State
1071 MR Imaging. Radiology 242(1):225–235.

1072 143. Chun KY, Choi YS, Lee SH, et al. 2015. Deltoid ligament and tibiofibular syndesmosis injury in
1073 chronic lateral ankle instability: Magnetic resonance imaging evaluation at 3t and comparison with
1074 arthroscopy. Korean J. Radiol. 16(5):1096–1103.

1075 144. Mei-Dan O, Carmont M, Laver L, et al. 2013. Standardization of the functional syndesmosis
1076 widening by dynamic U.S examination. BMC Sports Sci. Med. Rehabil. 5(1):1–8.

1077 145. Milz P, Milz S, Steinborn M, et al. 1998. Lateral ankle ligaments and tibiofibular syndesmosis: 13-
1078 MHz high-frequency sonography and MRI compared in 20 patients. Acta Orthop. Scand. 69(1):51–55.

1079 146. Oae K, Takao M, Uchio Y, Ochi M. 2010. Evaluation of anterior talofibular ligament injury with
1080 stress radiography, ultrasonography and MR imaging. Skeletal Radiol. 39(1):41–47.

1081 147. Mei-Dan O, Kots E, Barchilon V, et al. 2009. A dynamic ultrasound examination for the diagnosis
1082 of ankle syndesmotic injury in professional athletes: A preliminary study. Am. J. Sports Med. 37(5):1009–
1083 1016.

1084 148. van Niekerk C, van Dyk B. 2017. Dynamic ultrasound evaluation of the syndesmosis ligamentous
1085 complex and clear space in acute ankle injury, compared to magnetic resonance imaging and surgical
1086 findings. Cannon Communications. 8 p.

1087 149. Fisher CL, Rabbani T, Johnson K, et al. 2019. Diagnostic capability of dynamic ultrasound
1088 evaluation of supination-external rotation ankle injuries: a cadaveric study. BMC Musculoskelet. Disord.
1089 20(1):502.

1090 150. Sri-Ram K, Robinson AHN. 2005. Arthroscopic assessment of the syndesmosis following ankle
1091 fracture. Injury 36(5):675–678.

1092 151. van den Bekerom MPJ, Lamme B, Hogervorst M, Bolhuis HW. 2007. Which Ankle Fractures Require
1093 Syndesmotic Stabilization? J. Foot Ankle Surg. 46(6):456–463.

1094 152. Schnetzke M, Vetter SY, Beisemann N, et al. 2016. Management of syndesmotic injuries: What is
1095 the evidence? World J. Orthop. 7(11):718.

1096 153. Ramsey PL, Hamilton W. 1976. Changes in tibiotalar area of contact caused by lateral talar shift.
1097 J. Bone Joint Surg. Am. 58(3):356–7.

1098 154. Miller AN, Paul O, Boraiah S, et al. 2010. Functional outcomes after syndesmotic screw fixation
1099 and removal. J. Orthop. Trauma 24(1):12–16.

1100 155. Hamid N, Loeffler BJ, Braddy W, et al. 2009. Outcome after fixation of ankle fractures with an
1101 injury to the syndesmosis. J. Bone Joint Surg. Br. 91-B(8):1069–1073.

1102 156. Lui TH. 2010. Tri-ligamentous Reconstruction of the Distal Tibiofibular Syndesmosis: A Minimally
1103 Invasive Approach. J. Foot Ankle Surg. 49(5):495–500.

1104 157. Kara AN, Esenyel CZ, Sener BT, Merih E. 1999. A different approach to the treatment of the lateral
1105 malleolar fractures with syndesmosis injury: The ANK nail. J. Foot Ankle Surg. 38(6):394–402.

1106 158. Nelson OA. 2006. Examination and repair of the AITFL in transmalleolar fractures. J. Orthop.
1107 Trauma 20(9):637–643.

1108 159. Regauer M, Mackay G, Lange M, et al. 2017. Syndesmotic InternalBraceTM for anatomic distal
1109 tibiofibular ligament augmentation. World J. Orthop. 8(4):301.

1110 160. Schepers T. 2012. Acute distal tibiofibular syndesmosis injury: A systematic review of suture-
1111 button versus syndesmotic screw repair. Int. Orthop. 36(6):1199–1206.

1112 161. Schottel PC, Baxter J, Gilbert S, et al. 2016. Anatomic ligament repair restores ankle and
1113 syndesmotic rotational stability as much as syndesmotic screw fixation. J. Orthop. Trauma 30(2):e36–e40.

1114 162. Teramoto A, Shoji H, Sakakibara Y, et al. 2018. Suture-Button Fixation and Mini-Open Anterior
1115 Inferior Tibiofibular Ligament Augmentation Using Suture Tape for Tibiofibular Syndesmosis Injuries. J.
1116 Foot Ankle Surg. 57(1):159–161.

1117 163. Yang Y, Zhou J, Li B, et al. 2013. Operative exploration and reduction of syndesmosis in weber type
1118 c ankle injury. Acta Ortop. Bras. 21(2):103–108.

1119 164. Vilá-Rico J, Sánchez-Morata E, Vacas-Sánchez E, Ojeda-Thies C. 2018. Anatomical Arthroscopic
1120 Graft Reconstruction of the Anterior Tibiofibular Ligament for Chronic Disruption of the Distal
1121 Syndesmosis. Arthrosc. Tech. 7(2):e165–e169.

1122 165. Grass R, Rammelt S, Biewener A, Zwipp H. 2003. Peroneus Longus Ligamentoplasty for Chronic
1123 Instability of the Distal Tibiofibular Syndesmosis. Foot Ankle Int. 24(5):392–397.

1124 166. Yasui Y, Takao M, Miyamoto W, et al. 2011. Anatomical reconstruction of the anterior inferior
1125 tibiofibular ligament for chronic disruption of the distal tibiofibular syndesmosis. Knee Surgery, Sport.
1126 Traumatol. Arthrosc. 19(4):691–695.

1127 167. Lee SH, Kim ES, Lee YK, et al. 2015. Arthroscopic Syndesmotic Repair. Foot Ankle Int. 36(2):229–
1128 231.

1129 168. Van Heest TJ, Lafferty PM. 2014. Injuries to the ankle syndesmosis. J. Bone Jt. Surg. - Ser. A
1130 96(7):603–613.

1131 169. Lambers KT, van den Bekerom MP, Doornberg JN, et al. 2013. Long-Term Outcome of Pronation-
1132 External Rotation Ankle Fractures Treated with Syndesmotic Screws Only. J. Bone Jt. Surgery-American
1133 Vol. 95(17):e122-1–7.

1134 170. Symeonidis PD, Iselin LD, Chehade M, Stavrou P. 2013. Common Pitfalls in Syndesmotic Rupture
1135 Management. Foot Ankle Int. 34(3):345–350.

1136 171. Wikerøy AKB, Høiness PR, Andreassen GS, et al. 2010. No Difference in Functional and
1137 Radiographic Results 8.4 years after quad vs tricortical syndesmosis fixation in ankle fractures. J. Orthop.
1138 Trauma 24(1):17–23.

1139 172. Høiness P, Strømsøe K. 2004. Tricortical Versus Quadricortical Syndesmosis Fixation in Ankle
1140 Fractures. J. Orthop. Trauma 18(6):331–337.

1141 173. McBryde A, Chiasson B, Wilhelm A, et al. 1997. Syndesmotic Screw Placement: A Biomechanical
1142 Analysis. Foot Ankle Int. 18(5):262–266.

1143 174. Miller RS, Weinhold PS, Dahners LE. 1999. Comparison of Tricortical Screw Fixation Versus a
1144 Modified Suture Construct for Fixation of Ankle Syndesmosis Injury: A Biomechanical Study. J. Orthop.
1145 Trauma 13(1):39–42.

1146 175. Verim O, Serhan Er M, Altinel L, Tasgetiren S. 2014. Biomechanical Evaluation of Syndesmotic
1147 Screw Position: A Finite-Element Analysis. J. Orthop. Trauma 28(4):210–215.

1148 176. Albers GH, de Kort AF, Middendorf PR, van Dijk CN. 1996. Distal tibiofibular synostosis after ankle
1149 fracture. A 14-year follow-up study. J. Bone Joint Surg. Br. 78(2):250–2.

1150 177. Sproule JA, Khalid M, O'Sullivan M, McCabe JP. 2004. Outcome after surgery for Maisonneuve
1151 fracture of the fibula. Injury 35(8):791–798.

1152 178. Kukreti S, Faraj A, Miles JNV. 2005. Does position of syndesmotic screw affect functional and
1153 radiological outcome in ankle fractures? Injury 36(9):1121–1124.

1154 179. Stuart K, Panchbhavi VK. 2011. The Fate of Syndesmotic Screws. Foot Ankle Int. 32(5):519–525.

1155 180. Thompson MC, Gesink DS. 2000. Biomechanical Comparison of Syndesmosis Fixation with 3.5-
1156 and 4.5-millimeter Stainless Steel Screws. Foot Ankle Int. 21(9):736–741.

1157 181. Fort NM, Aiyer AA, Kaplan JR, et al. 2017. Management of acute injuries of the tibiofibular
1158 syndesmosis. Eur. J. Orthop. Surg. Traumatol. 27(4).

182. Markolf KL, Jackson SR, McAllister DR. 2013. Syndesmosis Fixation Using Dual 3.5 mm and 4.5 mm Screws With Tricortical and Quadricortical Purchase. Foot Ankle Int. 34(5):734–739.

183. Amendola A. 1992. Controversies in Diagnosis and Management of Syndesmosis Injuries of the Ankle. Foot Ankle 13(1):44–50.

184. Nousiainen MT, McConnell AJ, Zdero R, et al. 2008. The Influence of the Number of Cortices of Screw Purchase and Ankle Position in Weber C Ankle Fracture Fixation. J. Orthop. Trauma 22(7):473–478.

185. Moore JA, Shank JR, Morgan SJ, Smith WR. 2006. Syndesmosis Fixation: A Comparison of Three and Four Cortices of Screw Fixation Without Hardware Removal. Foot Ankle Int. 27(8):567–572.

186. Karapinar H, Kalenderer O, Karapinar L, et al. 2007. Effects of Three- or Four-Cortex Syndesmotic Fixation in Ankle Fractures. J. Am. Podiatr. Med. Assoc. 97(6):457–459.

187. Liu G, Chen L, Gong M, et al. 2019. Clinical Evidence for Treatment of Distal Tibiofibular Syndesmosis Injury: A Systematic Review of Clinical Studies. J. Foot Ankle Surg. 58(6):1245–1250.

188. Schepers T. 2011. To retain or remove the syndesmotic screw: A review of literature. Arch. Orthop. Trauma Surg. 131(7):879–883.

189. Manjoo A, Sanders DW, Tieszer C, MacLeod MD. 2010. Functional and radiographic results of patients with syndesmotic screw fixation: Implications for screw removal. J. Orthop. Trauma 24(1):2–6.

190. Melvin JS, Downing KL, Ogilvie CM. 2008. A Technique for Removal of Broken Cannulated Tricortical Syndesmotic Screws. J. Orthop. Trauma 22(9):648–651.

191. Beumer A, Campo MM, Niesing R, et al. 2005. Screw fixation of the syndesmosis: A cadaver model comparing stainless steel and titanium screws and three and four cortical fixation. Injury 36(1):60–64.

192. van der Eng DM, Schep NWL, Schepers T. 2015. Bioabsorbable Versus Metallic Screw Fixation for Tibiofibular Syndesmotic Ruptures: A Meta-Analysis. J. Foot Ankle Surg. 54(4):657–662.

193. Ahmad J, Raikin SM, Pour AE, Haytmanek C. 2009. Bioabsorbable Screw Fixation of the Syndesmosis in Unstable Ankle Injuries. Foot Ankle Int. 30(02):99–105.

194. Böstman OM, Laitinen OM, Tynninen O, et al. 2005. Tissue restoration after resorption of polyglycolide and poly-laevo-lactic acid screws. J. Bone Joint Surg. Br. 87-B(11):1575–1580.

195. Cox S, Mukherjee D, Ogden A, et al. 2005. Distal tibiofibular syndesmosis fixation: a cadaveric, simulated fracture stabilization study comparing bioabsorbable and metallic single screw fixation. J. Foot Ankle Surg. 44(2):144–151.

196. Sun H, Luo CF, Zhong B, et al. 2014. A prospective, randomised trial comparing the use of absorbable and metallic screws in the fixation of distal tibiofibular syndesmosis injuries. Bone Joint J. 96-B(4):548–554.

197. Thordarson DB, Samuelson M, Shepherd LE, et al. 2001. Bioabsorbable Versus Stainless Steel Screw Fixation of the Syndesmosis in Pronation-Lateral Rotation Ankle Fractures: A Prospective Randomized Trial. Foot Ankle Int. 22(4):335–338.

198. Kaukonen JP, Lamberg T, Korkala O, Pajarinen J. 2005. Fixation of Syndesmotic Ruptures in 38 Patients With a Malleolar Fracture:A Randomized Study Comparing a Metallic and a Bioabsorbable Screw. J. Orthop. Trauma 19(6):392–395.

199. Böstman OM, Pihlajamäki HK. 2000. Adverse tissue reactions to bioabsorbable fixation devices. Clin. Orthop. Relat. Res. (371):216–227.

200. Frøkjær J, Møller BN. 1992. Biodegradable fixation of ankle fractures: Complications in a prospective study of 25 cases. Acta Orthop. 63(4):434–436.

201. Seitz WH, Bachner EJ, Abram LJ, et al. 1991. Repair of the tibiofibular syndesmosis with a flexible implant. J. Orthop. Trauma 5(1):78–82.

202. Schon JM, Williams BT, Venderley MB, et al. 2017. A 3-D CT Analysis of Screw and Suture-Button Fixation of the Syndesmosis. Foot Ankle Int. 38(2):208–214.

203. Soin SP, Knight TA, Dinah AF, et al. 2009. Suture-Button versus Screw Fixation in a Syndesmosis Rupture Model: A Biomechanical Comparison. Foot Ankle Int. 30(4):346–352.

204. Thornes B, Walsh A, Hislop M, et al. 2003. Suture-Endobutton Fixation of Ankle Tibio-Fibular Diastasis: A Cadaver Study. Foot Ankle Int. 24(2):142–146.

205. Benhardt HA, Cosgriff-Hernandez EM. 2009. The Role of Mechanical Loading in Ligament Tissue Engineering. Tissue Eng. Part B Rev. 15(4):467–475.

206. Thornton GM, Shrive NG, Frank CB. 2003. Healing ligaments have decreased cyclic modulus compared to normal ligaments and immobilization further compromises healing ligament response to cyclic loading. J. Orthop. Res. 21(4):716–722.

207. Hildebrand KA, Frank CB. 1998. Scar formation and ligament healing. Can. J. Surg. 41(6):425–429.

208. Lubberts B, Vopat BG, Wolf JC, et al. 2017. Arthroscopically measured syndesmotic stability after screw vs. suture button fixation in a cadaveric model. Injury 48(11):2433–2437.

209. Forsythe K, Freedman KB, Stover MD, Patwardhan AG. 2008. Comparison of a Novel FiberWire-Button Construct versus Metallic Screw Fixation in a Syndesmotic Injury Model. Foot Ankle Int. 29(1):49–54.

210. Laflamme M, Belzile EL, Bedard L, et al. 2015. A prospective randomized multicenter trial comparing clinical outcomes of patients treated surgically with a static or dynamic implant for acute ankle syndesmosis rupture. J. Orthop. Trauma 29(5):216–223.

211. Naqvi GA, Cunningham P, Lynch B, et al. 2012. Fixation of ankle syndesmotic injuries: Comparison of tightrope fixation and syndesmotic screw fixation for accuracy of syndesmotic reduction. Am. J. Sports Med. 40(12):2828–2835.

212. Sanders D, Schneider P, Taylor M, et al. 2019. Improved Reduction of the Tibiofibular Syndesmosis with Tightrope Compared to Screw Fixation: Results of a Randomized Controlled Study. J. Orthop. Trauma 3(3):2473011418S0012.

213. Andersen MR, Frihagen F, Hellund JC, et al. 2018. Randomized trial comparing suture button with single syndesmotic screw for syndesmosis injury. J. Bone Jt. Surg. - Am. Vol. 100(1):2–12.

214. Coetzee JC, Ortho M. 2009. Treatment of syndesmoses disruptions: A prospective, randomized study comparing conventional screw fixation vs TightRope® fiber wire fixation - medium term results. SA Orthop. J. 8(1):32–37.

1234 215. Colcuc C, Blank M, Stein T, et al. 2018. Lower complication rate and faster return to sports in
1235 patients with acute syndesmotic rupture treated with a new knotless suture button device. Knee Surgery,
1236 Sport. Traumatol. Arthrosc. 26(10):3156–3164.

1237 216. Seyhan M, Donmez F, Mahirogullari M, et al. 2015. Comparison of screw fixation with elastic
1238 fixation methods in the treatment of syndesmosis injuries in ankle fractures. Injury 46(S2):S19–S23.

1239 217. Shimozono Y, Hurley ET, Myerson CL, et al. 2019. Suture Button Versus Syndesmotic Screw for
1240 Syndesmosis Injuries: A Meta-analysis of Randomized Controlled Trials. Am. J. Sports Med. 47(11):2764–
1241 2771.

1242 218. Onggo JR, Nambiar M, Phan K, et al. 2020. Suture button versus syndesmosis screw constructs for
1243 acute ankle diastasis injuries: A meta-analysis and systematic review of randomised controlled trials. Foot
1244 Ankle Surg. 26(1):54–60.

1245 219. Grassi A, Samuelsson K, D'Hooghe P, et al. 2019. Dynamic Stabilization of Syndesmosis Injuries
1246 Reduces Complications and Reoperations as Compared With Screw Fixation: A Meta-analysis of
1247 Randomized Controlled Trials. Am. J. Sports Med. :1000–1013.

1248 220. Westermann RW, Rungprai C, Goetz JE, et al. 2014. The Effect of Suture-Button Fixation on
1249 Simulated Syndesmotic Malreduction: A Cadaveric Study. J. Bone Jt. Surgery-American Vol. 96(20):1732–
1250 1738.

1251 221. DeGroot H, Al-Omari AA, Ghazaly SA El. 2011. Outcomes of Suture Button Repair of the Distal
1252 Tibiofibular Syndesmosis. Foot Ankle Int. 32(3):250–256.

1253 222. Thornes B, Shannon F, Guiney A-MM, et al. 2005. Suture-button syndesmosis fixation: Accelerated
1254 rehabilitation and improved outcomes. Clin. Orthop. Relat. Res. (431):207–212.

1255 223. Solan MC, Sakellariou A. 2017. Posterior malleolus fractures: Worth fixing. Bone Jt. J.
1256 99B(11):1413–1419.

1257 224. Odak S, Ahluwalia R, Unnikrishnan P, et al. 2016. Management of Posterior Malleolar Fractures:
1258 A Systematic Review. J. Foot Ankle Surg. 55(1):140–145.

1259 225. Gardner MJ, Brodsky A, Briggs SM, et al. 2006. Fixation of posterior malleolar fractures provides
1260 greater syndesmotic stability. Clin. Orthop. Relat. Res. (447):165–171.

1261 226. Miller AN, Carroll EA, Parker RJ, et al. 2010. Posterior Malleolar Stabilization of Syndesmotic
1262 Injuries is Equivalent to Screw Fixation. Clin. Orthop. Relat. Res. 468(4):1129–1135.

1263 227. Hooper J. 1983. Movement at the ankle joint after driving a screw across the inferior tibiofibular
1264 joint. Injury 14(6):493–506.

1265 228. Boyle MJ, Gao R, Frampton CMA, Coleman B. 2014. Removal of the syndesmotic screw after the
1266 surgical treatment of a fracture of the ankle in adult patients does not affect one-year outcomes: A
1267 randomised controlled trial. Bone Jt. J. 96B(12):1699–1705.

1268 229. Bell DP, Wong MK. 2006. Syndesmotic screw fixation in Weber C ankle injuries-should the screw
1269 be removed before weight bearing? Injury 37(9):891–898.

1270 230. Dingemans SA, Rammelt S, White TO, et al. 2016. Should syndesmotic screws be removed after
1271 surgical fixation of unstable ankle fractures? a systematic review. Bone Jt. J. 98-B(11):1497–1504.

1272 231. Mendelsohn ES, Hoshino CM, Harris TG, Zinar DM. 2013. The Effect of Obesity on Early Failure
1273 After Operative Syndesmosis Injuries. J. Orthop. Trauma 27(4):201–206.

1274 232. Song DJ, Lanzi JT, Groth AT, et al. 2014. The effect of syndesmosis screw removal on the reduction
1275 of the distal tibiofibular joint: A prospective radiographic study. Foot Ankle Int. 35(6):543–548.

1276 233. Hsu Y-T, Wu C-C, Lee W-C, et al. 2011. Surgical treatment of syndesmotic diastasis: emphasis on
1277 effect of syndesmotic screw on ankle function. Int. Orthop. 35(3):359–64.

1278 234. Schepers T, Van Lieshout EMM, de Vries MR, Van der Elst M. 2011. Complications of Syndesmotic
1279 Screw Removal. Foot Ankle Int. 32(11):1040–1044.

1280 235. Andersen MR, Frihagen F, Madsen JE, Figved W. 2015. High complication rate after syndesmotic
1281 screw removal. Injury 46(11):2283–2287.

1282 236. Tucker A, Street J, Kealey D, et al. 2013. Functional outcomes following syndesmotic fixation: A
1283 comparison of screws retained in situ versus routine removal - Is it really necessary? Injury 44(12):1880–
1284 1884.

1285 237. Lalli TAJ, Matthews LJ, Hanselman AE, et al. 2015. Economic impact of syndesmosis hardware
1286 removal. Foot 25(3):131–133.

1287 238. Ramsey DC, Friess DM. 2018. Cost-Effectiveness Analysis of Syndesmotic Screw Versus Suture
1288 Button Fixation in Tibiofibular Syndesmotic Injuries. J. Orthop. Trauma 32(6):e198–e203.

1289 239. Neary KC, Mormino MA, Wang H. 2017. Suture Button Fixation Versus Syndesmotic Screws in
1290 Supination-External Rotation Type 4 Injuries. Am. J. Sports Med. 45(1):210–217.

1291 240. Hodgson P, Thomas R. 2011. Avoiding Suture Knot Prominence With Suture Button Along Distal
1292 Fibula: Technical Tip. Foot Ankle Int. 32(9):908–909.

1293 241. Peterson KS, Chapman WD, Hyer CF, Berlet GC. 2015. Maintenance of Reduction With Suture
1294 Button Fixation Devices for Ankle Syndesmosis Repair. Foot Ankle Int. 36(6):679–684.

1295 242. Zhang P, Liang Y, He J, et al. 2017. A systematic review of suture-button versus syndesmotic screw
1296 in the treatment of distal tibiofibular syndesmosis injury. BMC Musculoskelet. Disord. 18(1):1–12.

1297 243. Fantry AJ, O'Donnell SW, Born CT, Hayda RA. 2017. Deep Infections After Syndesmotic Fixation
1298 With a Suture Button Device. Orthopedics 40(3):e541–e545.

1299 244. Hong CC, Lee WT, Tan KJ. 2015. Osteomyelitis After TightRope® Fixation of the Ankle Syndesmosis:
1300 A Case Report and Review of the Literature. J. Foot Ankle Surg. 54(1):130–134.

1301 245. Storey P, Gadd RJ, Blundell C, Davies MB. 2012. Complications of Suture Button Ankle Syndesmosis
1302 Stabilization with Modifications of Surgical Technique. Foot Ankle Int. 33(9):717–721.

1303 246. Rigby RB, Cottom JM. 2013. Does the arthrex tightrope® provide maintenance of the distal
1304 tibiofibular syndesmosis? A 2-year follow-up of 64 tightropes® in 37 patients. J. Foot Ankle Surg.
1305 52(5):563–567.

1306 247. Inge SY, Pull ter Gunne AF, Aarts CAM, Bemelman M. 2016. A systematic review on dynamic versus
1307 static distal tibiofibular fixation. Injury 47(12):2627–2634.

1308 248. Taylor DC, Englehardt DL, Bassett FH. 1992. Syndesmosis sprains of the ankle. The influence of
1309 heterotopic ossification. Am. J. Sports Med. 20(2):146–50.

1310 249. Hinds RM, Lazaro LE, Burket JC, Lorich DG. 2014. Risk factors for posttraumatic synostosis and
1311 outcomes following operative treatment of ankle fractures. Foot Ankle Int. 35(2):141–147.

1312 250. Hohman DW, Affonso J, Marzo JM, Ritter CA. 2011. Pathologic Tibia/Fibula Fracture Through a
1313 Suture Button Screw Tract. Am. J. Sports Med. 39(3):645–648.

1314 251. M C, M B, G M, T K. 2011. Distal tibial fracture post syndesmotic screw removal: an adverse
1315 complication. Arch. Orthop. Trauma Surg. 131(10):1405–1408.

1316 252. Clarke M, Covey DC. 2010. Stress fracture of the distal tibia following syndesmosis screw removal.
1317 Curr. Orthop. Pract. 21(2):E8–E12.

1318 253. Kwon JY, Campbell JT, Myerson MS. 2012. Posterior Tibial Tendon Tear After 4-Cortex
1319 Syndesmotic Screw Fixation. J. Orthop. Trauma 26(6):e66–e69.

1320 254. Welck MJ, Ray P. 2013. Tibialis Anterior Tendon Entrapment After Ankle Tightrope Insertion for
1321 Acute Syndesmosis Injury. Foot Ankle Spec. 6(3):242–246.

1322 255. Nussbaum ED, Hosea TM, Sieler SD, et al. 2001. Prospective Evaluation of Syndesmotic Ankle
1323 Sprains without Diastasis. Am. J. Sports Med. 29(1):31–35.

1324 256. Vopat ML, Vopat BG, Lubberts B, DiGiovanni CW. 2017. Current trends in the diagnosis and
1325 management of syndesmotic injury. Curr. Rev. Musculoskelet. Med. 10(1):94–103.

1326 257. Ryan PM, Rodriguez RM. 2016. Outcomes and Return to Activity After Operative Repair of Chronic
1327 Latent Syndesmotic Instability. Foot Ankle Int. 37(2):192–197.

1328 258. Schuberth JM, Jennings MM, Lau AC. 2008. Arthroscopy-Assisted Repair of Latent Syndesmotic
1329 Instability of the Ankle. Arthrosc. J. Arthrosc. Relat. Surg. 24(8):868–874.

1330 259. Kitaoka HB, Alexander IJ, Adelaar RS, et al. 1994. Clinical Rating Systems for the Ankle-Hindfoot,
1331 Midfoot, Hallux, and Lesser Toes. Foot Ankle Int. 15(7):349–353.

1332 260. Ceccarelli F, Calderazzi F, Pedrazzi G. 2014. Is There a Relation between AOFAS Ankle-Hindfoot
1333 Score and SF-36 in Evaluation of Achilles Ruptures Treated by Percutaneous Technique? J. Foot Ankle Surg.
1334 53(1):16–21.

1335 261. Egol KA, Tejwani NC, Walsh MG, et al. 2006. Predictors of Short-Term Functional Outcome
1336 Following Ankle Fracture Surgery. J. Bone Jt. Surg. 88(5):974–979.

1337 262. Stufkens SAS, Van Den Bekerom MPJ, Kerkhoffs GMMJ, et al. 2011. Long-term outcome after 1822
1338 operatively treated ankle fractures: A systematic review of the literature. Injury 42(2):119–127.

1339 263. Shah NH, Sundaram RO, Velusamy A, Braithwaite IJ. 2007. Five-year functional outcome analysis
1340 of ankle fracture fixation. Injury 38(11):1308–1312.

1341 264. Day GA, Swanson CE, Hulcombe BG. 2001. Operative treatment of ankle fractures: A minimum
1342 ten-year follow-up. Foot Ankle Int. 22(2):102–106.

1343 265. Michelson JD, Wright M, Blankstein M. 2018. Syndesmotic ankle fractures. J. Orthop. Trauma
1344 32(1).

1345 266. Thordarson DB, Motamed S, Hedman T, et al. 1997. The effect of fibular malreduction on contact
1346 pressures in an ankle fracture malunion model. J. Bone Jt. Surg. - Ser. A 79(12 79A):1809–1815.

1347 267. Rigby RB, Cottom JM. 2013. Does the Arthrex TightRope® Provide Maintenance of the Distal
1348 Tibiofibular Syndesmosis? A 2-year Follow-up of 64 TightRopes® in 37 Patients. J. Foot Ankle Surg.
1349 52(5):563–567.

1350 268. Curtis MJ, Michelson JD, Urquhart MW, et al. 1992. Tibiotalar contact and fibular malunion in
1351 ankle fractures A cadaver study. Acta Orthop. Scand. 63(3):326–329.

1352 269. Pang EQ, Bedigrew K, Palanca A, et al. 2019. Ankle joint contact loads and displacement in
1353 syndesmosis injuries repaired with Tightropes compared to screw fixation in a static model. Injury
1354 50(11):1901–1907.

1355 270. Ray R, Koohnejad N, Clement ND, Keenan GF. 2019. Ankle fractures with syndesmotic stabilisation
1356 are associated with a high rate of secondary osteoarthritis. Foot Ankle Surg. 25(2):180–185.

1357 271. Tochigi Y, Rudert MJ, McKinley TO, et al. 2008. Correlation of dynamic cartilage contact stress
1358 aberrations with severity of instability in ankle incongruity. J. Orthop. Res. 26(9):1186–1193.

1359 272. McKinley TO, Tochigi Y, Rudert MJ, Brown TD. 2008. Instability-Associated Changes in Contact
1360 Stress and Contact Stress Rates Near a Step-Off Incongruity. J. Bone Jt. Surg. 90(2):375–383.

1361 273. Chissell HR, Jones J. 1995. The influence of a diastasis screw on the outcome of Weber type-C
1362 ankle fractures. J. Bone Jt. Surg. - Ser. B 77(3):435–438.

1363 274. Harper MC. 1984. Instability of the distal tibiofibular syndesmosis after bimalleolar and
1364 trimalleolar ankle fractures. J. Bone Jt. Surg. - Ser. A 66(8):1319–1320.

1365 275. Futamura K, Baba T, Mogami A, et al. 2017. Malreduction of syndesmosis injury associated with
1366 malleolar ankle fracture can be avoided using Weber's three indexes in the mortise view. Injury 48(4).

1367 276. Phisitkul P, Ebinger T, Goetz J, et al. 2012. Forceps reduction of the syndesmosis in rotational ankle
1368 fractures: A cadaveric study. J. Bone Jt. Surg. - Ser. A 94(24):2256–2261.

1369 277. Yamaguchi K, Martin CH, Boden SD, Labropoulos PA. 1994. Operative Treatment of Syndesmotic
1370 Disruptions Without Use of a Syndesmotic Screw: A Prospective Clinical Study. Foot Ankle Int. 15(8):407–
1371 414.

1372 278. Hovis WD, Kaiser BW, Watson JT, Bucholz RW. 2002. Treatment of Syndesmotic Disruptions of the
1373 Ankle with Bioabsorbable Screw Fixation. J. Bone Jt. Surgery-American Vol. 84(1):26–31.

1374 279. Miller AN, Carroll EA, Parker RJ, et al. 2009. Direct Visualization for Syndesmotic Stabilization of
1375 Ankle Fractures. Foot Ankle Int. 30(05):419–426.

1376 280. van den Heuvel SB, Dingemans SA, Gardenbroek TJ, Schepers T. 2019. Assessing Quality of
1377 Syndesmotic Reduction in Surgically Treated Acute Syndesmotic Injuries: A Systematic Review. J. Foot
1378 Ankle Surg. 58(1):144–150.

1379 281. Andersen MR, Diep LM, Frihagen F, et al. 2019. Importance of Syndesmotic Reduction on Clinical
1380 Outcome after Syndesmosis Injuries. J. Orthop. Trauma 33(8):397–403.

1381 282. Warner SJ, Fabricant PD, Garner MR, et al. 2015. The Measurement and Clinical Importance of
1382 Syndesmotic Reduction After Operative Fixation of Rotational Ankle Fractures. J. Bone Jt. Surg.
1383 97(23):1935–1944.

1384 283. Kocadal O, Yucel M, Pepe M, et al. 2016. Evaluation of Reduction Accuracy of Suture-Button and
1385 Screw Fixation Techniques for Syndesmotic Injuries. Foot Ankle Int. 37(12):1317–1325.

1386 284. Prior CP, Widnall JC, Rehman AK, et al. 2017. A simplified, validated protocol for measuring fibular
1387 reduction on ankle CT. Foot Ankle Surg. 23(1):53–56.

1388 285. HC L, MG E. 1984. Instability of the distal tibiofibular syndesmosis after bimalleolar and
1389 trimalleolar ankle fractures. J. Bone Joint Surg. Am. 66(4):490–503.

1390 286. Slobogean GP, Younger A, Apostle KL, et al. 2010. Preference-based quality of life of end-stage
1391 ankle arthritis treated with arthroplasty or arthrodesis. Foot Ankle Int. 31(7):563–566.

1392 287. Loizou CL, Sudlow A, Collins R, et al. 2017. Radiological assessment of ankle syndesmotic
1393 reduction. Foot 32:39–43.

1394 288. Grenier S, Benoit B, Rouleau DM, et al. 2013. APTF: Anteroposterior tibiofibular ratio, a new
1395 reliable measure to assess syndesmotic reduction. J. Orthop. Trauma 27(4):207–211.

1396 289. Koenig SJ, Tornetta P, Merlin G, et al. 2015. Can We Tell if the Syndesmosis Is Reduced Using
1397 Fluoroscopy? J. Orthop. Trauma 29(9):e326–e330.

1398 290. Franke J, von Recum J, Suda AJ, et al. 2014. Predictors of a Persistent Dislocation After Reduction
1399 of Syndesmotic Injuries Detected With Intraoperative Three-Dimensional Imaging. Foot Ankle Int.
1400 35(12):1323–1328.

1401 291. Franke J, Recum J Von, Suda AJ, et al. 2012. Intraoperative 3D imaging in the treatment of unstable
1402 syndesmotic injuries. J. Bone Jt. Surg. 94(15):1386.

1403 292. Davidovitch RI, Weil Y, Karia R, et al. 2013. Intraoperative syndesmotic reduction: Three-
1404 dimensional versus standard fluoroscopic imaging. J. Bone Jt. Surg. 95(20):1838–1843.

1405 293. Ruan Z, Luo C, Shi Z, et al. 2011. Intraoperative reduction of distal tibiofibular joint aided by three-
1406 dimensional fluoroscopy. Technol. Heal. Care 19(3):161–166.

1407 294. Richter M, Zech S. 2009. Intraoperative 3-Dimensional Imaging in Foot and Ankle Trauma-
1408 Experience With a Second-Generation Device (ARCADIS-3D). J. Orthop. Trauma 23(3):213–220.

1409 295. Richter M, Geerling J, Zech S, et al. 2005. Intraoperative Three-Dimensional Imaging With a
1410 Motorized Mobile C-Arm (SIREMOBIL ISO-C-3D) in Foot and Ankle Trauma Care. J. Orthop. Trauma
1411 19(4):259–266.

1412 296. Kendoff D, Citak M, Gardner MJ, et al. 2009. Intraoperative 3D Imaging: Value and Consequences
1413 in 248 Cases. J. Trauma Inj. Infect. Crit. Care 66(1):232–238.

1414 297. Atesok K, Finkelstein J, Khoury A, et al. 2007. The use of intraoperative three-dimensional imaging
1415 (ISO-C-3D) in fixation of intraarticular fractures. Injury 38(10):1163–1169.

1416 298. Kennedy MT, Carmody O, Leong S, et al. 2014. A computed tomography evaluation of two
1417 hundred normal ankles, to ascertain what anatomical landmarks to use when compressing or placing an
1418 ankle syndesmosis screw. Foot 24(4):157–160.

1419 299. Putnam SM, Linn MS, Spraggs-Hughes A, et al. 2017. Simulating clamp placement across the trans-
1420 syndesmotic angle of the ankle to minimize malreduction: A radiological study. Injury 48(3):770–775.

1421 300. Cosgrove CT, Spraggs-Hughes AG, Putnam SM, et al. 2018. A novel indirect reduction technique
1422 in ankle syndesmotic injuries: A cadaveric study. J. Orthop. Trauma 32(7):361–367.

1423 301. Miller AN, Barei DP, Iaquinto JM, et al. 2013. Iatrogenic syndesmosis malreduction via clamp and
1424 screw placement. J. Orthop. Trauma 27(2):100–106.

1425 302. Cosgrove CT, Putnam SM, Cherney SM, et al. 2017. Medial Clamp Tine Positioning Affects Ankle
1426 Syndesmosis Malreduction. In: Journal of Orthopaedic Trauma. p 440–446.

1427 303. Schon JM, Mikula JD, Backus JD, et al. 2017. 3D Model Analysis of Ankle Flexion on Anatomic
1428 Reduction of a Syndesmotic Injury. Foot Ankle Int. 38(4):436–442.

1429 304. Mahapatra P, Rudge B, Whittingham-Jones P. 2018. Is It Possible to Overcompress the
1430 Syndesmosis? J. Foot Ankle Surg. 57(5):1005–1009.

1431 305. Park YH, Ahn JH, Choi GW, Kim HJ. 2018. Comparison of Clamp Reduction and Manual Reduction
1432 of Syndesmosis in Rotational Ankle Fractures: A Prospective Randomized Trial. J. Foot Ankle Surg.
1433 57(1):19–22.

1434 306. Haynes J, Cherney S, Spraggs-Hughes A, et al. 2016. Increased Reduction Clamp Force Associated
1435 With Syndesmotic Overcompression. Foot Ankle Int. 37(7):722–729.

1436 307. Cherney SM, Haynes JA, Spraggs-Hughes AG, et al. 2015. In Vivo Syndesmotic Overcompression
1437 After Fixation of Ankle Fractures With a Syndesmotic Injury. J. Orthop. Trauma 29(9):414–9.

1438 308. Morellato J, Louati H, Bodrogi A, et al. 2017. The Effect of Varying Tension of a Suture Button
1439 Construct in Fixation of the Tibiofibular Syndesmosis - Evaluation Using Stress Computed Tomography. J.
1440 Orthop. Trauma 31(2):103–110.

1441 309. Pelton K, Thordarson DB, Barnwell J. 2010. Open versus closed treatment of the fibula in
1442 Maissoneuve injuries. Foot Ankle Int. 31(7):604–608.

1443 310. Dubois-Ferrière V, Gamulin A, Chowdhary A, et al. 2016. Syndesmosis reduction by computer-
1444 assisted orthopaedic surgery with navigation: Feasibility and accuracy in a cadaveric study. Injury
1445 47(12):2694–2699.

1446 311. Nault ML, Marien M, Hébert-Davies J, et al. 2017. MRI Quantification of the Impact of Ankle
1447 Position on Syndesmosis Anatomy. Foot Ankle Int. 38(2):215–219.

1448 312. Kwong Y, Mel AO, Wheeler G, Troupis JM. 2015. Four-dimensional computed tomography (4DCT):
1449 A review of the current status and applications. J. Med. Imaging Radiat. Oncol. 59(5):545–554.

1450 313. Gondim Teixeira PA, Gervaise A, Louis M, et al. 2015. Musculoskeletal Wide-Detector CT
1451 Kinematic Evaluation: From Motion to Image. Semin. Musculoskelet. Radiol. 19(05):456–462.

1452 314. Hu H. 1999. Multi-slice helical CT: Scan and reconstruction. Med. Phys. 26(1):5–18.

1453 315. Hurlock GS, Higashino H, Mochizuki T. 2009. History of cardiac computed tomography: Single to
1454 320-detector row multislice computed tomography. Int. J. Cardiovasc. Imaging 25(SUPPL. 1):31–42.

1455 316. Hsiao EM, Rybicki FJ, Steigner M. 2010. CT Coronary Angiography: 256-Slice and 320-Detector Row
1456 Scanners. Curr. Cardiol. Rep. 12(1):68–75.

1457 317. Wassilew GI, Janz V, Heller MO, et al. 2013. Real time visualization of femoroacetabular
1458 impingement and subluxation using 320-slice computed tomography. J. Orthop. Res. 31(2):275–281.

318. Gondim Teixeira PA, Formery A-S, Jacquot A, et al. 2017. Quantitative Analysis of Subtalar Joint Motion With 4D CT: Proof of Concept With Cadaveric and Healthy Subject Evaluation. Am. J. Roentgenol. 208(1):150–158.

319. Alta TD, Bell SN, Troupis JM, et al. 2012. The new 4-dimensional computed tomographic scanner allows dynamic visualization and measurement of normal acromioclavicular joint motion in an unloaded and loaded condition. J. Comput. Assist. Tomogr. 36(6):749–754.

320. Goh YP LK. 2012. Using the 320-Multidetector computed tomography scanner for four-dimensional functional assessment of the elbow joint. Am J Orthop . 41(2):E20-4.

321. Shores JT, Demehri S, Chhabra A. 2013. Kinematic “4 Dimensional” CT Imaging in the Assessment of Wrist Biomechanics Before and After Surgical Repair. Eplasty 13:e9.

322. Tanaka MJ, Elias JJ, Williams AA, et al. 2016. Characterization of patellar maltracking using dynamic kinematic CT imaging in patients with patellar instability. Knee Surgery, Sport. Traumatol. Arthrosc. 24(11):3634–3641.

323. Gondim Teixeira PA, Formery AS, Balazuc G, et al. 2019. Comparison between subtalar joint quantitative kinematic 4-D CT parameters in healthy volunteers and patients with joint stiffness or chronic ankle instability: A preliminary study. Eur. J. Radiol. 114(November 2018):76–84.

324. Yamaguchi S, Sasho T, Kato H, et al. 2009. Ankle and Subtalar Kinematics during Dorsiflexion-Plantarflexion Activities. Foot Ankle Int. 30(4):361–366.

3. Four-Dimensional Computed Tomography: Musculoskeletal Applications

3.1. Introduction

3.1.1. CT Technology

CT has advanced substantially since its introduction in the 1970's. The first CT scanners had limited resolution (matrix size 80x80), higher radiation (17mSv for a 6 slice CT head), and time consuming scanning and processing times (35 minutes).[1] However, improvements in hardware and imaging processing techniques have allowed CT to become ubiquitous in the medical field and the area of MSK health. Reduced ionizing radiation dose, rapid image acquisition speeds, and vastly improved image resolution has made CT the gold standard for diagnosis and treatment planning in many MSK conditions.[2] Multi-row detector CT (MDCT) scanners were introduced in 1999, which allowed the capture of multiple image slices at once by using adjacent detector rows along the gantry axis to detect a single x-ray source.[3] The gantry could complete a full rotation in 0.8 seconds and the field-of-view was 20mm along the axis of rotation. Gradual improvements in the technology reduced the time required for gantry rotation and increased the number of detector rows from four to a 320 row detector scanner which is currently available.[4] These modern scanners have the ability to image a 160mm field of view along the axis of rotation in under 0.3 seconds and further improvements are ongoing.[5]

3.1.2. 4DCT Development

With the introduction of wide field of view detector arrays and ultra-fast gantry rotation 4DCT, also known as dynamic CT or kinematic CT, has flourished over the last decade. By repeating the acquisition of the same volume with a single gantry rotation at multiple timepoints, a kinematic volume is created of the

subject's position at each time. Though technically possible since the advent of MDCT, small fields-of-view made the dynamic technique impractical. Further, slower gantry rotations made the images subject to motion artifact, and higher radiation doses made the practice unsafe for human participants. In contrast, recent techniques allow clinicians and researchers to capture large volumes in real time, with radiation exposure below that of a routine chest x-ray, depending on the anatomic region and acquisition protocol.[6,7]

3.1.3. Non-musculoskeletal Applications

Some of the first applications of 4DCT were in radiation oncology, especially for thoracic and abdominal tumors where lesions are shown to move with respiration. Quantifying this motion with 4DCT can allow for precise delivery of therapeutic radiation to the lesion.[8] 4DCT can also evaluate dynamic structures such as the heart by imaging the entire heart through the cardiac cycle to investigate flow and valvular pathology, and may be of utility in cases where echocardiography is technically challenging or for patients with MRI contraindications.[9] Vascular disease has been investigated with 4DCT, providing more information than conventional CT angiography, including the response of aneurysms to the cardiac cycle, giving new insight into disease progression risk.[10] With an increasing body of evidence for the safety and utility of 4DCT in these fields, more widespread adoption of the technology is occurring. Clinicians and researchers are realizing that 4DCT provides insight into dynamic phenomena not previously possible to image.

3.2. Musculoskeletal Applications

In the MSK field, questions regarding joint kinematics, instability, and impingement have all been addressed using 4DCT.

1523

1524 ### 3.2.1. Shoulder Girdle

1525 4DCT imaging has been used to image the sternoclavicular and acromioclavicular joints, as well as
1526 scapulothoracic motion in order to investigate shoulder instability and impingement. In the
1527 sternoclavicular joint, a case report describes visualization of the medial clavicle translating posteriorly
1528 with arm range of motion to abut the trachea in a patient who complained of an intermittent choking
1529 sensation.[11] 4DCT revealed this compression, which was not evident on conventional CT or MRI, and led
1530 to the decision to perform surgical stabilization with a good outcome.[11] 4DCT has also been used as a
1531 diagnostic tool to measure the degree of sternoclavicular joint instability based on translation during arm
1532 range of motion.[12] This information was used to recommend surgical versus conservative treatment with
1533 successful outcomes.[12] The acromioclavicular joint has also been imaged dynamically and revealed that
1534 cases of persistent pain with seemingly low grade injuries could be attributed to unexpectedly large
1535 translations with glenohumeral joint range of motion, giving a more accurate prognosis for functional
1536 impairment with and without reconstructive surgery of the joint.[13] In the acromioclavicular joint, 4DCT
1537 has provided normative data on uninjured joint motion and has also been able to detect pathologic
1538 motion in patients with uncertain diagnosis such as instability versus arthrosis via conventional
1539 examinations.[13,14] Clinicians have also used 4DCT to investigate snapping scapula syndrome. In the case of
1540 impingement of the scapula on the posterior ribs, preoperative 4DCT has allowed clinicians to determine
1541 the precise point of impingement to minimize unnecessary bone resection and to ensure the site of
1542 pathology is addressed.[15] These clinical applications of 4DCT improved diagnosis, prognostication, and
1543 informed surgical planning throughout the shoulder girdle.

1544

3.2.2. Elbow

To our knowledge, only one study has investigated the elbow using 4DCT. Work by Goh et al.[16] demonstrated a use for 4DCT imaging of the ulnohumeral joint in which 4DCT demonstrated impingement of osteophytes on the coronoid process and olecranon, preventing both terminal flexion and extension. These findings highlight the advantage 4DCT has over conventional CT to confirm restrictions in motion due to impingement, rather than capsular fibrosis or adhesions, as is common after elbow injuries. As the technology matures, further 4DCT investigations are warranted in the elbow.

3.2.3. Wrist

Within the wrist, numerous studies have made use of 4DCT to investigate carpal motion. Given that subtle changes can be responsible for functional limitations and severe symptoms, standard imaging methods including MRI often lack the required sensitivity for diagnosis.[17] Normal kinematics for the proximal carpus have been described as well as post surgical changes.[17–19] Mechanical symptoms, including the catching or clunking seen in trigger lunate syndrome, or instability, such as in scapholunate instability, have also been identified with 4DCT.[20–23] In these conditions, the mechanical cause of symptoms was only detected on dynamic imaging, without which appropriate treatment is challenging. The complexity of the carpal joints, coupled with the small field-of-view required and minimal radiosensitivity, make wrist pathology an ideal application for 4DCT and clinical indications for 4DCT continue to expand and evolve.

3.2.4. Hip

At present, there has been limited 4DCT examination of the hip joint, in part due to the high effective radiation dose from proximity to radiosensitive tissues and higher energy required for x-ray exposure.[2,24] However, one study has investigated femoroacetabular impingement and found that 4DCT more

accurately predicted the location of cam and pincer type impingement on the femur and acetabulum versus traditional radiographs or MRI, when compared to gold-standard surgical hip dislocation.[24] These findings demonstrate the benefits of 4DCT to allow surgeons to accurately plan minimally invasive interventions to remove the sites of impingement via hip arthroscopy, thus minimizing arthroscopy times and morbidity while improving the localization of required resection. It is expected that further use of 4DCT for understanding hip pathology will follow as newer image reconstruction methods and hardware are developed to reduce radiation exposure to the patient.

3.2.5. Knee

With respect to the knee, several studies have developed 4DCT acquisition protocols in order to analyse patellar tracking through knee range of motion to investigate patellofemoral pain syndrome and the nebulous etiology that is commonly related to patellar mal-tracking and subluxation.[25–27] 4DCT is well suited to investigate patellar tracking though knee range of motion in this patient population. When determining whether to perform a tibial tubercle osteotomy (TTO) versus medial patellofemoral ligament reconstruction, one group has demonstrated that tibial tubercle-trochlear groove distance (TTTG) varies significantly with knee flexion angle which is non-uniform on review of conventional imaging.[28] Their results show that 70% of symptomatic patients would qualify for TTO with the knee flexed to 30 degrees based on accepted TTTG thresholds versus only 24% of patients at 0 degrees.[28] Using dynamic imaging, quantitative and repeatable measures of instability and mal-tracking are possible which help to identify the etiology of patellofemoral pain, stratify patients, and select surgical candidates.[27–30]

3.2.6. Foot and Ankle

Multiple 4DCT studies have quantified subtalar joint motion and recent work has expanded into the distal tibiofibular joint. In the subtalar joint, 4DCT has demonstrated motion changes between healthy ankles and those with chronic instability symptoms or stiffness.[31] Dynamic imaging of the subtalar joint with the application of an external stress throughout a range of motion gives an objective measure of the etiology of instability. 4DCT can also measure patient response to therapy and motion patterns can be linked to specific injury patterns for precise treatment.[32] Motion at the distal tibiofibular joint, or syndesmosis, has also been reliably quantified with 4DCT.[33] Figure 3.1 demonstrates physiologic changes in syndesmotic distances with ankle range of motion which are important to appreciate when assessing reduction. Understanding physiologic motion at this joint is crucial for developing surgical repair techniques after ligamentous injury. Imaging throughout an active ROM can also compare fixation methods in order to further understand causes of residual functional impairment.

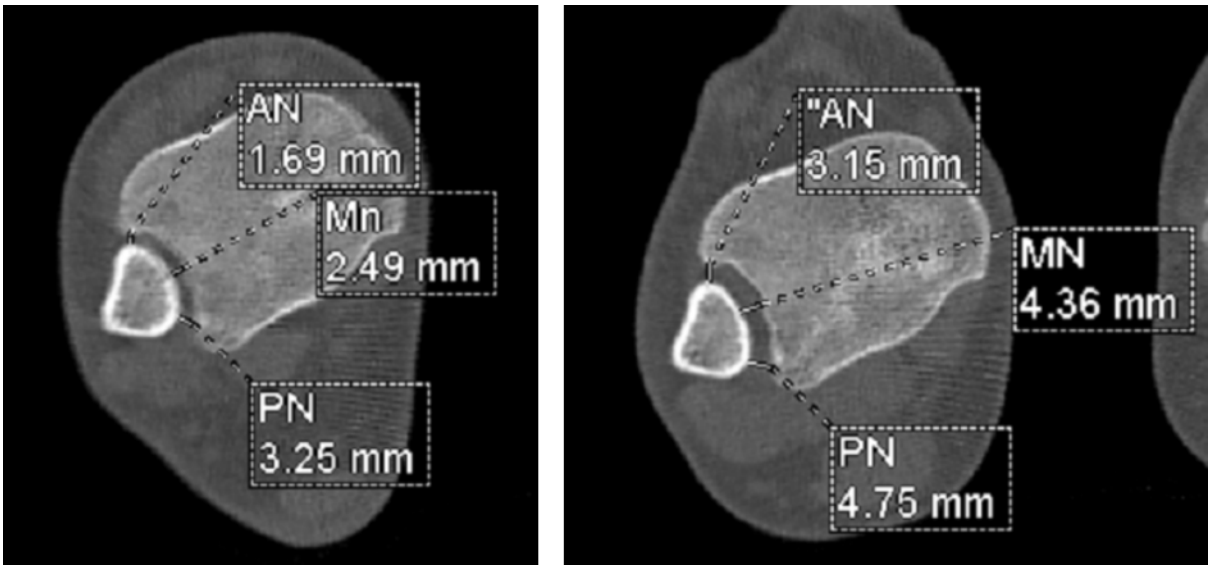

Figure 3.1: Syndesmotic reduction in plantarflexion (left) and dorsiflexion (right) as measured by the anterior (AN), middle (MN), and posterior (PN) syndesmotic distances.

3.3. Challenges and Future Directions

4DCT is a relatively new modality and continuous advancements are being made to this technology. It is anticipated that increasing availability and understanding of 4DCT will lead to an expansive scope for research and application to clinical practice.[34] Advances in field-of-view can be achieved through increasing the number of detector rows or increasing detector size.[4] However, the latter method would decrease axial resolution. Optimal acquisition protocols need to be determined to minimize dose and motion artifact without sacrificing resolution and the ability to track motions as desired.

Motion artifact is another challenge which ongoing work is dedicated to resolving. Recommendations have been made to design protocols to limit artifact by orienting the plane of motion optimally and promoting smooth patient motion through training, external cues, or custom devices to constrain range of motion or even simulate weightbearing conditions.[35–37] These recommendations regarding positioning and speed are not always feasible however as this motion must be achievable within the confined CT gantry and some phenomena are only observed under particular conditions. Half reconstruction methods use only one half of a gantry rotation to create an image, compared to a full rotation of projections. In dynamic applications this serves to improve motion artifact as well as reduce radiation exposure.[35] Other advancements such as implementation of scanners with dual x-ray source technology and increased gantry rotation speeds can also serve to reduce motion artifact.[35]

When investigating post-surgical motion, metal artifact from implants also poses significant challenges for image interpretation and processing. To date, no studies have incorporated metal suppression via dual-

energy CT into dynamic protocols, likely because dual-energy CT would decrease the temporal resolution and increase radiation dose. As a result, metal artifact reduction is currently limited to post-processing algorithms and manual correction, which requires increased user time and may reduce the accuracy of results.

Concerns of radiation exposure continue to limit the adoption of 4DCT exposure as well. In general, the more proximal the area to be imaged, the higher effective radiation dose.[2] Improvements continue to be made in x-ray source hardware and iterative reconstruction techniques to lower the dose produced by the source, while still maintaining image quality.[38]

Finally, 4DCT produces large data sets which result in substantial image processing time and effort, especially in the case of routine clinical adoption. Qualitative analysis of motion is possible and multiple manufacturers and software packages provide the ability to visualize three-dimensional reconstructions at each timepoint. However, quantitative analysis requires further post-processing with segmentation of individual bones and registration of these bones across timepoints. Currently, there are limited commercially available software packages which can semi-automate measurement and analysis protocols, but more work is required to make versatile tools available for ease of use and clinical implementation.

3.4. Conclusion

4DCT technology remains in its early phases but has promising clinical and research applicability in numerous areas, including diagnostic, prognostic, and surgical outcome assessment for many MSK

pathologies. As the technology matures and gains further adoption it can be applied to joint kinematics and the quantification of instability, mal-tracking, and impingement. Future work should focus on improving image quality and patient safety to enable wider adoption of the technology. Consequently, we can expect novel uses of 4DCT to create improvements in the diagnosis and treatment of a wide variety of MSK conditions.

3.5. References

1. Hounsfield, GN: Computerized transverse axial scanning (tomography): I. Description of system. *Br J Radiol* 1973;46:1016–1022.

2. Biswas, D, Bible, JE, Bohan, M, Simpson, AK, Whang, PG, Grauer, JN: Radiation exposure from musculoskeletal computerized tomographic scans. *J Bone Jt Surg - Ser A* 2009;91:1882–1889.

3. Hu, H: Multi-slice helical CT: Scan and reconstruction. *Med Phys* 1999;26:5–18.

4. Hurlock, GS, Higashino, H, Mochizuki, T: History of cardiac computed tomography: Single to 320-detector row multislice computed tomography. *Int J Cardiovasc Imaging* 2009;25:31–42.

5. Hsiao, EM, Rybicki, FJ, Steigner, M: CT Coronary Angiography: 256-Slice and 320-Detector Row Scanners. *Curr Cardiol Rep* 2010;12:68–75.

6. Gondim Teixeira, PA, Gervaise, A, Louis, M, Lecocq, S, Raymond, A, Aptel, S, Blum, A: Musculoskeletal wide detector CT: Principles, techniques and applications in clinical practice and research. *Eur J Radiol* 2015;84:892–900.

7. Kalia, V, Obray, RW, Filice, R, Fayad, LM, Murphy, K, Carrino, JA: Functional joint imaging using 256-MDCT: Technical feasibility. *Am J Roentgenol* 2009;192:295–299.

8. Wang, L, Hayes, S, Paskalev, K, Jin, L, Buyyounouski, MK, Ma, CC-M, Feigenberg, S: Dosimetric comparison of stereotactic body radiotherapy using 4D CT and multiphase CT images for treatment planning of lung cancer: Evaluation of the impact on daily dose coverage. *Radiother Oncol* 2009;91:314–324.

9. Numata, S, Tsutsumi, Y, Ohashi, H: Evaluation of stuck mechanical valve with four-dimensional computed tomography. *Eur J Cardio-thoracic Surg* 2012;42:594.

10. Kuroda, J, Kinoshita, M, Tanaka, H, Nishida, T, Nakamura, H, Watanabe, Y, Tomiyama, N, Fujinaka, T, Yoshimine, T: Cardiac cycle-related volume change in unruptured cerebral aneurysms: A detailed volume quantification study using 4-dimensional ct angiography. *Stroke* 2012;43:61–66.

11. Hislop-Jambrich, JL, Troupis, JM, Moaveni, AK: The use of a dynamic 4-dimensional computed tomography scan in the diagnosis of atraumatic posterior sternoclavicular joint instability. *J Comput Assist Tomogr* 2016;40:576–577.

12. Goh, YP, Kamali Moaveni, A, Hoy, G, Tate, J, Rotstein, A: Dynamic assessment of sternoclavicular joint instability using four-dimensional computed tomography. *J Med Imaging Radiat Oncol* 2019;63:216–221.

13. Dyer, DR, Troupis, JM, Kamali Moaveni, A: Wide field of view CT and acromioclavicular joint instability: A technical innovation. *J Med Imaging Radiat Oncol* 2015;59:326–330.

14. Alta, TD, Bell, SN, Troupis, JM, Coghlan, JA, Miller, D: The new 4-dimensional computed tomographic scanner allows dynamic visualization and measurement of normal acromioclavicular joint motion in an unloaded and loaded condition. *J Comput Assist Tomogr* 2012;36:749–754.

15. Bell, SN, Troupis, JM, Miller, D, Alta, TD, Coghlan, JA, Wijeratna, MD: Four-dimensional computed tomography scans facilitate preoperative planning in snapping scapula syndrome. *J Shoulder Elb Surg* 2015;24:e83–e90.

16. Goh YP, LK: Using the 320-Multidetector computed tomography scanner for four-dimensional functional assessment of the elbow joint. *Am J Orthop* 2012;41:E20-4.

17. Zhao, K, Breighner, R, Holmes, D, Leng, S, McCollough, C, An, K-N: A Technique for Quantifying Wrist Motion Using Four-Dimensional Computed Tomography: Approach and Validation. *J Biomech Eng* 2015;137:074501.

18. Shores, JT, Demehri, S, Chhabra, A: Kinematic “4 Dimensional” CT Imaging in the Assessment of Wrist Biomechanics Before and After Surgical Repair. *Eplasty* 2013;13:e9.

19. Demehri, S, Hafezi-Nejad, N, Morelli, JN, Thakur, U, Lifchez, SD, Means, KR, Eng, J, Shores, JT: Scapholunate kinematics of asymptomatic wrists in comparison with symptomatic contralateral wrists using four-dimensional CT examinations: initial clinical experience. *Skeletal Radiol* 2016;45:437–446.

20. Troupis, JM, Amis, B: Four-dimensional Computed Tomography and Trigger Lunate Syndrome. *J Comput Assist Tomogr* 2013;37:639–643.

21. Leng, S, Zhao, K, Qu, M, An, K-N, Berger, R, McCollough, CH: Dynamic CT technique for assessment of wrist joint instabilities. *Med Phys* 2011;38 Suppl 1:S50.

22. Kakar, S, Breighner, R, Leng, S, McCollough, C, Moran, S, Berger, R, Zhao, K: The Role of Dynamic (4D) CT in the Detection of Scapholunate Ligament Injury. *J Wrist Surg* 2016;05:306–310.

23. Repse, SE, Koulouris, G, Troupis, JM: Wide field of view computed tomography and mid carpal instability: The value of the sagittal radius-lunate-capitate axis - Preliminary experience. *Eur J Radiol* 2015;84:908–914.

24. Wassilew, GI, Janz, V, Heller, MO, Tohtz, S, Rogalla, P, Hein, P, Perka, C: Real time visualization of femoroacetabular impingement and subluxation using 320-slice computed tomography. *J Orthop Res* 2013;31:275–281.

25. de Sá Rebelo, M, Moreno, RA, Gobbi, RG, Camanho, GL, de Ávila, LFR, Demange, MK, Pecora, JR, Gutierrez, MA: Description of patellar movement by 3D parameters obtained from dynamic CT acquisition. *Med Imaging 2014 Comput Diagnosis* 2014;9035:903538.

26. Forsberg, D, Lindblom, M, Quick, P, Gauffin, H: Quantitative analysis of the patellofemoral motion pattern using semi-automatic processing of 4D CT data. *Int J Comput Assist Radiol Surg* 2016;11:1731–1741.

27. Tanaka, MJ, Elias, JJ, Williams, AA, Demehri, S, Cosgarea, AJ: Characterization of patellar maltracking using dynamic kinematic CT imaging in patients with patellar instability. *Knee Surgery, Sport Traumatol Arthrosc* 2016;24:3634–3641.

28. Tanaka, MJ, Elias, JJ, Williams, AA, Carrino, JA, Cosgarea, AJ: Correlation between Changes in Tibial Tuberosity-Trochlear Groove Distance and Patellar Position during Active Knee Extension on Dynamic Kinematic Computed Tomographic Imaging. *Arthrosc - J Arthrosc Relat Surg* 2015;31:1748–1755.

29. Demehri, S, Thawait, GL, Williams, AA, Kompel, A, Elias, JJ, Carrino, JA, Cosgarea, AJ: Imaging Characteristics of Contralateral Asymptomatic Patellofemoral Joints in Patients with Unilateral instability. *Radiology* 2014;273:821–830.

30. Williams, AA, Elias, JJ, Tanaka, MJ, Thawait, GK, Demehri, S, Carrino, JA, Cosgarea, AJ: The relationship between tibial tuberosity-trochlear groove distance and abnormal patellar tracking in patients with unilateral patellar instability. *Arthrosc - J Arthrosc Relat Surg* 2016;32:55–61.

31. Gondim Teixeira, PA, Formery, AS, Balazuc, G, Lux, G, Loiret, I, Hossu, G, Blum, A: Comparison between subtalar joint quantitative kinematic 4-D CT parameters in healthy volunteers and patients with joint stiffness or chronic ankle instability: A preliminary study. *Eur J Radiol* 2019;114:76–84.

32. Gondim Teixeira, PA, Formery, A-S, Jacquot, A, Lux, G, Loiret, I, Perez, M, Blum, A: Quantitative Analysis of Subtalar Joint Motion With 4D CT: Proof of Concept With Cadaveric and Healthy Subject Evaluation. *Am J Roentgenol* 2017;208:150–158.

33. Mousavian, A, Shakoor, D, Hafezi-Nejad, N, Haj-Mirzaian, A, de Cesar Netto, C, Orapin, J, Schon, LC, Demehri, S: Tibiofibular syndesmosis in asymptomatic ankles: initial kinematic analysis using four-dimensional CT. *Clin Radiol* 2019;74:571.e1-571.e8.

34. Kwong, Y, Mel, AO, Wheeler, G, Troupis, JM: Four-dimensional computed tomography (4DCT): A review of the current status and applications. *J Med Imaging Radiat Oncol* 2015;59:545–554.

35. Gondim Teixeira, PA, Gervaise, A, Louis, M, Raymond, A, Formery, A-S, Lecocq, S, Blum, A: Musculoskeletal Wide-Detector CT Kinematic Evaluation: From Motion to Image. *Semin Musculoskelet Radiol* 2015;19:456–462.

36. Gondim Teixeira, PA, Formery, AS, Hossu, G, Winninger, D, Batch, T, Gervaise, A, Blum, A: Evidence-based recommendations for musculoskeletal kinematic 4D-CT studies using wide area-detector scanners: a phantom study with cadaveric correlation. *Eur Radiol* 2017;27:437–446.

37. Tay, SC, Primak, AN, Fletcher, JG, Schmidt, B, An, K-N, McCollough, CH: Understanding the Relationship Between Image Quality and Motion Velocity in Gated Computed Tomography: Preliminary Work for 4-Dimensional Musculoskeletal Imaging. *J Comput Assist Tomogr* 2008;32:634–639.

38. Lombard, C, Gervaise, A, Villani, N, Louis, M, Raymond, A, Blum, A, Teixeira, PAG: The Impact of Dose Reduction in Quantitative Kinematic CT of Ankle Joints Using a Full Model-Based Iterative Reconstruction Algorithm: A Cadaveric Study. *Am J Roentgenol* 2018;210:396–403.

4. Imaging Protocol

In order to measure syndesmotic position and motion accurately and efficiently, custom image acquisition and analysis protocols were developed as part of this thesis work. Participants underwent standardized 4DCT scans of bilateral ankles followed by manual 3D bony model creation. Subsequently, we utilized an automated process to register these models to each timepoint to calculate various clinical measurements without requiring further user input. Linear mixed effects models were used to determine syndesmotic position and motion throughout full ankle ROM.

4.1. Image Acquisition

4.1.1. Patient Positioning

Participants were positioned supine on the CT scanner platform. Their lower legs were supported on 2 pillows to allow their ankles to hang freely and induce knee flexion. A foam sponge was placed between their legs and lower legs were secured to the platform using straps. Securing their lower legs restricted tibial motion, in order to reduce motion artifact and allow for image capture within a restricted field of view (Figure 4.1). We used a standardized instruction form to direct participants to actively move their ankles between full dorsiflexion and plantarflexion with two seconds between maximal positions. Participants were asked to avoid eversion and inversion as well as internal and external rotation. We also asked that they concentrated on slow, smooth motion without changing speed throughout the arc of motion. Participants practiced the motion and were coached as necessary prior to image acquisition. A flashing light mounted on the CT scanner housing was used to assist patients with timing.

Figure 4.1: Participant positioning on scanner platform. Legs were supported on pillows to allow the ankles to move freely and a sponge was placed between the legs. Fabric straps (not pictured) secured the legs to minimize tibial motion.

4.1.2. 4DCT Scan Parameters

The same GE Medical Systems Revolution™ CT scanner (General Electric, Boston, USA) was used for all studies. First a standard, static CT scan of bilateral ankles was completed, during which patients held their ankles in neutral (0° of dorsiflexion), or as close as comfortably possible. The field of view was 300 mm by 300 mm in the axial plane, centred between the middle of the left and middle of the right plafond, based on scout images. Default scan length along the axial plane was 160 mm, centred 10 mm above the plafonds. If participants had implants that extended proximally beyond the field of view, the scan length was increased to capture all implants. Imaging was performed at 120 kVp and 110 mA. Slices were taken 0.3125 mm apart, with a 0.5859 mm by 0.5859 mm resolution in the axial plane.

Following the static scan, patients were instructed to perform the previously taught motion continuously until completion of the 4DCT scan. A 4DCT volume was acquired with 10 imaging timepoints 0.9 seconds apart. Field of view was again 300 mm by 300 mm in the axial plane, however axial length was fixed at 140 mm, centred 10 mm above the plafond, regardless of implants. Scout images taken in plantarflexion ensured the entire talus would be captured in the field of view. The first timepoint was initiated when ankles were at maximal plantarflexion. Imaging voltage was 120 kVp and current was 70 mA. Space between axial slices was 0.625 mm imaging resolution was 0.5859 mm by 0.5859 mm in the axial plane. Gantry rotation time was 280 ms and complete rotations were used for image reconstruction.[1] Total effective radiation dose between scout, static CT, and 4DCT imaging combined was 0.059 mSv (95% CI 0.057-0.061 mSv).[2–4]

4.2. Model Creation

Using Mimics inPrint 3.0 (Materialize, Leuven, Belgium), we created 3D reference models of the tibia, fibula, and talus bilaterally. Axial images from the static CT volumes were imported and bone was isolated using a 226-2500 HU window to threshold the volume. These thresholds reduced soft tissues and metalwork. Manual correction was necessary, commonly to remove small connections between the talus and calcaneus and navicular, as well as remove persistent metal artifact. Holes in the individual bone models were filled using the built-in hole fill function, without affecting bony outlines and contours. These created models were exported in stereolithography (STL) format (Figure 4.2).

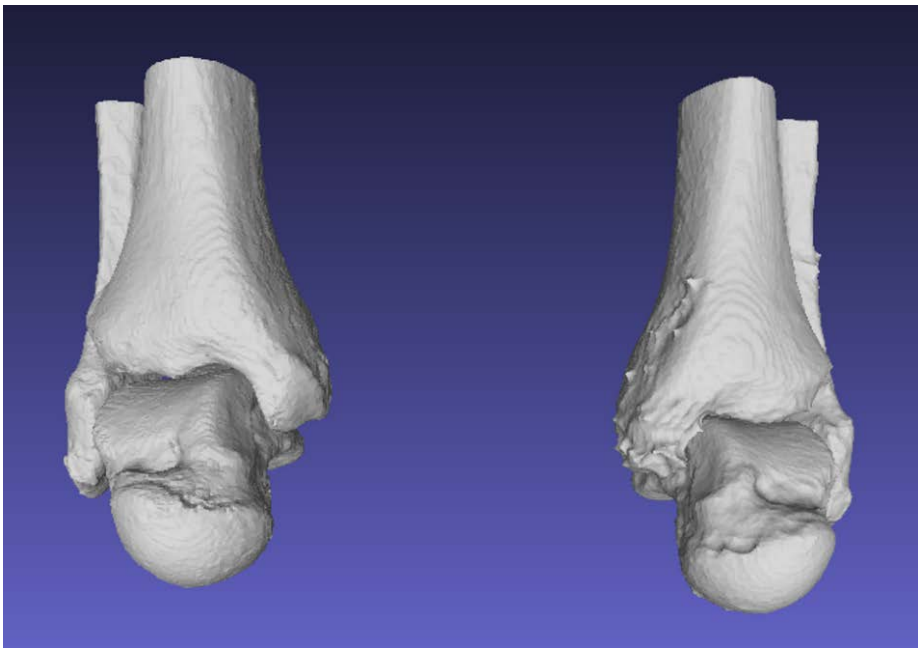

Figure 4.2: 3D reference models created.

To assist with model processing in later steps, basic measurements were taken on these reference models. The three-dimensional coordinate of the most medial point on the medial malleolus was measured, as was the anterior and posterior border of the incisura, 10 mm above the plafond. The plafond was localized using the most distal slice that captured the entire bony plafond without discontinuity (Figure 4.3). Borders of the incisura were the most prominent points of the anterior and posterior tibial tubercles. These coordinates were automatically refined in subsequent analysis steps. In the 4DCT volume, at the first timepoint, we measured the axial (Z) coordinate of the first and last slices which contained the fibula to calculate its approximate length.

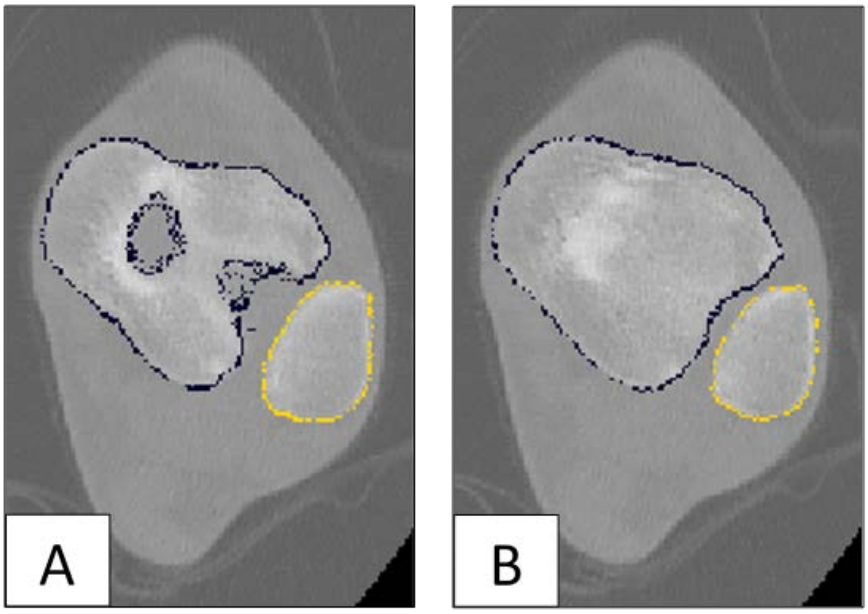

Figure 4.3: Axial slice determining the level of the tibial plafond showing (A) discontinuity and (B) the complete plafond.

4.3. Automated Registration Process

To improve efficiency, an automated program was developed in Matlab® (MathWorks, Natick, USA) so that models would not have to be manually created at each dynamic timepoint (Figure 4.4).

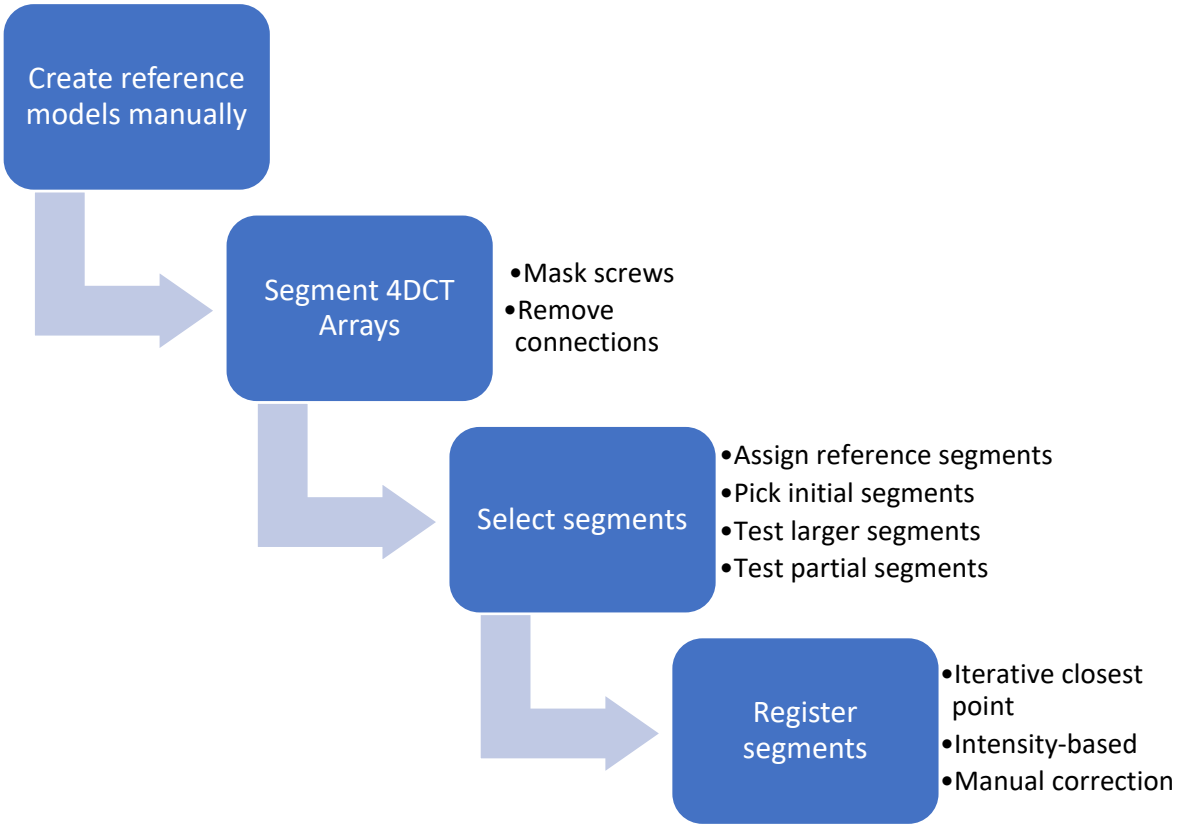

Figure 4.4: Flowchart of automated registration process steps.

4.3.1. Array Alignment

Both the static volume and 4DCT volumes were loaded into the program and DICOM files converted into 3D and 4D arrays of Hounsfield units (HU), respectively. Next, the axial height of each reference fibula was calculated from the previous models. This was compared to the measured fibular length from the first 4DCT model. If both reference fibulas were 5 mm longer or greater than the 4DCT fibulas, the reference array was truncated proximally so that the reference array captured only 5 mm more of the proximal legs compared to the 4DCT volume. This step served to improve future registration between arrays.

4.3.2. Array Segmentation

A segmentation routine was then performed on both volumes. In order to remove connections between the tibia and fibula caused by syndesmotic screws, a blocking mask was applied to each array where any cluster of voxels greater than 2,222 HU, oriented in a linear horizontal direction, and a length greater than 30 mm was overwritten with a box of minimum intensity (Figure 4.5).

Figure 4.5: Syndesmotic screws in (A) shown on axial and coronal CT slices in (B) and (C). Blocking mask applied on the same slices in (D) and (E).

Following this, a gaussian blurring filter of size 5 and standard deviation 1.0 was applied to help reduce the impact of metallic ring artifact. A 500-2,222 HU window was used to threshold the volumes into binary

arrays. A more restrictive window was used than in the model creation process to automatically reduce the number of connections that had previously been manually removed. Voxels were divided into groups where each voxel within a group was connected to another voxel in the same group by at least one face. Any groups of fewer than 800 voxels were removed as they would not substantially impact the registration process. Each remaining voxel group was stored as a separate segment. This process led to some over-segmentation of individual bones, but was successful in greatly reducing the number of unwanted connections between bones (Figure 4.6).

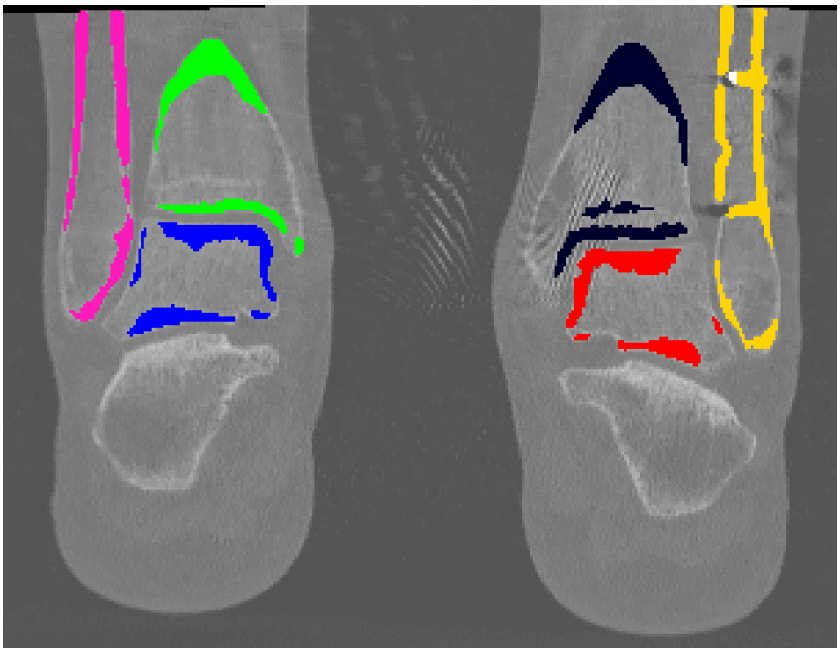

Figure 4.6: Segmented bones from the custom program.

4.3.3. Segment Assignment

For the reference array, the manually created STL models were imported and converted to 3D arrays using the Möller-Trumbore algorithm.[5] These models were overlaid on the segmented reference array.

Intersections between the segments and model for each bone were combined and chosen as the reference segment for that bone.

Next, appropriate segments had to be selected from each 4DCT timepoint. At each timepoint and for each bone, all 4DCT segments were registered to the reference segment using an iterative closest point algorithm, calculating 3D transformations and root mean square errors (RMSE).[6–8] Error minimization criteria were developed to determine the most likely 4DCT segment corresponding to the reference segment. Initial error minimization of forward RMSE (segment registered to reference) times backward RMSE (reference registered to segment), divided by the square root of the segment size in voxels produced the best accuracy. Since segmentation was imperfect, the process could potentially create segments which comprised only a portion of the reference bone, or segments which had parts of the reference bone and another bone combined. Smaller, partial segments would have low forward error but high backward error, while the larger combined segments would have high forward error but low backward error. Therefore, this initial error minimization criterion helped to ensure these imperfect segments were selected, giving preference to larger segments which would produce more accurate registration. Segments were ranked on the initial error minimization criterion. Any segments with initial criterion 10 times greater than the minimum criterion were excluded. If greater than six segments remained, only the lowest 6 segments were included for further evaluation.

Of these candidate segments, the most likely segment was chosen from the lowest initial criteria and the lower of the forward or backward RMSE was saved for comparison. Next larger, possibly combined segments were trialed to determine if better registration could be achieved. Any segment that had either a convex hull volume of greater than 25% of the reference model or a maximum length of greater than

40% of the reference model were tested. If these segments had a lower backward error than the current most likely segment, they were reassigned as the new most likely segment and the process continued.

Next, possible partial segments were analyzed for inclusion in a composite segment. Any partial segment should have a low forward error, so all segments were sorted by forward error and a threshold of twice the second lowest forward error was set. The second lowest error was chosen since some bones had been segmented into multiple pieces and one piece with a small volume may have much lower error than the other pieces, despite the others being crucial for accurate registration. Any segments that were below this threshold and included in the candidate segments were assessed. These potential partial segments were amalgamated, and the backward registration of the amalgamation was calculated. Sequentially, each part of the amalgamation was removed, and the backward registration was recalculated. If the minimum RMSE found with a removed segment was less than or equal to the total amalgamation RMSE, the segment in question was removed. This method assumed that the iterative closest point algorithm accurately registered the reference segment to the correct partial segments and was not affected by incorrect segments since the reference model would not be registering to them in the backward direction. The amalgamation was recreated less the segment in question and the process of eliminating incorrect segments continued until the minimum RMSE was found or a single segment remained. If the remaining combined segments had a lower forward or backward RMSE of less than the current most likely segment's minimum RMSE, the combination of partial segments replaced the most likely segment. The segment selection process was performed for each bone at every timepoint.

4.3.4. Iterative Closest Point Registration

Once the most likely 4DCT segment(s) and reference segments were selected, the relative transformation between segments was calculated. Again, using an iterative closest point algorithm, the forward and backward transformation between each bone at the 4DCT timepoint and the corresponding bone in reference coordinates was calculated and the transformation resulting in lower RMSE was saved.

4.3.5. Intensity-Based Registration

When registration failed by iterative closest point methods, intensity-based registration was performed between 4DCT and reference volumes. When RMSE for a specific bone and timepoint was greater than 0.4 mm, the program launched an intensity registration module to attempt to improve automated registration. The reference array of Hounsfield units was cropped to encompass only the reference bone based on STL model. To isolate only the reference bone, any voxels where the reference array and STL model did not overlap were removed from registration calculations, as were voxels below 226 HU or above 2222 HU.

The initial 4DCT array was based on the most likely 4DCT segment(s). The array was cropped to be centred on the chosen segment(s) with a length of 120% of the chosen segment(s) in each principal direction. Any voxels below 226 HU or above 2222 HU were removed from registration calculations. An intensity-based registration was then performed where the difference between voxel intensities between arrays was used to register the transformation between cropped reference and 4DCT arrays, minimizing mean squares.[8] An initial transformation from the iterative closest point registration was provided and used if it improved RMSE. The intensity registration was performed iteratively, where the reference model was transformed into 4DCT array coordinates according to the new intensity-based transform and the 4DCT array was re-

cropped to fit the transformed model. Intensity-based transformation was repeated using the new 4DCT input array until less than a 1 mm difference between successive transformations was found. If the resulting RMSE from intensity-based registration was less than the iterative closest point RMSE, the intensity-based transformation was used instead.

4.3.6. Manual Correction

All registrations were confirmed visually by overlaying the transformed reference model outline onto the 4DCT array. If any malalignment between the model and 4DCT cortical outline was observed, registration was considered to have failed. In case of program failure, 4DCT segments could be manually selected, or a model from the 4DCT array could be created as described in section 4.2 in order to calculate the transformation between the reference and 4DCT models (Figure 4.7).

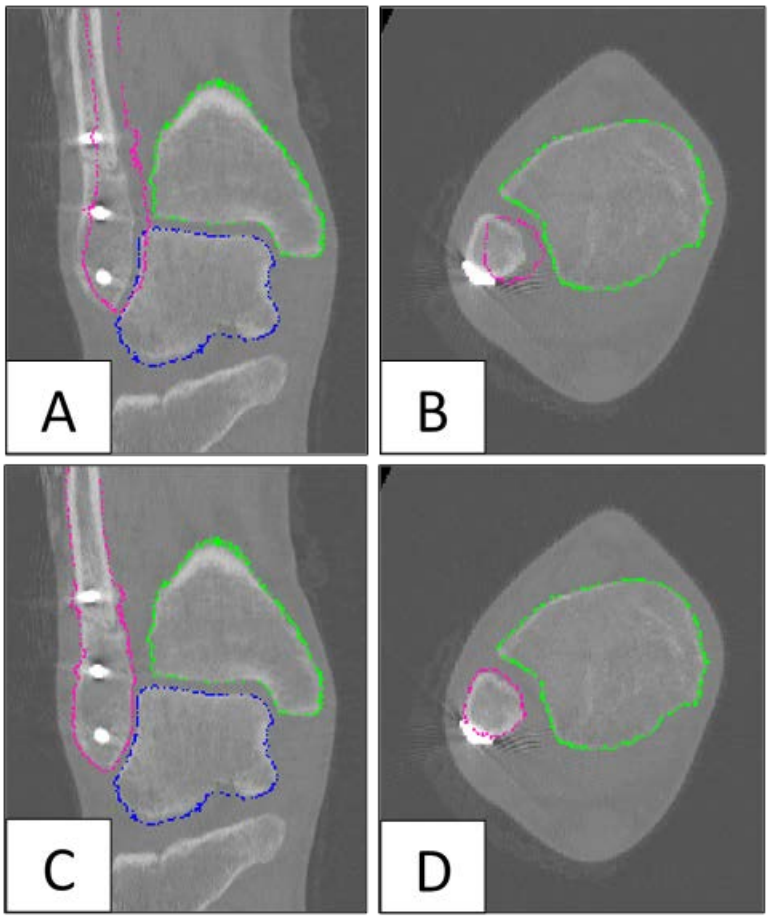

Figure 4.7: Failure of automatic registration for the fibula on coronal and axial CT slices in (A) and (B). Correction of registration via manual segment selection in (C) and (D).

4.3.7. Automated Registration Accuracy

Prior to processing, 2.8% of 4DCT timepoints were excluded due to excessive motion artifact that would have compromised results. Using our outlined image acquisition procedure, the automated process accurately registered bones between the reference model and 4DCT images 99% of the time for specimen without metal implants, and 96% of the time in patients with metal implants (98% overall). Manual segment selection was required in 1.5% of the time in specimen without metal implants and 3.3% of the time in patients with metal implants (2.1% overall). 4DCT model creation was not required in uninjured

ankles and only 0.7% of the time in patients with metal implants (0.2% overall). We achieved sub-voxel size accuracy. The mean RMSE achieved by the automated process was 0.33 mm.

4.4. Radiographic Measurements

At each 4DCT timepoint, the transformation from reference models to 4DCT space was used to determine the relative positions of the tibia, fibula, and talus bilaterally. From there, various radiographic measures were calculated to describe syndesmotic position and motion.

4.4.1. Model Orientation

Reference models were transformed into their 4DCT timepoint positions then oriented in a consistent manner. Z axis was determined by calculating the long axis of the tibia. The centroids of the tibia at its most proximal aspect and at the level of the incisura, as measured on the reference model 10 mm above the plafond in section 4.2, determined this axis (Figure 4.8). The level of the incisura was used to avoid skewing of the axis by the medial malleolus distally. The Y axis was determined as the axis from medial malleolus to the midpoint between the anterior and posterior incisura, again as measured on the reference model. The cross product of the Y axis and Z axis determined the X axis, and the cross product of the Z axis and X axis then refined the Y axis. The models were oriented in this reference space and translated so that the origin was at the midpoint of the anterior and posterior incisura.

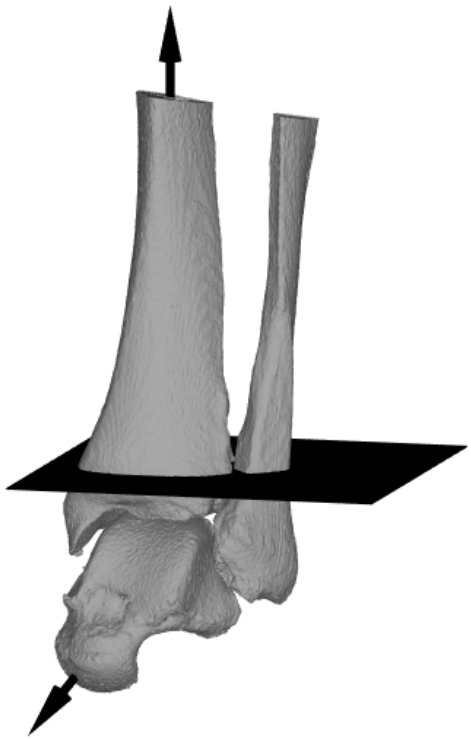

Figure 4.8: Long axis of the tibia and talar axis. Plane slices through the incisura perpendicular to the tibial axis.

4.4.2. Tibiotalar Angle

Once oriented in the anatomic coordinate system, the talar axis was calculated as the first principal moment of inertia axis (Figure 4.8). Directed anteriorly, the angle between this axis and the XY plane was recorded as the tibiotalar angle. The axis pointing distally is positive for plantarflexion, and when angled proximal to the XY plane the value is negative for dorsiflexion.

4.4.3. Syndesmotic Slicing

The oriented tibia and fibular models were sliced in the XY plane through the origin to perform common syndesmotic measurements (Figure 4.8). A tangent line was fit to the lateral outline of the tibia in order to find the points of contact at the anterior and posterior edges of the incisura. The incisura axis was the

vector from posterior to anterior. Then the slice was rotated so that the incisura axis was parallel to the X axis (Figure 4.9). The middle incisura point was the midpoint between the anterior and posterior incisura points, along the tibial perimeter.

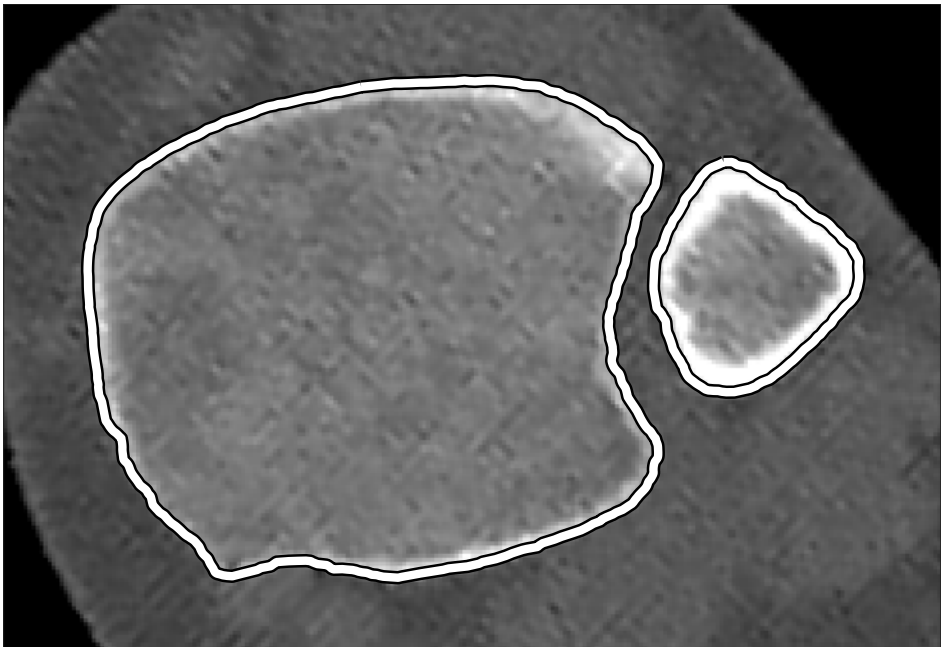

Figure 4.9: Sliced model overlaid on transformed CT volume.

4.4.4. Fibular Axis Definition

Due to variable cross section of the fibula at the level of the syndesmosis, a fibular cross section was taken 5 mm distal to the plafond to more reliably define the fibular axis.[9,10] A linear regression line was fit to the medial fibular articular border at that level, adjusting the section of fibula used by minimizing residuals. This linear regression slope was used at the level of the syndesmosis to define the fibular axis. The furthest apart points along the slope were used to define the anterior and posterior fibular points at 10 mm above the plafond.

4.4.5. Calculated Measurements

Using the anterior, middle, and posterior incisura points, the anterior (ASD), middle (MSD), and posterior (PSD) syndesmotic distances were calculated (Figure 4.10). The distances from these points to the closest corresponding points on the fibula were used.[11] TFCS and TFO were also measured as the distance from the most medial incisura to the most medial fibula and the most lateral incisura to the most medial incisura, respectively, perpendicular to the incisura axis (Figure 4.11).[9,12] Negative values for TFO indicate no overlap between the incisura and fibula. Sagittal translation was the distance from the most anterior point of the incisura to the most anterior part of the fibula, parallel to the incisura axis where negative values mean the fibula is anterior to the incisura (Figure 4.12).[11] Fibular rotation was also measured, as the angle between the fibular and incisura axes, where internal rotation of the fibula is positive (Figure 4.13).[11,13–15] The final measurement was syndesmotic area, which was the area bounded by tangent lines between the tibia and fibula anteriorly and posteriorly, and the outline of the tibia and fibula medially and laterally (Figure 4.14).[16]

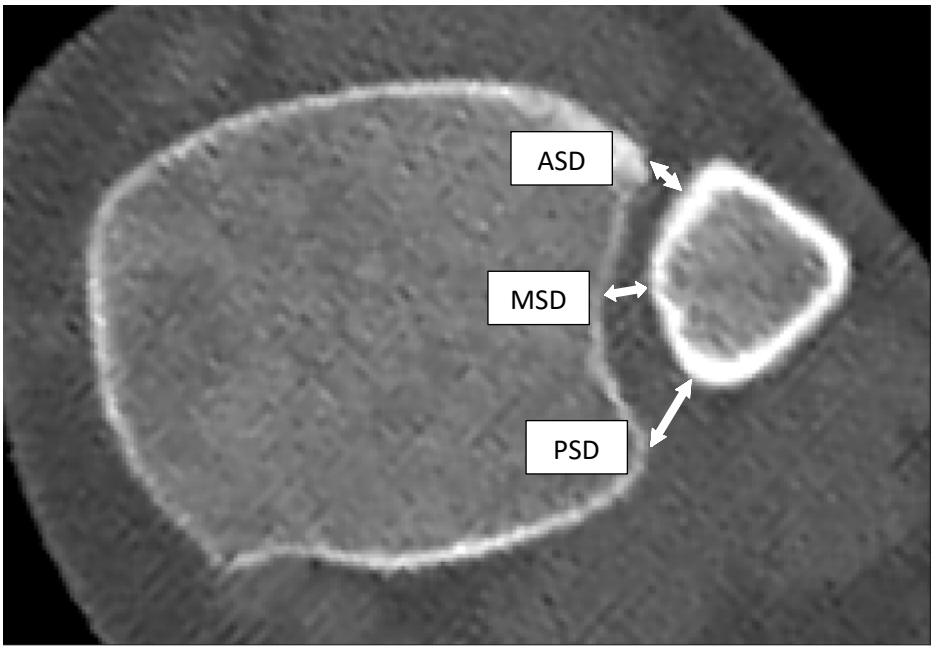

Figure 4.10: Anterior, middle, and posterior syndesmotic distances.

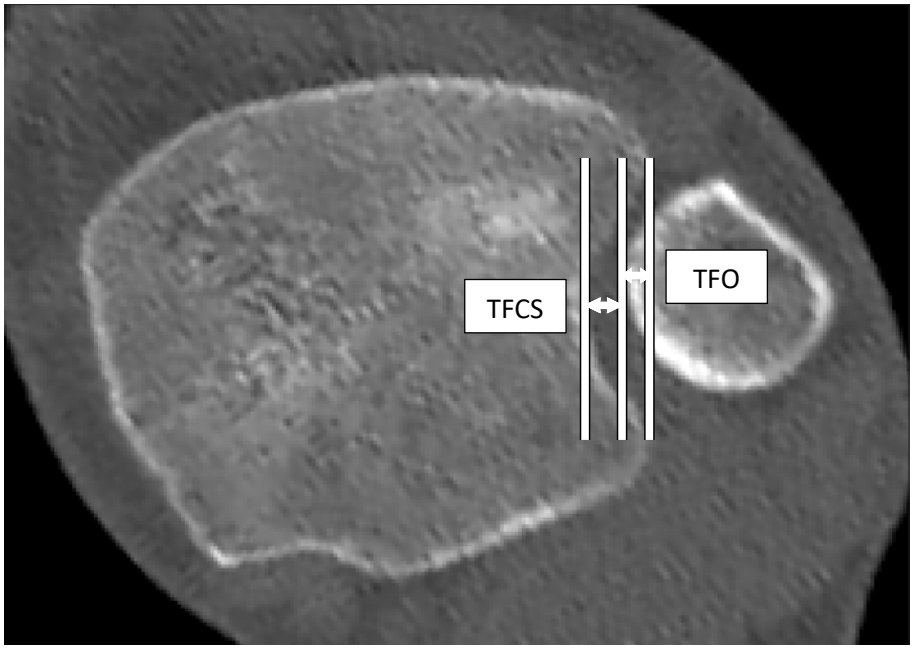

Figure 4.11: Tibiofibular clear space and tibiofibular overlap.

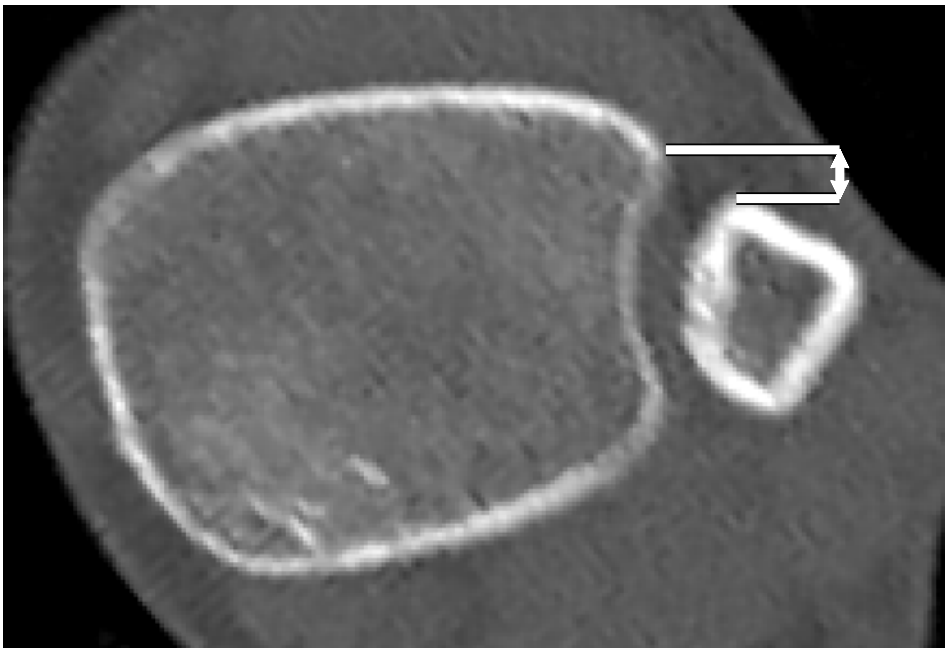

Figure 4.12: Sagittal translation.

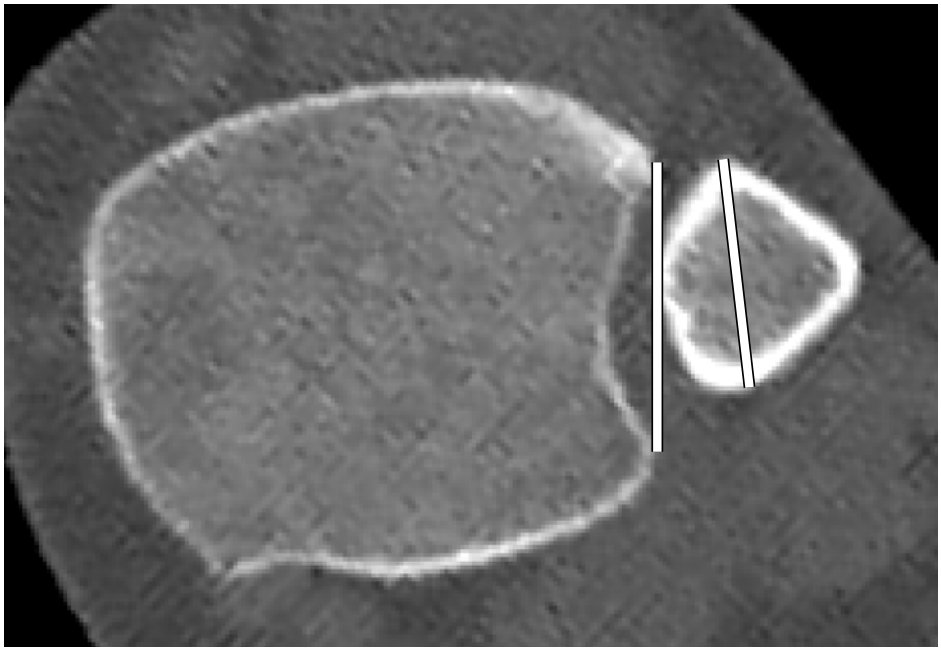

Figure 4.13: Fibular rotation between the incisura axis and fibula axis.

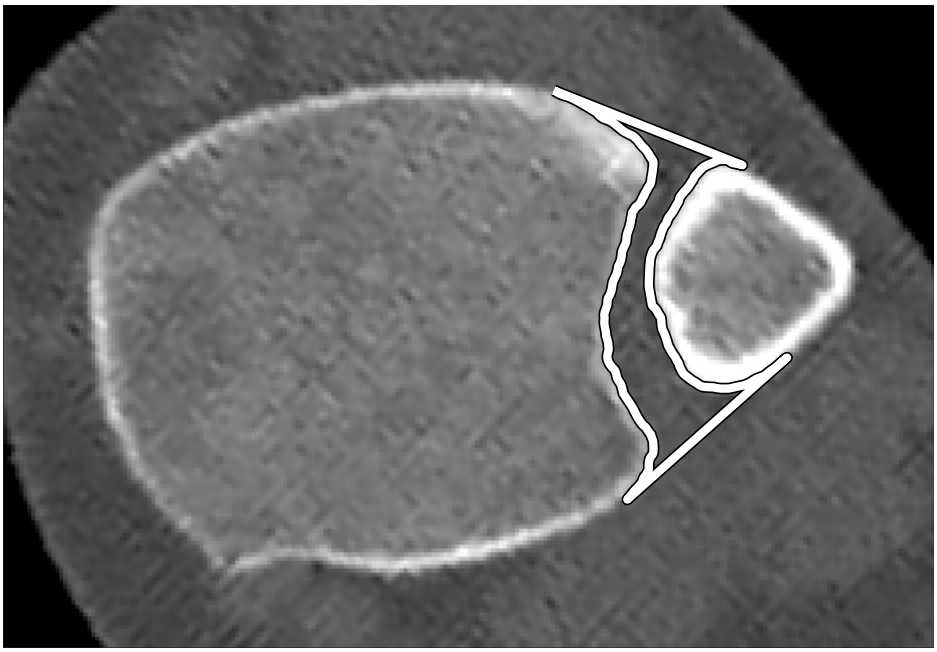

Figure 4.14: Syndesmotic area.

As transformations between reference models and 4DCT timepoints were available, the 3D, 6 degree of freedom transformations could be calculated from the relative transformations. Using the most dorsiflexed timepoint as the neutral position, the relative translation and rotations about the X, Y, and Z axes were found for each timepoint. A Z-Y-X Euler angle convention was used when decomposing the rotation matrix.

4.5. Statistical Analysis

Linear mixed effects models were used to investigate the impact of ankle range of motion and various parameters on the above measurements. Data were nested by ankle then specimen to avoid pseudo-replication. The fixed effects portion of the model estimated the impact of patient demographics, tibiotalar angle, and treatment variables on the measurements calculated. The impact of demographic

and treatment variables on motion was explored by examining their respective interactions with tibiotalar angle on the various measurements. Goodness of fit of the model was investigated using an adjusted R-squared value. Side to side variability of each measurement was found using linear regression modelling within each ankle across ankle position and comparing the intercepts and slopes generated from the regression models. Significance of alpha < 0.05 was used.

4.6. References

1. Gondim Teixeira, PA, Formery, AS, Hossu, G, Winninger, D, Batch, T, Gervaise, A, Blum, A: Evidence-based recommendations for musculoskeletal kinematic 4D-CT studies using wide area-detector scanners: a phantom study with cadaveric correlation. *Eur Radiol* 2017;27:437–446.

2. Biswas, D, Bible, JE, Bohan, M, Simpson, AK, Whang, PG, Grauer, JN: Radiation exposure from musculoskeletal computerized tomographic scans. *J Bone Jt Surg - Ser A* 2009;91:1882–1889.

3. Gervaise, A, Teixeira, P, Villani, N, Lecocq, S, Louis, M, Blum, A: CT dose optimisation and reduction in osteoarticular disease. *Diagn Interv Imaging* 2013;94:371–388.

4. Lombard, C, Gervaise, A, Villani, N, Louis, M, Raymond, A, Blum, A, Teixeira, PAG: The Impact of Dose Reduction in Quantitative Kinematic CT of Ankle Joints Using a Full Model-Based Iterative Reconstruction Algorithm: A Cadaveric Study. *Am J Roentgenol* 2018;210:396–403.

5. Möller, T, Trumbore, B: Fast, Minimum Storage Ray-Triangle Intersection. *J Graph Tools* 1997;2:21–28.

6. Besl, PJ, McKay, ND: A method for registration of 3-D shapes. *IEEE Trans Pattern Anal Mach Intell* 1992;14:239–256.

7. Chen, Y, Medioni, G: Object modelling by registration of multiple range images. *Image Vis Comput* 1992;10:145–155.

8. MATLAB: version 9.6.0 (R2019a). *Natick, Massachusetts MathWorks Inc* 2019;

9. Morellato, J, Louati, H, Bodrogi, A, Stewart, A, Papp, S, Liew, A, Gofton, W: The Effect of Varying Tension of a Suture Button Construct in Fixation of the Tibiofibular Syndesmosis - Evaluation Using Stress Computed Tomography. *J Orthop Trauma* 2017;31:103–110.

10. Vasarhelyi, A, Lubitz, J, Gierer, P, Gradl, G, Rosler, K, Hopfenmuller, W, Klaue, K, Mittlmeier, TWF: Detection of fibular torsional deformities after surgery for ankle fractures with a novel CT method. *Foot Ankle Int* 2006;27:1115–1121.

11. Nault, M-LL, Hébert-Davies, J, Laflamme, G-YY, Leduc, S: CT scan assessment of the syndesmosis: A new reproducible method. *J Orthop Trauma* 2013;27:638–641.

12. Lepojärvi, S, Pakarinen, H, Savola, O, Haapea, M, Sequeiros, RB, Niinimäki, J: Posterior translation of the fibula may indicate malreduction: CT study of normal variation in uninjured ankles. *J Orthop Trauma* 2014;28:205–209.

13. Dikos, GD, Heisler, J, Choplin, RH, Weber, TG: Normal Tibiofibular Relationships at the Syndesmosis on Axial CT Imaging. *J Orthop Trauma* 2012;26:433–438.

14. Futamura, K, Baba, T, Mogami, A, Morohashi, I, Kanda, A, Obayashi, O, Sato, K, Ueda, Y, Kurata, Y, Tsuji, H, *et al.*: Malreduction of syndesmosis injury associated with malleolar ankle fracture can be avoided using Weber's three indexes in the mortise view. *Injury* 2017;48:

15. Warner, SJ, Fabricant, PD, Garner, MR, Schottel, PC, Helfet, DL, Lorich, DG: The Measurement and Clinical Importance of Syndesmotic Reduction After Operative Fixation of Rotational Ankle Fractures. *J Bone Jt Surg* 2015;97:1935–1944.

16. Malhotra, G, Cameron, J, Toolan, BC: Diagnosing chronic diastasis of the syndesmosis: A novel measurement using computed tomography. *Foot Ankle Int* 2014;35:483–488.

5. 4DCT Analysis of Normal Syndesmotic Motion

5.1. Introduction

The tibiofibular syndesmosis plays an important role in ankle stability. The syndesmosis primarily resists fibular external rotation and lateral translation.[1,2] In addition, the syndesmosis increases joint contact area between the distal tibia and talus and transmits axial loads from the tibia to the fibula throughout the gait cycle.[3,4] Small but significant amounts of motion are seen at the distal tibiofibular joint throughout ankle range of motion (ROM) as well as in response to loading. This motion can provide additional ankle stability when accommodating motion of the irregularly shaped talus.[5] In cadaveric and imaging studies, when the ankle moves from dorsiflexion to plantarflexion, there is up to 1.3 mm of anterior fibular translation, 3.0 mm of medial translation, and 3.7° of internal rotation relative to the tibia.[5–7]

Injuries to the syndesmosis are common, occurring in up to 18% of all ankle sprains[4,8] and in up to one-quarter of ankle fractures.[9,10] When injured, the historical gold standard for treatment has been rigid screw fixation.[10] However, due to concerns regarding excessive rigidity and screw breakage or loosening, flexible suture-button devices, such as the Tightrope® (Arthrex, Naples, USA), have been introduced.[11,12] These flexible devices reduce the rate of malreduction, but malreduction still occurs in up to 20% of flexible cases compared with up to 52% of rigid cases.[13,14] Malreduction is the most important predictor of inferior outcomes after injury, leading to chronic pain, stiffness, instability, or arthritis.[15–18] Efforts to improve reduction such as direct visualization of the syndesmosis, avoidance of reduction clamps which may introduce over-compression, and intraoperative CT have limited success.[19–23]

Malreduction is commonly judged based on side-to-side differences on bilateral ankle CT.[24–26] However, the syndesmosis is a dynamic structure and conventional CT does not provide a complete picture of syndesmotic position. A CT volume taken at a single non-standardized, patient-selected ankle position may give inaccurate and potentially misleading results. 4DCT, also known as dynamic CT, is an emerging technology which can image a joint in real-time as it moves through a range of motion.[27] Multi-detector arrays and fast gantry speeds allow the capture of an entire volume in under 0.3 seconds which can be repeated to create a moving image.[28]

Given the consequences of syndesmotic malreduction as well as demonstrated motion at the distal tibiofibular joint, it is important to account for this motion when treating syndesmotic injuries. Treating reduction as a static measurement rather than a parameter affected by ankle ROM may predispose patients to worse functional outcomes. Therefore, the purpose of this study was to use 4DCT to investigate the *in vivo* effect of ankle ROM on syndesmotic measurements in uninjured, asymptomatic participants. By understanding normal syndesmotic motion, we can develop reduction and fixation strategies to recreate physiologic motion and reduce impairment after syndesmotic injury. We hypothesized that syndesmotic measurements would change significantly throughout ankle ROM and that side-to-side differences would be minimal, as defined as below accepted thresholds of malreduction.

5.2. Methods

5.2.1. Inclusion Criteria

Uninjured ankles were gathered from a combination of three studies. First, a subset of patients from a multicentre randomized controlled trial comparing rigid and flexible fixation after syndesmotic injury were recruited to undergo bilateral ankle 4DCT at 12 months after their index surgery were included

(ClinicalTrials.gov identifier NCT02199249).[14] In addition, a prospective cohort study comparing reduction after rigid and flexible fixation is underway in which all patients undergo a bilateral ankle 4DCT scan at three months after their index surgery. Finally, a prospective cohort of healthy, adult volunteers was recruited from our Level 1 trauma centre and affiliated university to undergo bilateral ankle 4DCT. The contralateral uninjured ankle was analyzed in the two injury cohorts and both ankles were used from the control cohort. All participants were skeletally mature and 18 years old or over with a unilateral uninjured ankle (bilateral in the control cohort). Participants were excluded if they had prior lower extremity fractures or known syndesmotic injuries, were non-ambulatory or required gait aids, had congenital lower extremity deformities or neuromuscular disease, or were pregnant or attempting to become pregnant. The study was approved by our institutional research ethics review board (REB14-1142 and REB18-2146).

5.2.2. Data Acquisition

Each participant underwent a single 4DCT of their bilateral ankles using a GE Medical Systems Revolution™ CT scanner (General Electric, Boston, USA) at 120 kVp and 70 mA. A 140 mm axial scan length with a 300 mm by 300 mm field of view in the axial plane was used. Axial slice resolution was 0.586 mm by 0.586 mm with 0.625 mm between axial slices. Participants were instructed to move their ankles freely between maximal comfortable dorsiflexion and plantarflexion continuously with two seconds between extremes. Ten imaging timepoints were captured each 0.9 seconds apart. The effective radiation dose for the entire scanning protocol was 0.06 mSv, which is well below the radiation exposure of a standard chest x-ray.[29–31] To ensure the bilateral uninjured cohort represented an asymptomatic population, validated functional outcome measures were administered including the AOFAS, Foot and Ankle Ability Measure (FAAM), OM, and a visual analog pain scale (VAS).

5.2.3. Measurement Process

From CT data, 3D models were created of the tibia, fibula, and talus bilaterally for each participant using Mimics software (Materialise, Leuven, Belgium). A custom Matlab® (MathWorks, Natick, USA) program was then used to automatically segment the CT volume and register the 3D model to each timepoint. A 500-2,222 Hounsfield Unit intensity threshold was used to segment the imaging volume, followed by a combination of iterative closest point and intensity matching algorithms to register the 3D reference model to each 4DCT timepoint (Figure 5.1). The mean root-mean-square error in registration was 0.33 mm. At each timepoint, the tibiotalar angle was calculated between the long axis of the tibia and the long axis of the talus. The long axis of the tibia was defined as the line between the centroid of the tibia taken at its most proximal aspect and at the level of the incisura, as measured on axial CT slices (Figure 5.2). The talar long axis was found by calculating the first principal moment of inertia axis. The fibular rotation axis was defined as the tangent line along the medial fibular border at 5 mm below the plafond, as the fibular axis can be defined more reliably at this level.[32] Syndesmotic measurements were taken 10 mm above the plafond. These measurements included ASD, MSD, and PSD distances, which were measured from the most anterior and posterior points of the incisura, as well as the midpoint of the incisura, to the closest corresponding points on the fibula (Figure 5.3).[25] TFCS was the distance between the most medial fibula and most medial part of the incisura measured perpendicular to the incisura while the TFO was the distance between the most medial fibula and most lateral part of the incisura.[32,33] Sagittal translation was the distance from the most anterior incisura to the most anterior fibula parallel to the incisura, and fibular rotation was the angle between the fibular axis and the incisura tangent.[25] Syndesmotic area was determined by fitting tangents between the tibia and fibula anteriorly and posteriorly then finding the area bounded by the tangents.[34] All measurements were automated calculated based off the registered 3D models in Matlab®. After manual reference model creation, the registration, model orientation, and measurement process were fully automated. Therefore, no user input was required to generate

syndesmotic measurements, giving complete measurement reproducibility, and eliminating error related to subjective landmark selection.

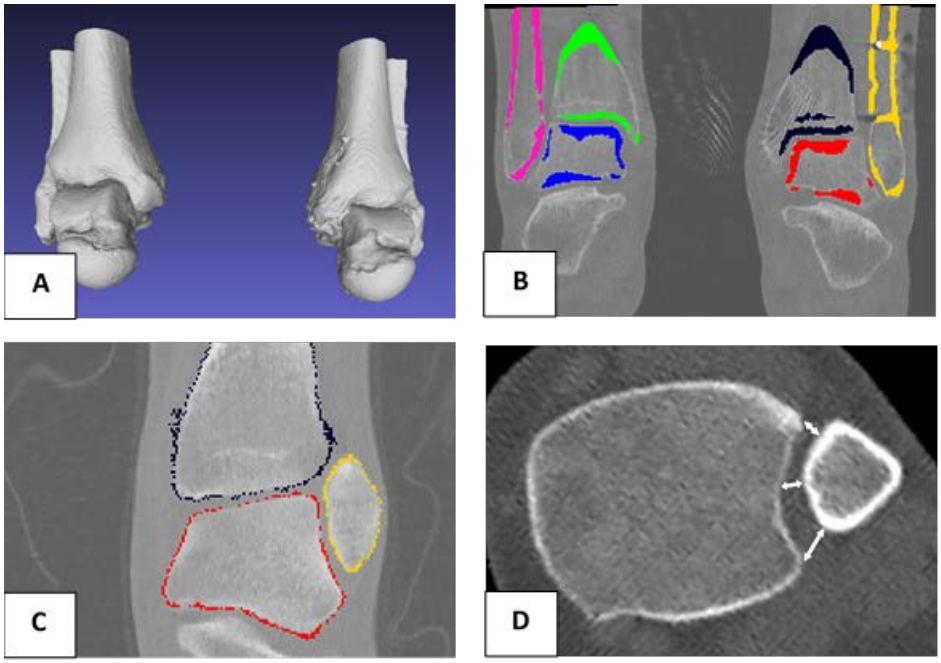

Figure 5.1: Automated measurement process. A: 3D reference models, B: Threshold based segmentation, C: reference models registered to 4DCT data, D: Automated syndesmosis measurements calculated based on registered models. An automated measurement process calculates multiple measurements at each 4DCT timepoint.

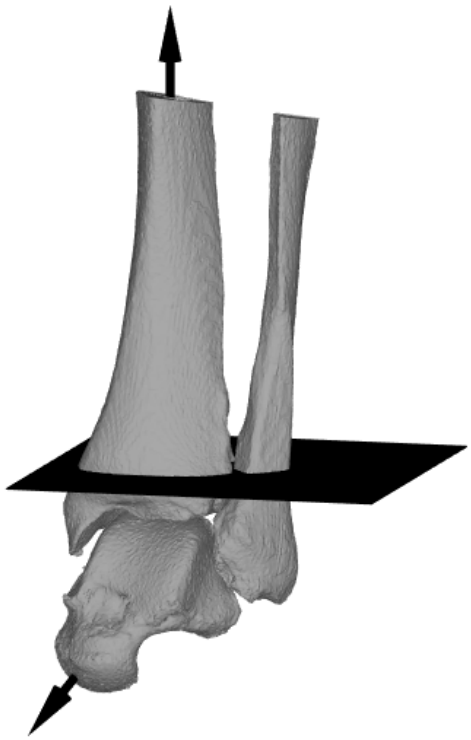

Figure 5.2: Long axis of the tibia and talar axis. Plane slices through the incisura perpendicular to the tibial axis.

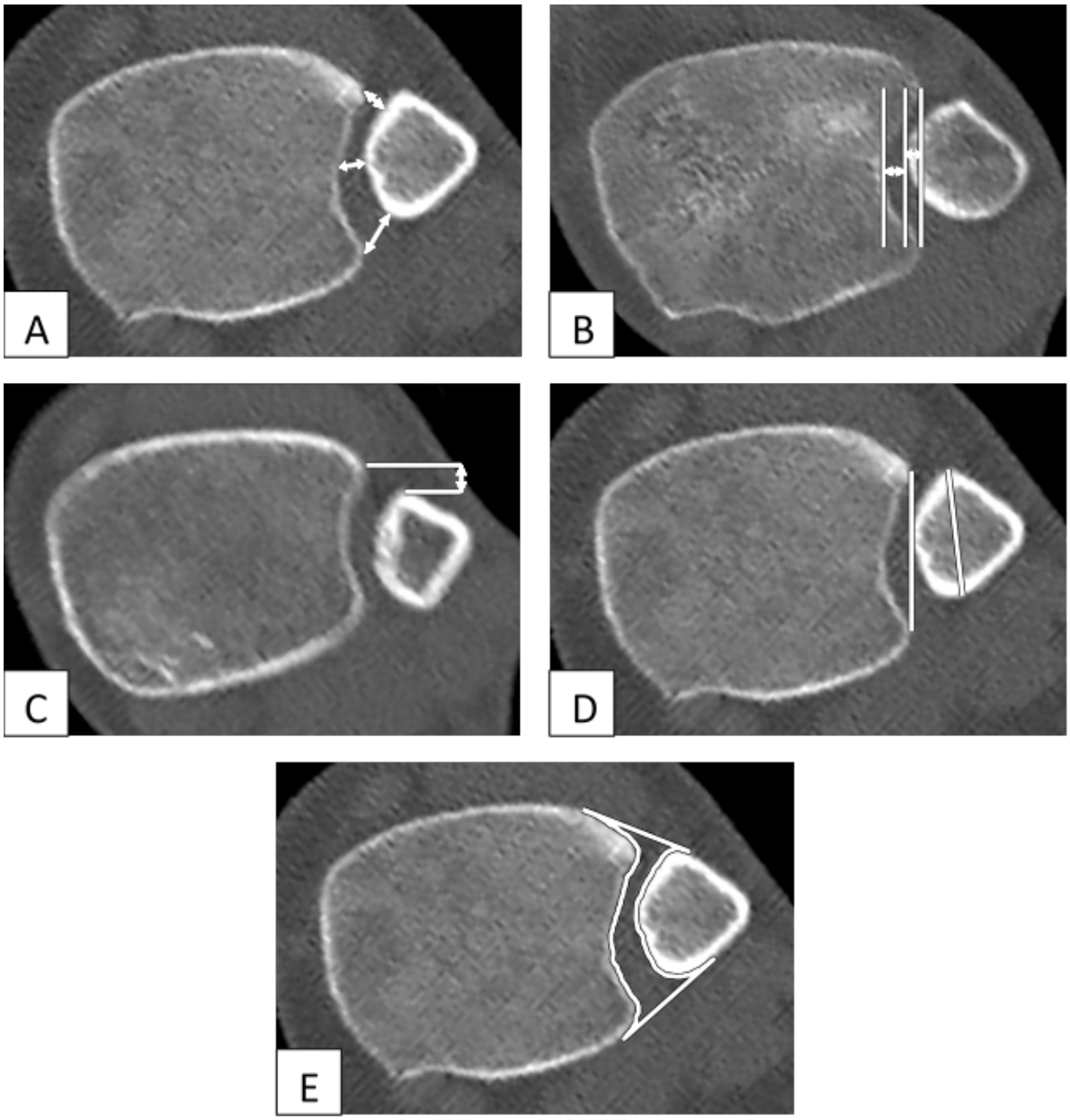

Figure 5.3: Syndesmosis measurements generated from 3D models overlain on 4DCT data. (A) Anterior, middle, and posterior syndesmosis distances, (B) tibiofibular clear space and tibiofibular overlap, (C) sagittal translation, (D) fibular rotation, and (E) syndesmotic area.

5.2.4. Statistical Analysis

A linear mixed effects model was used to determine the position of the syndesmosis in the neutral (0° dorsiflexion) ankle position as well as the syndesmotic motion across ankle ROM. Adjusted r-squared values were calculated to determine the model fit and Shapiro-Wilk tests were used to assess normality. Data were nested within specimen to avoid pseudo-replication within the bilateral control cohort. Side-to-side variability of syndesmotic position and motion was evaluated by comparing the slope and intercept fit to each individual ankle with a linear regression model. P-values less than 0.05 were deemed significant.

5.3. Results

5.3.1. Demographics

Fifty-eight ankles in 39 different patients were included in the analysis. Thirteen patients came from the randomized control trial, seven from the prospective cohort of injury patients, and 19 from the bilateral control group. The bilateral control group was asymptomatic based on AOFAS, FAAM, OM, and VAS scores (Supplementary Table 5.3). There were 24 males and 15 females. The mean age was 35 years (range 18 to 75 years). The mean maximal dorsiflexion was -2° (range -20° to 19°) and the mean maximal plantarflexion was 44° (range 27° to 61°). The adjusted marginal r-squared value of the linear mixed effects models ranged from 0.91 to 0.97 indicating good model fit for each measurement. No significant differences between the three patient groups were detected for any measurement (Supplementary Table 5.4).

5.3.2. Normal Syndesmotic Measurements

The mean ASD in neutral position was 3.3 mm, which decreased by 0.7 mm from dorsiflexion to plantarflexion ($p < 0.001$). The MSD was 3.4 mm and decreased by 1.1 mm with plantarflexion ($p < 0.001$). The PSD was 6.1 mm and decreased by 0.8mm with plantarflexion ($p < 0.001$) (Table 5.1). Age did not have a significant impact on syndesmotic position or motion. Males demonstrated less change in PSD with ROM than females (0.6 mm versus 1.0 mm, $p = 0.048$), but no differences in neutral position in ASD, MSD, or PSD were detected, nor were there differences in ASD or MSD motion. Syndesmotic measurements as a function of tibiotalar angle for each individual ankle are shown in Supplementary Figures 5.6-5.13.

Table 5.1: Normal syndesmotic position in neutral dorsiflexion and motion from dorsiflexion to plantarflexion.

	Position		**Motion**	
	Mean (SD)	95% CI	Mean (SD)	95% CI
ASD (mm)	3.3 (0.9)	3.0 – 3.6	-0.7 (0.5)	-0.9 – -0.5
MSD (mm)	3.4 (0.9)	3.1 – 3.7	-1.1 (0.5)	-1.2 – -0.9
PSD (mm)	6.1 (1.2)	5.7 – 6.5	-0.8 (0.6)	-1.0 – -0.6
TFCS (mm)	3.9 (0.9)	3.6 – 4.2	-1.1 (0.5)	-1.3 – -0.9
TFO (mm)	-0.3 (1.3)	-0.7 – 0.1	1.1 (0.5)	0.9 – 1.3
Sagittal Translation (mm)	0.5 (1.2)	0.1 – 0.9	0.1 (0.6)	-0.1 – 0.3
Fibular Rotation (degrees)	18.3 (7.0)	16.1 – 20.6	-1.2 (1.6)	-1.7 – -0.7
Syndesmotic Area (mm^2)	122 (23)	115 – 130	-26 (11)	-29 – -22

The mean TFCS was 3.9 mm, which decreased by 1.1 mm during plantarflexion ($p < 0.001$). TFO was -0.3 mm indicating lack of overlap between the medial fibular border and the lateral border of the incisura. This overlap increased by 1.1 mm with plantarflexion ($p < 0.001$). No age- or sex-related differences were found for TFCS and TFO position or motion.

The fibula was situated 0.5 mm posterior to the anterior border of the incisura but did not translate significantly in the sagittal plane with ankle ROM ($p = 0.43$). In neutral position, the fibular axis was 18.3° internally rotated relative to the incisura axis and externally rotated 1.2° with plantarflexion ($p < 0.001$). Fibular internal rotation was found to increase significantly with age by 0.2° per year ($p = 0.041$). No other age- or sex-related changes were significant for sagittal translation or fibular rotation.

The mean syndesmotic area in neutral position was 122 mm^2. From dorsiflexion to plantarflexion, syndesmotic area decreased 26 mm^2 ($p < 0.001$). Though males had a greater syndesmotic area by 14 mm^2, this failed to reach statistical significance ($p = 0.069$). There was no difference in change in area between sexes and no age-related differences for area or change in area.

5.3.3. Side-to-Side Variability

The 19 uninjured participants were analyzed to determine side-to-side variability of the syndesmotic measurements (Table 5.2). Using ASD, MSD, PSD, TFCS, or TFO no participants had a side-to-side difference of 2 mm or greater (Figure 5.4). One participant was above the 2 mm threshold for sagittal translation, at 3.1 mm. If a lower threshold of a 1.5 mm difference is used, no participants would be considered abnormal by ASD, two by MSD, one by PSD, none by TFCS, one by TFO, and three by sagittal

translation. The greatest side-to-side difference in fibular rotation was 9°. The greatest difference in syndesmotic area was 27 mm^2. The side-to-side differences in syndesmotic motion with ankle ROM are depicted in Figure 5.5.

Table 5.2: Side-to-side differences in syndesmotic position in neutral dorsiflexion and motion from dorsiflexion to plantarflexion.

	Side-to-Side Position Difference		**Side-to-Side Motion Difference**	
	Mean (SD)	95% CI	Mean (SD)	95% CI
ASD (mm)	0.7 (0.4)	0.5 – 0.9	0.6 (0.5)	0.3 – 0.8
MSD (mm)	0.6 (0.6)	0.3 – 0.9	0.5 (0.5)	0.3 – 0.7
PSD (mm)	0.8 (0.4)	0.5 – 1.0	0.5 (0.5)	0.2 – 0.7
TFCS (mm)	0.5 (0.3)	0.4 – 0.7	0.5 (0.4)	0.3 – 0.7
TFO (mm)	0.7 (0.5)	0.5 – 0.9	0.4 (3)	0.2 – 0.6
Sagittal Translation (mm)	0.9 (0.8)	0.5 – 1.3	0.6 (0.5)	0.3 – 0.8
Fibular Rotation (degrees)	3.1 (2.4)	1.9 – 4.3	2.3 (1.8)	1.5 – 3.2
Syndesmotic Area (mm^2)	11 (7)	8 – 15	10 (10)	5 – 15

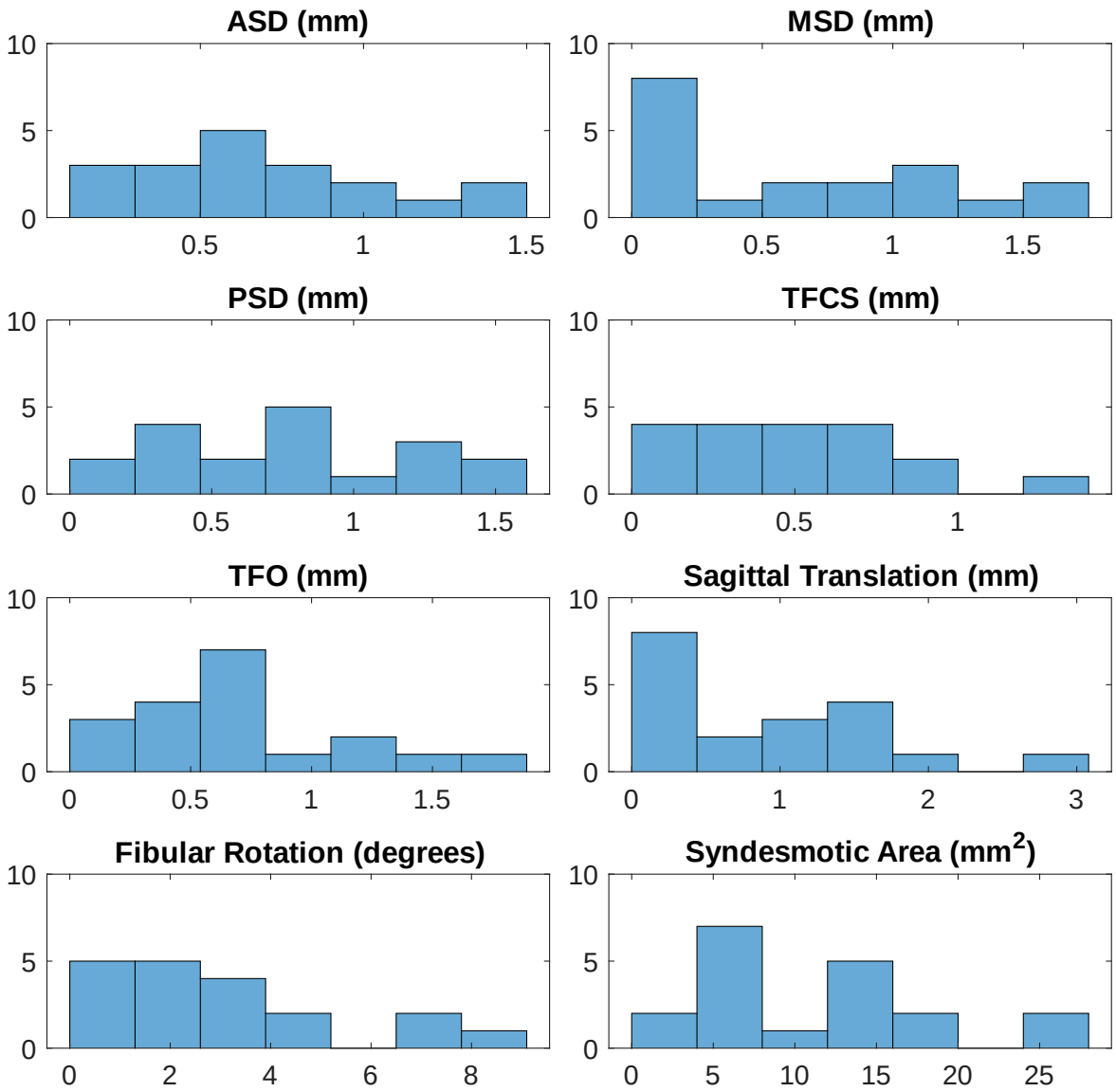

Figure 5.4: Distribution of side-to-side differences in syndesmotic position with the ankle in neutral. The y-axis indicates number of patients and the x-axis indicates the value for each syndesmotic measurement.

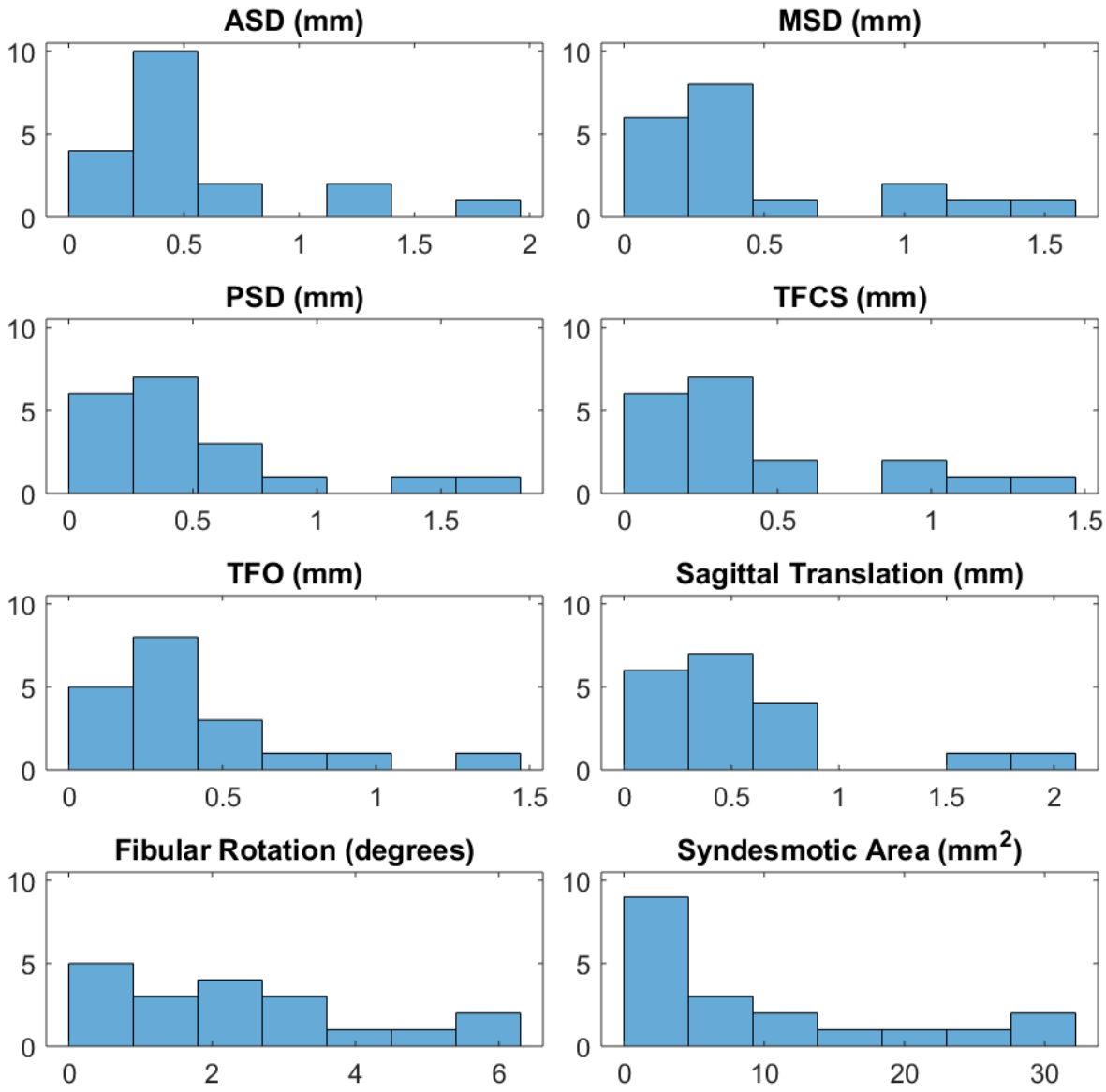

Figure 5.5: Distribution of side-to-side differences in syndesmotic motion between dorsiflexion and plantarflexion. The y-axis indicates number of patients and the x-axis indicates the value for each syndesmotic measurement.

5.4. Discussion

Achieving accurate reduction of the syndesmosis is challenging, especially given the wide variation in normal anatomy and numerous different measures of reduction. Current measures have not accounted

for normal syndesmotic motion when judging reduction which puts patients at risk of inferior functional outcomes.

5.4.1. Normal Position and Motion

This study shows that commonly used measures of syndesmotic width and fibular rotation vary significantly with ankle ROM. These measurements were chosen due to their common use in clinical practice, demonstrated repeatability, and sensitivity in detecting injury.[24,25,34–38]

The values determined for each syndesmotic measurement at neutral dorsiflexion are comparable to those previously reported.[24,25,34] We show slightly less variation in values than previously. This may be due to our calculation of these values from a mixed effects model incorporating 10 timepoints per ankle, or from the resulting standardized ankle position.

In various biomechanical studies, the fibula translates medially 0.8 – 3 mm, 0.9 – 1.3 mm anteriorly, and rotates 0.5° – 3.7° internally with plantarflexion.[5,6] Mousavian et al.[7] have also investigated the change in syndesmotic measurements through ankle ROM using 4DCT. When investigating 10 uninjured, unilateral ankles, the only significant change was 0.7 mm of posterior translation with plantarflexion, contrary to the prior studies showing anterior translation.[7] The current study found a decrease in syndesmotic width of up to 1.1 mm and area by 26 mm^2, consistent with existing literature, which can be explained by the greater width of the talar dome in dorsiflexion compared to plantarflexion. No change in sagittal translation was detected in the present study, perhaps due to our imaging protocol which was unloaded and had subjects perform a comfortable range of motion. This protocol could potentially lead to

submaximal motion and extremes of motion may not have been captured with the 0.9 second imaging intervals. Differences in methodology may explain discrepancies between our results and biomechanical motion studies. These studies were either cadaveric experiments where the soft tissues were denuded and the ankle was moved passively, or *in vivo* studies using radiostereometric analysis. In either case, these subjects were imaged in an upright position compared to our supine study. Prior work has also demonstrated that x-rays have poor accuracy for detecting positional changes at the distal tibiofibular joint.[39,40] Mousavian et al.'s[7] findings may also be different due to their method of measuring sagittal translation, based off a tangent line drawn from the anterolateral fibula, which would also be impacted by fibular rotation. Our automated measurement program found 1.2° of fibular external rotation with ankle plantarflexion on average. Some amount of external rotation was seen in 70% of ankles (35 of 50). While previous studies have shown predominantly internal rotation, external rotation has been reported in some subjects.[5] Estimates of fibular rotation from x-ray are inaccurate,[41,42] so prior estimates of the change in fibular rotation are based on cadaveric studies.[5,43] Again, it is possible that contributions from intact soft tissue attachments and active muscular contraction could explain why external rotation was found *in vivo*.

Normal syndesmotic motion has important implications on imaging and fixation of syndesmotic injuries. Previous authors demonstrated that rigid fixation of the syndesmosis need not be performed at a specific ankle position.[44,45] However, these conclusions were based off the restoration of ankle ROM, and not syndesmotic reduction. In addition to this study, Nault et al.[46] demonstrated increases in syndesmotic width with ankle plantarflexion, as did Koretkangas et al.,[47] who performed intraoperative CT scans and detected seven malreductions after flexible fixation. In these cases, open exploration was performed intending to revise the reduction, but each ankle was found to be well reduced under direct inspection and on subsequent CT scans at 0° dorsiflexion.[47] Therefore, ankle position should be considered when

performing fixation and imaging of these injuries if we wish to obtain an anatomic reduction. A syndesmosis rigidly fixed in dorsiflexion may become under compressed and internally rotated in plantarflexion while fixation in plantarflexion may produce over-compression and external rotation of the syndesmosis in dorsiflexion. If not accounted for, syndesmotic motion may explain why even when using intraoperative CT malreduction rates can remain as high as 38%.[20,48]

Given the demonstrated motion at the syndesmosis, we should seek to restore both position and motion of the syndesmosis to optimize outcomes for patients after injury. Though seemingly small, this syndesmotic motion impacts ankle kinematics and joint contact mechanics. If motion is not restored, joint contact area is reduced, leading to earlier cartilage degradation, and impingement or instability are possible.[49–51]

5.4.2. Side-to-Side Variability

Imaging of bilateral ankles demonstrated mild side-to-side variability, as shown previously.[24,36,52] Only one subject out of 19 had a single side-to-side measurement difference of 2 mm, a common threshold for malreduction.[51,53,54] Three of 19 had asymmetry in rotational measurements greater than 5° indicating that wider thresholds should be used when determining rotational malreduction based on the contralateral side. This supports work by Warner et al.[55] who found no functional difference in patients with a mean rotational asymmetry of 5.75° after syndesmotic injury, and Vasarhelyi et al.[51] who proposed 10° – 15° as a cutoff after which AOFAS scores worsened. Like position, side-to-side motion demonstrated only mild variability.

5.4.3. Age and Sex Related Changes

The only impact of age found was a small increase in fibular internal rotation with increasing age. It is possible that this finding represents type I error. If not, one potential explanation is that the distal fibular articular cartilage is in closer proximity anteriorly, and may thin with aging, leading to increased internal rotation. If degenerative changes do occur, they are not large enough to detect significant changes in syndesmotic widths. Most studies found no age related changes in syndesmotic measurements, though increased internal rotation has been reported.[56]

This study found no difference in position measurements between sexes, though there was a significant difference in PSD motion between males and females. Studies of normal position using various modalities have varying results, but in general show greater measurements of syndesmotic width or sagittal translation in males due to larger joint sizes overall.[24,36,52] Syndesmotic area is highly sensitive to changes in syndesmotic width and was larger in males in the current study, but failed to reach statistical significance ($p = 0.067$), indicating the effect size was too small to detect in our sample. Currently, no separate malreduction cutoffs for males and females exist, though some advocate for this, based on different average joint sizes.[36]

5.4.4. Limitations

The study investigated the impact of ankle ROM on syndesmotic position in a supine position. Therefore, the presented data is in a non-weightbearing condition and it is known that gravity imparts a posterior force on the fibula. One study has shown a change in syndesmotic position with weightbearing,[43] though it was performed on denuded cadavers, while other studies have failed to find significant changes between loaded and unloaded conditions in both *in vitro* and *in vivo* experiments.[1,57] As the CT protocol

captured 4DCT timepoints at regular intervals, we cannot guarantee that extremes of motion or specific positions were captured for direct comparison. This was overcome with the linear mixed effects model which was able to model each syndesmotic measurement as a function of tibiotalar angle and interpolate or extrapolate to a standard position as required, while still accounting for the variation within individual ankle datasets.

5.4.5. Strengths

Strengths of this study include use of an emerging technology, 4DCT, to accurately measure motion *in vivo*. 4DCT in peripheral extremities has a low radiation dose, less than a chest x-ray in our study, or approximately equivalent to 10 days of background atmospheric radiation. Syndesmotic measurements were calculated 10 times per specimen to model reduction throughout ROM. The automated measurement process achieved sub-voxel size registration accuracy and completed measurements automatically ensuring repeatable and accurate measurements. This process has allowed us to perform the largest study of motion to our knowledge and is the first to report on side-to-side motion variation in normal individuals. We also included a substantial cohort of healthy control participants to ensure truly asymptomatic, normal ankles.

5.5. Conclusion

This study has demonstrated that there is significant syndesmotic motion during ankle ROM, thereby impacting common measures of reduction. It is important to appreciate and standardize foot position when using conventional imaging and performing reductions of the syndesmosis. Consideration should be given to restoring motion as well as position after syndesmotic injuries. Syndesmotic position and

motion are consistent within subjects, therefore the contralateral ankle may be used to template for anatomic reduction, provided ankle position is standardized.

5.6. Supplementary Tables and Figures

Table 5.3: Functional outcome measures for the uninjured control population.

PARTICIPANT	AOFAS	FAAM: ACTIVITIES OF DAILY LIVING SUBSECTION	FAAM: SPORTS SUBSECTION	OLERUD AND MOLANDER	VAS
1	100	100	100	100	0
2	100	100	100	100	0
3	100	100	100	100	0
4	100	100	100	100	0
5	100	100	100	100	0
6	100	100	100	100	0
7	100	100	100	100	0
8	100	100	100	100	0
9	100	100	100	100	0
10	100	100	100	100	0
11	100	100	100	100	0
12	100	100	100	100	0
13	100	100	100	100	0

14	100	100	100	100	0
15	100	100	100	100	0
16	100	100	100	100	0
17	100	100	100	95	0
18	100	100	100	100	0
19	100	100	100	100	0

Table 5.4: Syndesmotic position and motion stratified by study group.

	POSITION				MOTION			
	Uninjured Controls	RCT	Prospective Cohort	P-value between groups	Uninjured Controls	RCT	Prospective Cohort	P-value between groups
ASD (MM)	3.26	3.41	3.31	0.91	-0.63	-0.81	-0.71	0.69
MSD (MM)	3.40	3.29	3.66	0.74	-1.14	-1.03	-1.06	0.87
PSD (MM)	6.08	5.95	6.66	0.56	-0.97	-0.48	-0.61	0.15
TFCS (MM)	3.83	3.74	4.14	0.72	-1.15	-1.05	-1.09	0.9
TFO (MM)	-0.32	-0.37	-0.29	0.99	1.15	1.05	1.09	0.9
SAGITTAL TRANSLATION (MM)	0.35	0.98	0.41	0.4	0.25	-0.23	0.01	0.15
FIBULAR ROTATION (DEGREES)	18.18	17.86	19.15	0.93	-1.42	-1.20	-0.09	0.32
SYNDESMOTIC AREA (MM^2)	118.57	123.44	131.75	0.54	-26.13	-25.24	-25.72	0.98

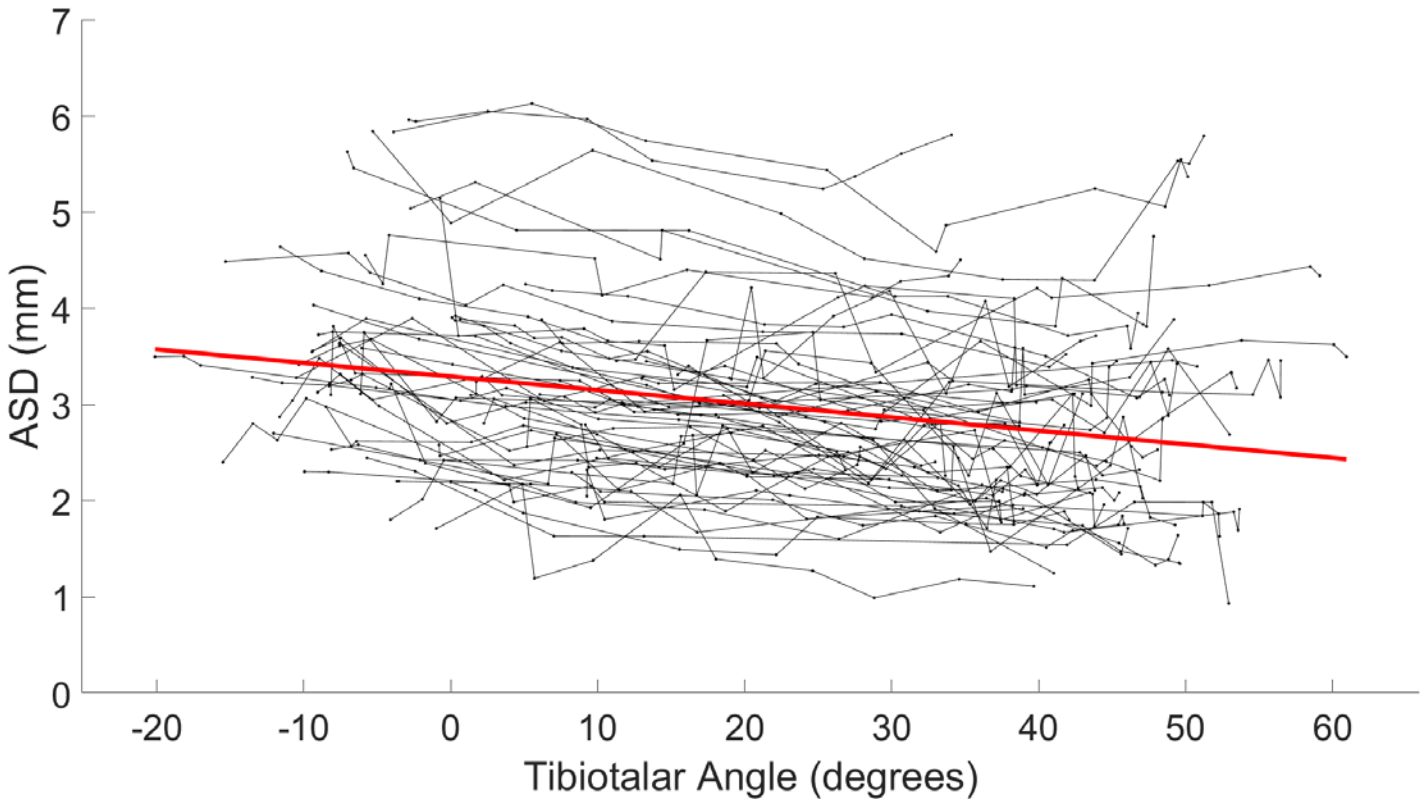

Figure 5.6: Individual ankle ASD versus tibiotalar angle plots with overall trendline.

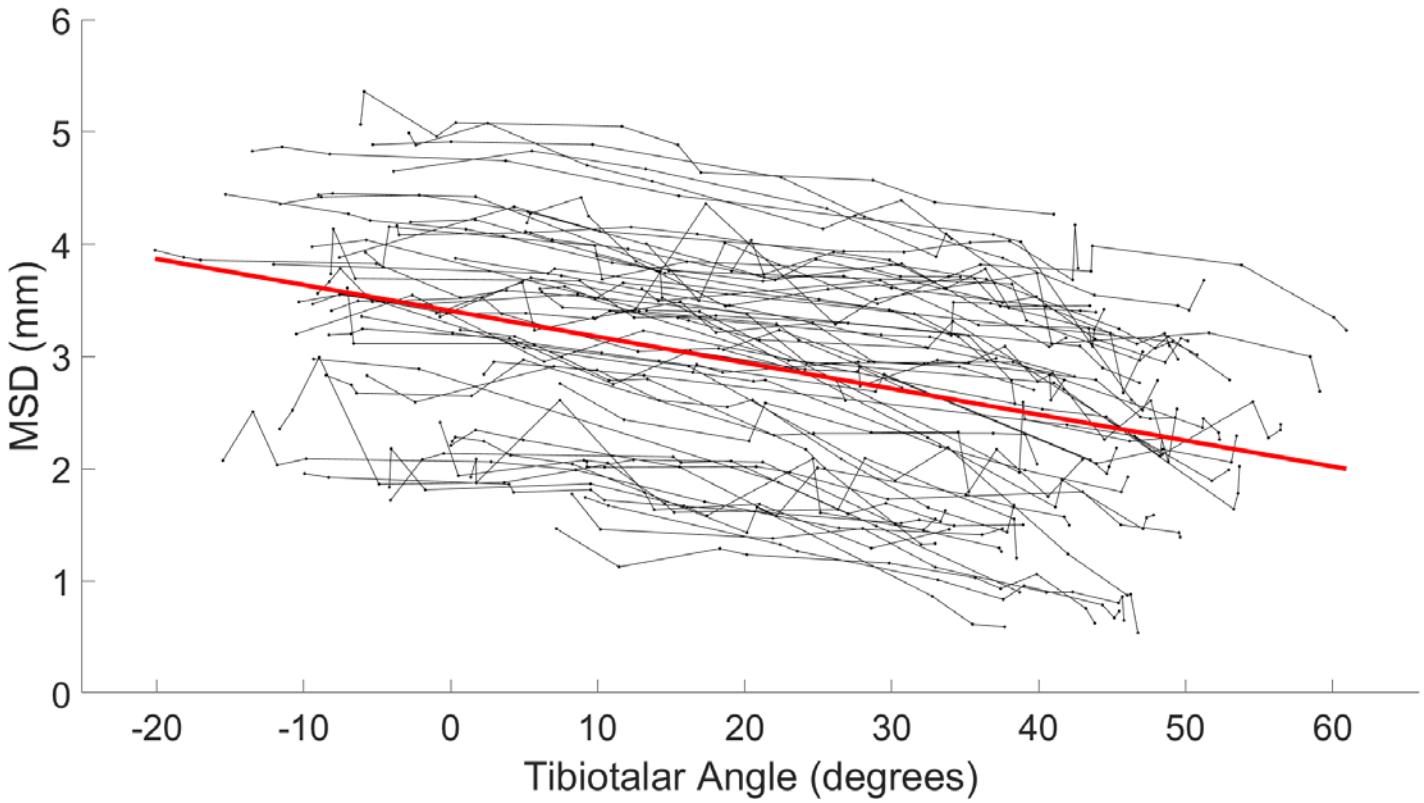

Figure 5.7: Individual ankle MSD versus tibiotalar angle plots with overall trendline.

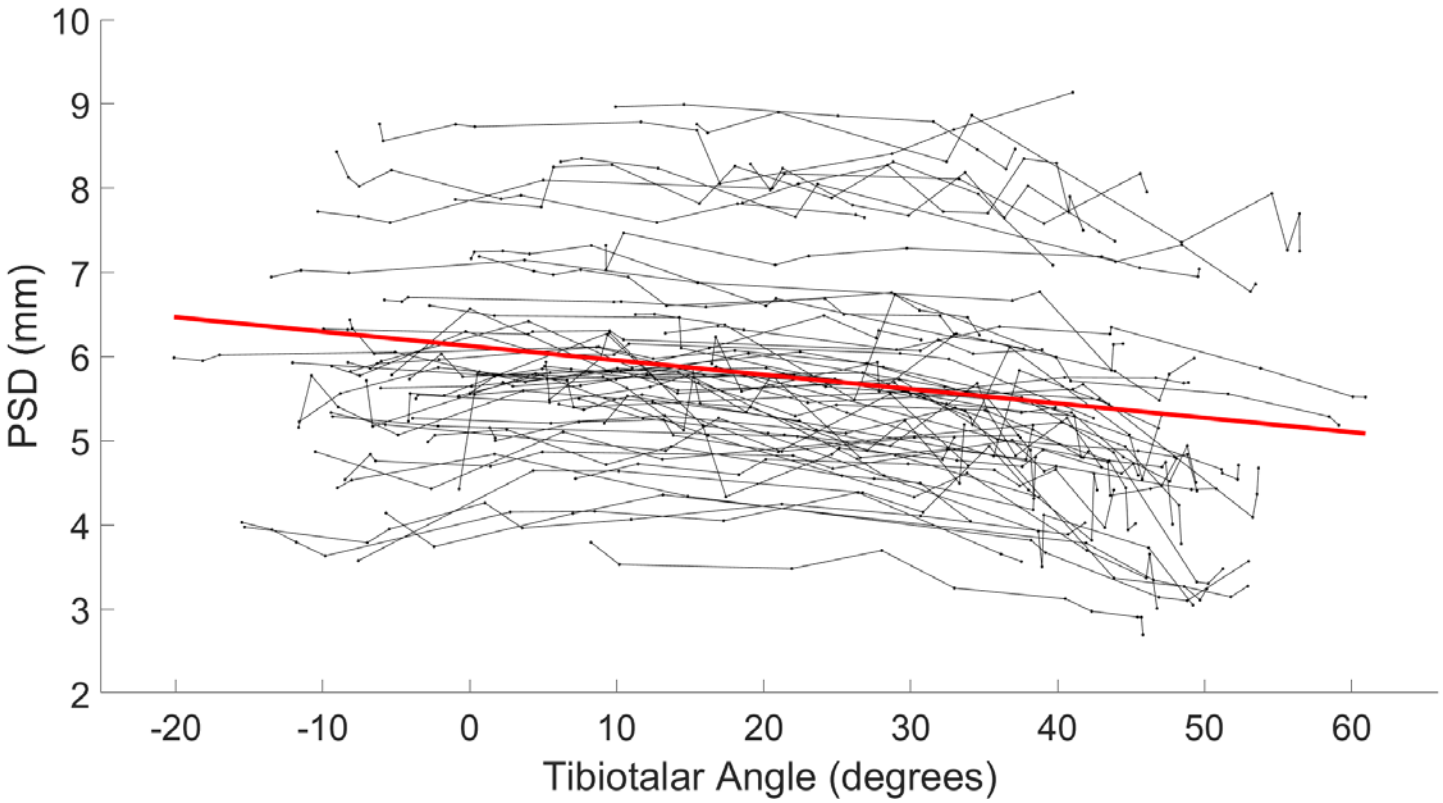

Figure 5.8: Individual ankle PSD versus tibiotalar angle plots with overall trendline.

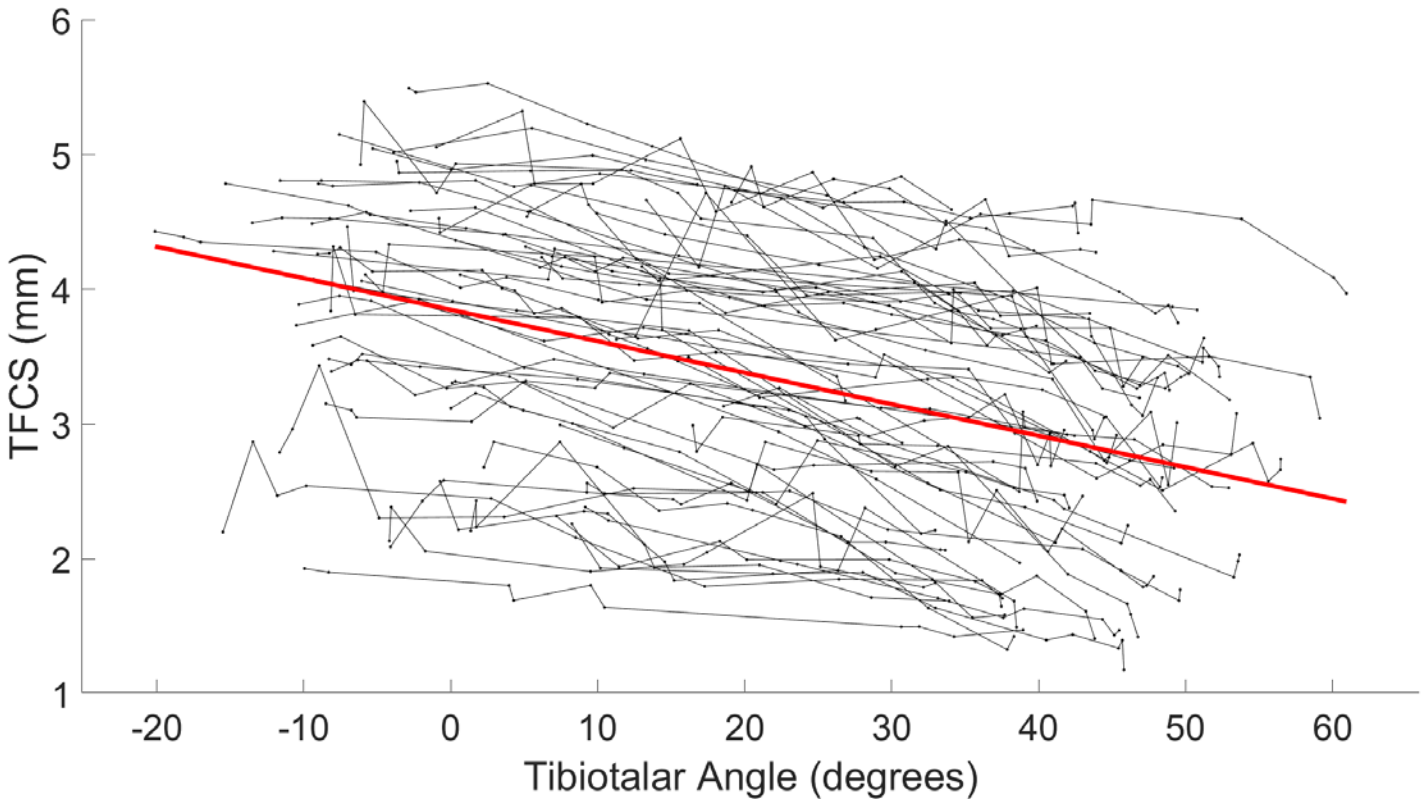

Figure 5.9: Individual ankle TFCS versus tibiotalar angle plots with overall trendline.

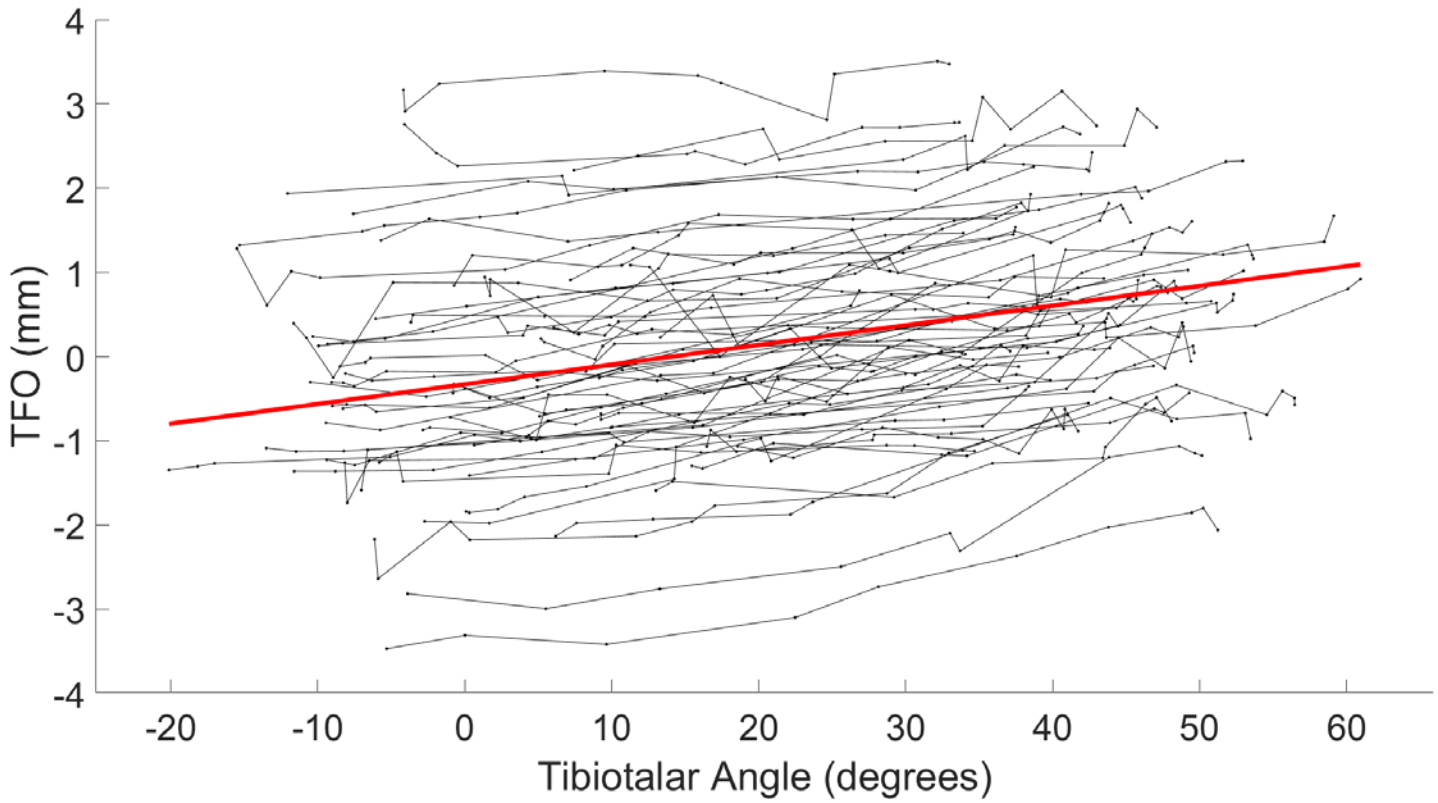

Figure 5.10: Individual ankle TFO versus tibiotalar angle plots with overall trendline.

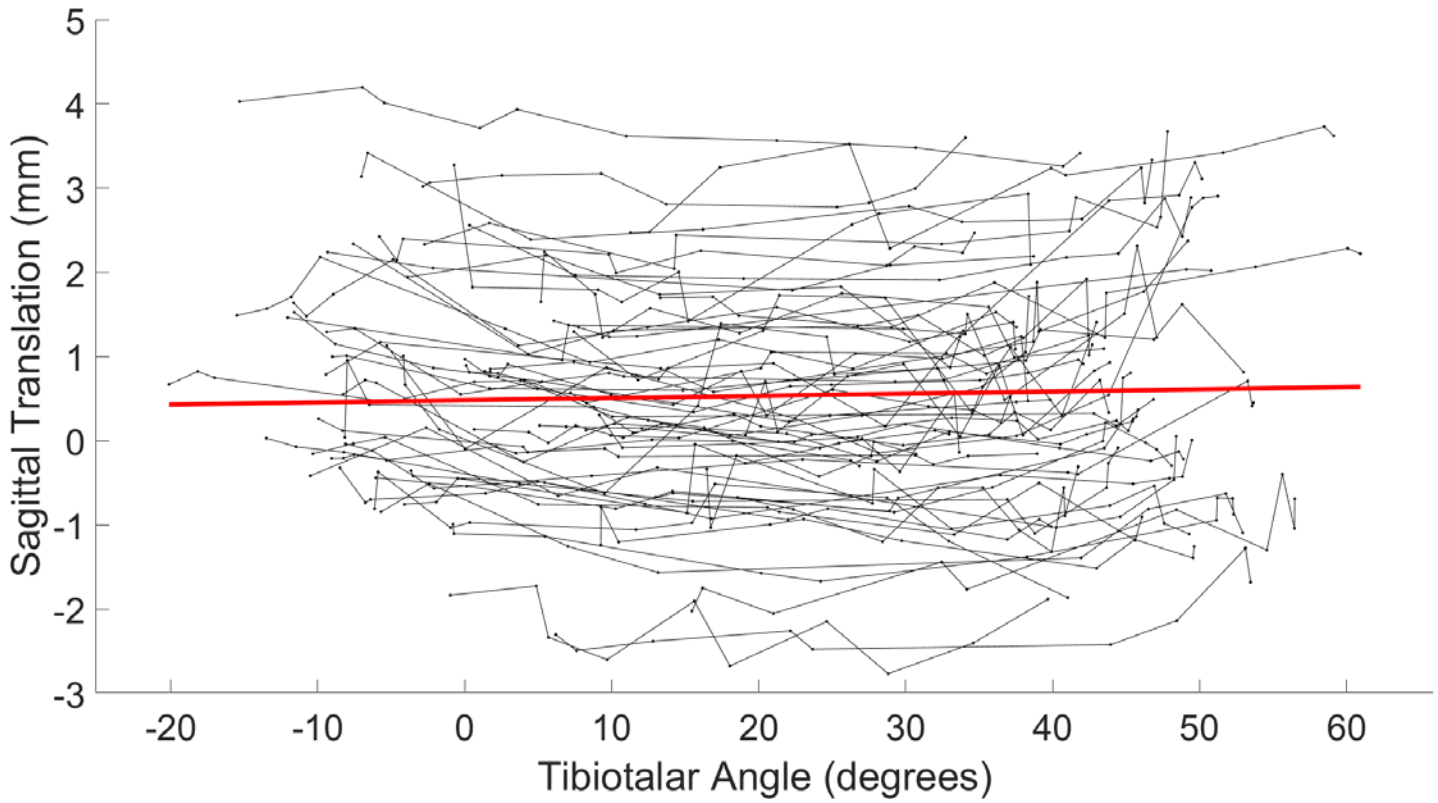

Figure 5.11: Individual ankle sagittal translation versus tibiotalar angle plots with overall trendline.

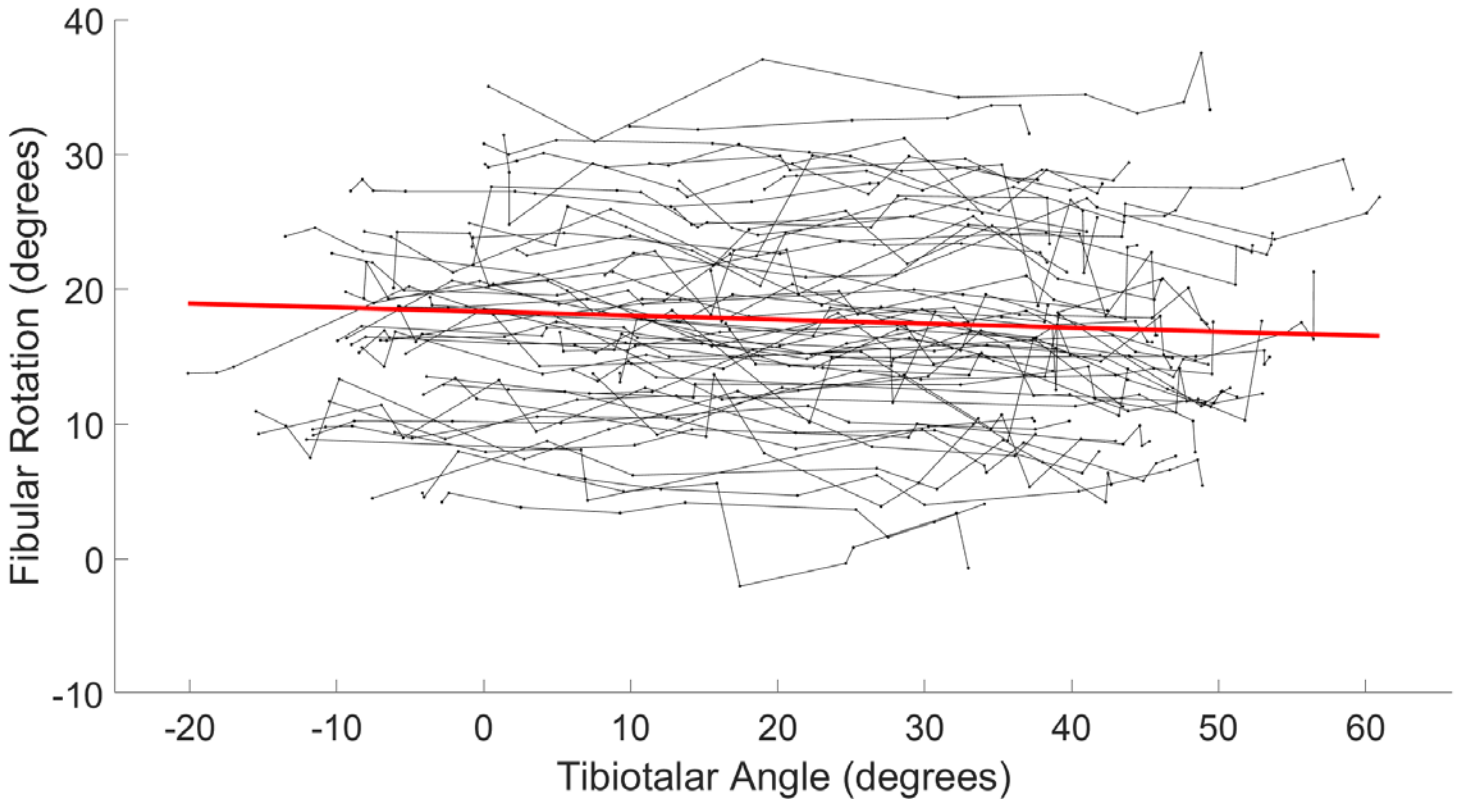

Figure 5.12: Individual ankle fibular rotation versus tibiotalar angle plots with overall trendline.

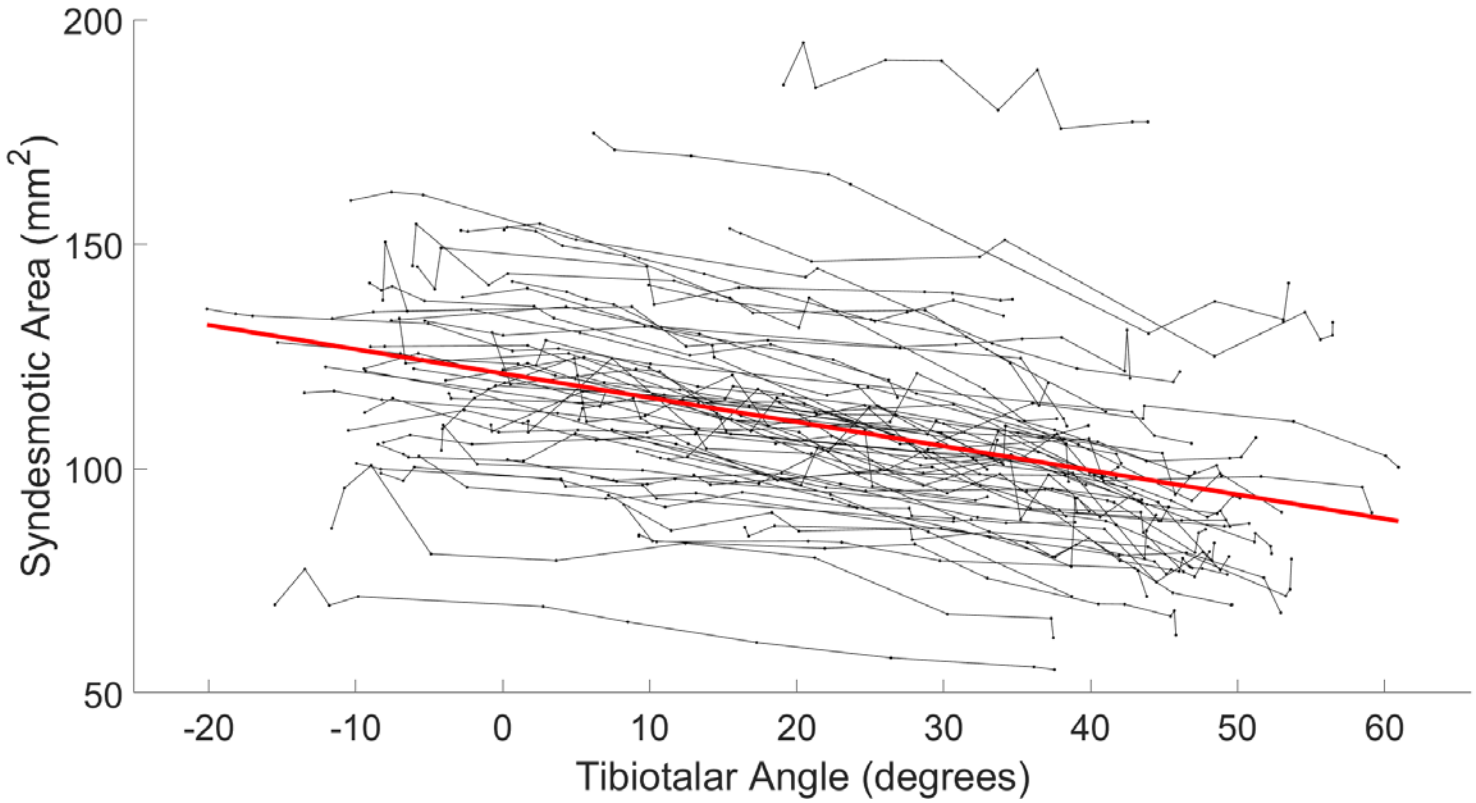

Figure 5.13: Individual ankle syndesmotic area versus tibiotalar angle plots with overall trendline.

5.7. References

1. Clanton, TO, Williams, BT, Backus, JD, Dornan, GJ, Liechti, DJ, Whitlow, SR, Saroki, AJ, Turnbull, TL, Laprade, RF: Biomechanical Analysis of the Individual Ligament Contributions to Syndesmotic Stability. *Foot Ankle Int* 2017;38:66–75.

2. Ebraheim, NA, Taser, F, Shafiq, Q, Yeasting, RA: Anatomical evaluation and clinical importance of the tibiofibular syndesmosis ligaments. *Surg Radiol Anat* 2006;28:142–149.

3. Hermans, JJ, Beumer, A, De Jong, TAW, Kleinrensink, GJ: Anatomy of the distal tibiofibular syndesmosis in adults: A pictorial essay with a multimodality approach. *J Anat* 2010;217:633–645.

4. Lin, CF, Gross, MT, Weinhold, P: Ankle syndesmosis injuries: Anatomy, biomechanics, mechanism of injury, and clinical guidelines for diagnosis and intervention. *J Orthop Sports Phys Ther* 2006;36:372–384.

5. Huber, T, Schmoelz, W, Bölderl, A: Motion of the fibula relative to the tibia and its alterations with syndesmosis screws: A cadaver study. *Foot Ankle Surg* 2012;18:203–209.

6. Rammelt, S, Obruba, P: An update on the evaluation and treatment of syndesmotic injuries. *Eur J Trauma Emerg Surg* 2015;41:601–614.

7. Mousavian, A, Shakoor, D, Hafezi-Nejad, N, Haj-Mirzaian, A, de Cesar Netto, C, Orapin, J, Schon, LC, Demehri, S: Tibiofibular syndesmosis in asymptomatic ankles: initial kinematic analysis using four-dimensional CT. *Clin Radiol* 2019;74:571.e1-571.e8.

8. Krähenbühl, N, Weinberg, MW, Davidson, NP, Mills, MK, Hintermann, B, Saltzman, CL, Barg, A: Imaging in syndesmotic injury: a systematic literature review. *Skeletal Radiol* 2017;47:631–648.

9. Zalavras, C, Thordarson, D: Ankle syndesmotic injury. *J Am Acad Orthop Surg* 2007;15:330–339.

10. Carr, JC, Werner, BC, Yarboro, SR: An Update on Management of Syndesmosis Injury: A National US Database Study. *Am J Orthop (Belle Mead NJ)* 2016;45:E472–E477.

11. Hamid, N, Loeffler, BJ, Braddy, W, Kellam, JF, Cohen, BE, Bosse, MJ: Outcome after fixation of ankle fractures with an injury to the syndesmosis. *J Bone Joint Surg Br* 2009;91-B:1069–1073.

12. Schepers, T: Acute distal tibiofibular syndesmosis injury: A systematic review of suture-button versus syndesmotic screw repair. *Int Orthop* 2012;36:1199–1206.

13. Andersen, MR, Frihagen, F, Hellund, JC, Madsen, JE, Figved, W: Randomized trial comparing suture button with single syndesmotic screw for syndesmosis injury. *J Bone Jt Surg - Am Vol* 2018;100:2–12.

14. Sanders, D, Schneider, P, Taylor, M, Tieszer, C, Lawendy, A-R: Improved Reduction of the Tibiofibular Syndesmosis with Tightrope Compared to Screw Fixation: Results of a Randomized Controlled Study. *J Orthop Trauma* 2019;3:2473011418S0012.

15. Ray, R, Koohnejad, N, Clement, ND, Keenan, GF: Ankle fractures with syndesmotic stabilisation are associated with a high rate of secondary osteoarthritis. *Foot Ankle Surg* 2019;25:180–185.

16. Hunt, KJ, Goeb, Y, Behn, AW, Criswell, B, Chou, L: Ankle Joint Contact Loads and Displacement with Progressive Syndesmotic Injury. *Foot Ankle Int* 2015;36:1095–1103.

17. Weening, B, Bhandari, M: Predictors of functional outcome following transsyndesmotic screw fixation of ankle fractures. *J Orthop Trauma* 2005;19:102–108.

18. Sagi, HC, Shah, AR, Sanders, RW: The Functional Consequence of Syndesmotic Joint Malreduction at a Minimum 2-Year Follow-Up. *J Orthop Trauma* 2012;26:439–443.

19. LaMothe, J, Baxter, JR, Gilbert, S, Murphy, CI, Karnovsky, SC, Drakos, MC: Effect of Complete Syndesmotic Disruption and Deltoid Injuries and Different Reduction Methods on Ankle Joint Contact Mechanics. *Foot Ankle Int* 2017;38:694–700.

20. Davidovitch, RI, Weil, Y, Karia, R, Forman, J, Looze, C, Liebergall, M, Egol, K: Intraoperative syndesmotic reduction: Three-dimensional versus standard fluoroscopic imaging. *J Bone Jt Surg* 2013;95:1838–1843.

21. Franke, J, Recum, J Von, Suda, AJ, Gr, PA, Wendl, K: Intraoperative 3D imaging in the treatment of unstable syndesmotic injuries. *J Bone Jt Surg* 2012;94:1386.

22. Park, YH, Ahn, JH, Choi, GW, Kim, HJ: Comparison of Clamp Reduction and Manual Reduction of Syndesmosis in Rotational Ankle Fractures: A Prospective Randomized Trial. *J Foot Ankle Surg* 2018;57:19–22.

23. Cosgrove, CT, Spraggs-Hughes, AG, Putnam, SM, Ricci, WM, Miller, AN, McAndrew, CM, Gardner, MJ: A novel indirect reduction technique in ankle syndesmotic injuries: A cadaveric study. *J Orthop Trauma* 2018;32:361–367.

24. Dikos, GD, Heisler, J, Choplin, RH, Weber, TG: Normal Tibiofibular Relationships at the Syndesmosis on Axial CT Imaging. *J Orthop Trauma* 2012;26:433–438.

25. Nault, M-LL, Hébert-Davies, J, Laflamme, G-YY, Leduc, S: CT scan assessment of the syndesmosis: A new reproducible method. *J Orthop Trauma* 2013;27:638–641.

26. Elgafy, H, Semaan, HB, Blessinger, B, Wassef, A, Ebraheim, NA: Computed tomography of normal distal tibiofibular syndesmosis. *Skeletal Radiol* 2010;39:559–564.

27. Kwong, Y, Mel, AO, Wheeler, G, Troupis, JM: Four-dimensional computed tomography (4DCT): A review of the current status and applications. *J Med Imaging Radiat Oncol* 2015;59:545–554.

28. Hurlock, GS, Higashino, H, Mochizuki, T: History of cardiac computed tomography: Single to 320-detector row multislice computed tomography. *Int J Cardiovasc Imaging* 2009;25:31–42.

29. Lombard, C, Gervaise, A, Villani, N, Louis, M, Raymond, A, Blum, A, Teixeira, PAG: The Impact of Dose Reduction in Quantitative Kinematic CT of Ankle Joints Using a Full Model-Based Iterative Reconstruction Algorithm: A Cadaveric Study. *Am J Roentgenol* 2018;210:396–403.

30. Biswas, D, Bible, JE, Bohan, M, Simpson, AK, Whang, PG, Grauer, JN: Radiation exposure from musculoskeletal computerized tomographic scans. *J Bone Jt Surg - Ser A* 2009;91:1882–1889.

31. Gervaise, A, Teixeira, P, Villani, N, Lecocq, S, Louis, M, Blum, A: CT dose optimisation and reduction in osteoarticular disease. *Diagn Interv Imaging* 2013;94:371–388.

32. Morellato, J, Louati, H, Bodrogi, A, Stewart, A, Papp, S, Liew, A, Gofton, W: The Effect of Varying Tension of a Suture Button Construct in Fixation of the Tibiofibular Syndesmosis - Evaluation Using Stress Computed Tomography. *J Orthop Trauma* 2017;31:103–110.

33. Lepojärvi, S, Niinimäki, J, Pakarinen, H, Leskelä, HV: Rotational Dynamics of the Normal Distal Tibiofibular Joint With Weight-Bearing Computed Tomography. *Foot Ankle Int* 2016;37:627–635.

34. Malhotra, G, Cameron, J, Toolan, BC: Diagnosing chronic diastasis of the syndesmosis: A novel measurement using computed tomography. *Foot Ankle Int* 2014;35:483–488.

35. Schon, JM, Brady, AW, Krob, JJ, Lockard, CA, Marchetti, DC, Dornan, GJ, Clanton, TO: Defining the three most responsive and specific CT measurements of ankle syndesmotic malreduction. *Knee Surgery, Sport Traumatol Arthrosc* 2019;27:

36. Lepojärvi, S, Pakarinen, H, Savola, O, Haapea, M, Sequeiros, RB, Niinimäki, J: Posterior translation of the fibula may indicate malreduction: CT study of normal variation in uninjured ankles. *J Orthop Trauma* 2014;28:205–209.

37. van den Heuvel, SB, Dingemans, SA, Gardenbroek, TJ, Schepers, T: Assessing Quality of Syndesmotic Reduction in Surgically Treated Acute Syndesmotic Injuries: A Systematic Review. *J Foot Ankle Surg* 2019;58:144–150.

38. Hagemeijer, NC, Chang, SH, Abdelaziz, ME, Casey, JC, Waryasz, GR, Guss, D, DiGiovanni, CW: Range of Normal and Abnormal Syndesmotic Measurements Using Weightbearing CT. *Foot Ankle Int* 2019;40:

39. Ebraheim, NA, Lu, J, Yang, H, Mekhail, AO, Yeasting, RA: Radiographic and CT Evaluation of Tibiofibular Syndesmotic Diastasis: A Cadaver Study. *Foot Ankle Int* 1997;18:693–698.

40. Beumer, A, Van Hemert, WLW, Niesing, R, Entius, CAC, Ginai, AZ, Mulder, PGH, Swierstra, BA: Radiographic measurement of the distal tibiofibular syndesmosis has limited use. *Clin Orthop Relat Res* 2004;227–234.doi:10.1097/01.blo.0000129152.81015.ad.

41. Marmor, M, Hansen, E, Han, HK, Buckley, J, Matityahu, A: Limitations of standard fluoroscopy in detecting rotational malreduction of the syndesmosis in an ankle fracture model. *Foot Ankle Int* 2011;32:616–622.

42. Knops, SP, Kohn, MA, Hansen, EN, Matityahu, A, Marmor, M: Rotational malreduction of the syndesmosis: Reliability and accuracy of computed tomography measurement methods. *Foot Ankle Int* 2013;34:1403–1410.

43. Hu, WK, Chen, DW, Li, B, Yang, YF, Yu, GR: Motion of the distal tibiofibular syndesmosis under different loading patterns: A biomechanical study. *J Orthop Surg* 2019;27:1–6.

44. Gonzalez, T, Egan, J, Ghorbanhoseini, M, Blais, M, Lechtig, A, Velasco, B, Nazarian, A, Kwon, JY: Overtightening of the syndesmosis revisited and the effect of syndesmotic malreduction on ankle dorsiflexion. *Injury* 2017;48:1253–1257.

45. Tornetta, P, Spoo, JE, Reynolds, FA, Lee, C: Overtightening of the ankle syndesmosis: Is it really possible? *J Bone Jt Surg - Ser A* 2001;83:489–492.

46. Nault, ML, Marien, M, Hébert-Davies, J, Laflamme, GY, Pelsser, V, Rouleau, DM, Gosselin-Papadopoulos, N, Leduc, S: MRI Quantification of the Impact of Ankle Position on Syndesmosis Anatomy. *Foot Ankle Int* 2017;38:215–219.

47. Kortekangas, T, Savola, O, Flinkkilä, T, Lepojärvi, S, Nortunen, S, Ohtonen, P, Katisko, J, Pakarinen, H: A prospective randomised study comparing TightRope and syndesmotic screw fixation for accuracy and

maintenance of syndesmotic reduction assessed with bilateral computed tomography. *Injury* 2015;46:1119–1126.

48. Cherney, SM, Spraggs-Hughes, AG, McAndrew, CM, Ricci, WM, Gardner, MJ: Incisura Morphology as a Risk Factor for Syndesmotic Malreduction. *Foot Ankle Int* 2016;37:748–754.

49. Pereira, DS, Koval, KJ, Resnick, RB, Sheskier, SC, Kummer, F, Zuckerman, JD: Tibiotalar Contact Area and Pressure Distribution: The Effect of Mortise Widening and Syndesmosis Fixation. *Foot Ankle Int* 1996;17:269–274.

50. Lamothe, JM, Baxter, JR, Murphy, C, Gilbert, S, Desandis, B, Drakos, MC: Three-Dimensional Analysis of Fibular Motion after Fixation of Syndesmotic Injuries with a Screw or Suture-Button Construct. *Foot Ankle Int* 2016;37:1350–1356.

51. Vasarhelyi, A, Lubitz, J, Gierer, P, Gradl, G, Rosler, K, Hopfenmuller, W, Klaue, K, Mittlmeier, TWF: Detection of fibular torsional deformities after surgery for ankle fractures with a novel CT method. *Foot Ankle Int* 2006;27:1115–1121.

52. Shah, AS, Kadakia, AR, Tan, GJ, Karadsheh, MS, Wolter, TD, Sabb, B: Radiographic Evaluation of the Normal Distal Tibiofibular Syndesmosis. *Foot Ankle Int* 2012;33:870–876.

53. Ramsey, PL, Hamilton, W: Changes in tibiotalar area of contact caused by lateral talar shift. *J Bone Joint Surg Am* 1976;58:356–7.

54. Gardner, MJ, Demetrakopoulos, D, Briggs, SM, Helfet, DL, Lorich, DG: Malreduction of the Tibiofibular Syndesmosis in Ankle Fractures. *Foot Ankle Int* 2006;27:788–792.

55. Warner, SJ, Fabricant, PD, Garner, MR, Schottel, PC, Helfet, DL, Lorich, DG: The Measurement and Clinical Importance of Syndesmotic Reduction After Operative Fixation of Rotational Ankle Fractures. *J Bone Jt Surg* 2015;97:1935–1944.

56. Prakash, AA: Syndesmotic stability: Is there a radiological normal?—A systematic review. *Foot Ankle Surg* 2018;24:174–184.

57. Beumer, A, Valstar, ER, Garling, EH, Niesing, R, Ranstam, J, Löfvenberg, R, Swierstra, BA: Kinematics of the distal tibiofibular syndesmosis: Radiostereometry in 11 normal ankles. *Acta Orthop Scand* 2003;74:337–343.

6. Syndesmotic Motion after Injury

6.1. Introduction

Syndesmotic injuries are present in up to 25% of ankle fractures.[1,2] The historic gold standard treatment of syndesmotic injuries is rigid screw fixation.[2] However, increasing evidence demonstrates improved reduction and functional outcomes with flexible fixation using suture button devices such as the Tightrope® (Arthrex, Naples, USA).[3,4] Despite advances in fixation methods, malreduction and impaired function remain common problems.[3,5,6]

Biomechanical studies have revealed that ankle dorsiflexion and plantarflexion leads to important syndesmotic motion in the coronal and sagittal planes, as well as fibular rotation.[7–10] This motion provides ankle stability, accommodating the irregularly shaped talus, and minimizes joint contact stresses through a congruent ankle joint.[8,11–15] Rigid fixation decreases this motion,[8,15–17] while there is concern flexible fixation does not adequately constrain fibular motion.[18–20]

Differences between the injured and uninjured ankle on CT are commonly used to assess syndesmotic reduction.[21–23] These measures of reduction change throughout ankle ROM.[24,25] Therefore, a syndesmosis that is reduced in dorsiflexion may appear malreduced in plantarflexion, and vice versa. 4DCT, also known as dynamic CT, is a capability of many modern CT scanners which captures multiple three-dimensional CT volumes of the same region in rapid succession to create a moving four-dimensional image volume.[26]

Understanding the impact of fixation methods on syndesmotic motion using modalities such as 4DCT is important to achieve accurate reduction throughout ankle ROM. Restoring normal motion, as well as

position, after syndesmotic injuries may help improve functional outcomes as well. The purpose of this study was to investigate the impact of fixation methods on *in vivo* syndesmotic kinematics through ankle ROM. We hypothesized that flexible fixation of syndesmotic injuries would better recreate normal, uninjured motion when compared to rigid fixation.

6.2. Methods

6.2.1. Inclusion Criteria

A subset of patients from a multicentre randomized controlled trial were recruited for an *a priori* planned subgroup analysis (ClinicalTrials.gov identifier NCT02199249).[3] In this trial, patients with Weber C (AO/OTA 44C) fractures were recruited and randomized to rigid or flexible fixation. Inclusion criteria were a diagnosis of a closed Weber C fibula fracture, age greater than 18 years, and radiographic talar instability, as defined by medial clear space widening greater than 5 mm or talar shift greater than 1 mm on stress views. Exclusion criteria were patients with open or pathologic fractures, lack of instability on intraoperative imaging, concurrent injuries affecting rehabilitation, or history of severe ankle injury, ligamentous laxity, neuropathy, or osteoporosis. Patients were randomized using an online randomization tool prior to surgery. The study was approved by the institutional ethics review board (REB14-1142).

6.2.2. Surgical Technique

Surgery was performed within 14 days of injury. Standard AO Foundation technique was used to perform fibular, medial malleolar, and posterior malleolar fixation as required. Following fracture fixation, a fluoroscopic external rotation stress test assessed stability of the syndesmosis. Patients not meeting inclusion criteria for instability were withdrawn. Patients with instability had a direct, open reduction of

the syndesmosis performed followed by provisional clamp or thumb stabilization. If randomized to rigid fixation, patients underwent fixation with at least two 3.5 mm cortical screws with tri- or quadra-cortical fixation as per the surgeon's preference. Screws were at least 15 mm above the tibial plafond and a minimum of 10 mm apart. In the flexible fixation group, a knotless Tightrope® (Arthex, Naples, USA) suture-button was inserted following the manufacturer's technique guide, at least 15 mm above the tibial plafond. An ACL graft tensioner was used to apply a uniform tension of 20 lb to the suture-button, based on the optimal tension found by Morellato et al.[27] Post-operative rehabilitation was standardized with a plaster splint applied for the first two weeks, followed by a removable boot for four weeks, with ROM encouraged. Weightbearing began at six weeks post-operatively and the boot was discontinued by 12 weeks.

6.2.3. Data Acquisition

At 12 months post-operatively, a 4DCT of bilateral ankles was performed on the subgroup of patients from our centre who consented to 4DCT imaging. The same GE Medical Systems Revolution™ CT scanner (General Electric, Boston, USA) was used for all participants. A static CT scan at 120 kVp and 110 mA was completed prior to the 4DCT portion at 120 kVp and 70 mA. Slice dimensions were 300 mm by 300 mm and the axial scan length was 140 mm. Patients moved their ankles continuously between dorsiflexion and plantarflexion to the comfortable limits of motion. Ten 4DCT timepoints were imaged over a 9-second span. Effective radiation dose for the entire static CT and 4DCT scanning process was 0.06 mSv.[28]

6.2.4. Measurement Process

Using the initial static CT scan, 3D models of bilateral tibias, fibulas, and tali for each specimen were created with Mimics software (Materialise, Leuven, Belgium). At each 4DCT timepoint, a custom Matlab®

(MathWorks, Natick, USA) routine automatically segmented the CT volume into individual bones and registered the 3D models to their respective bones (Figure 6.1). The relative positions of the 3D models at each timepoint were used to automatically calculate multiple syndesmotic measurements without requiring user input. The tibiotalar angle was measured between the long axis of the tibia and the long axis of the talus where 0° was the talar axis perpendicular to the tibial axis and values increased with plantarflexion. The fibular axis was measured along the medial fibular articular border 5 mm below the plafond, then translated to bisect the fibula at the level of the syndesmosis (Figure 6.2D).[27] The plane used for syndesmotic measurements was perpendicular to the long axis of the tibia, 10 mm proximal to the plafond. The incisura axis was a tangent line fit to the lateral tibial border contacting the anterior and posterior edges of the incisura. ASD, MSD, and PSD were measured from the anterior- and posterior-most points of the incisura, and their midpoint along the incisura, to the closest corresponding edge of the fibula (Figure 6.2).[22] Analogous to plain x-ray measurements, TFCS was measured along a line perpendicular to the incisura axis between the most medial point on the fibula and most medial part of the incisura.[12,27] TFO was the distance along the same line between the most medial point on the fibula and most lateral part of the incisura.[12,27] Sagittal translation was measured parallel to the incisura axis from the anterior edge of the incisura to the most anterior point on the fibula, where positive values showed a fibula posterior to the anterior incisura edge.[22] The angle between the incisura axis and the fibular axis was used to measure fibular rotation, where fibular internal rotation was defined as positive values.[22] Syndesmotic area was determined by fitting tangent lines between the tibia and fibula anteriorly and posteriorly then finding the area bounded by these tangents.[29]

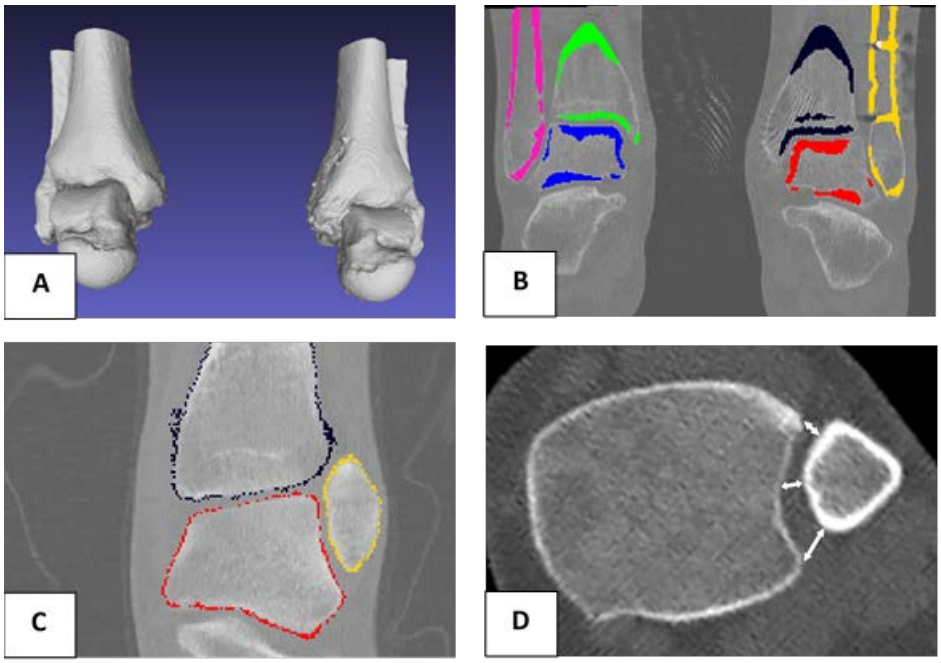

Figure 6.1: Automated measurement process. A: 3D reference models, B: Threshold based segmentation, C: reference models registered to 4DCT data, D: Automated syndesmosis measurements calculated based on registered models. An automated measurement process calculates multiple measurements at each 4DCT timepoint.

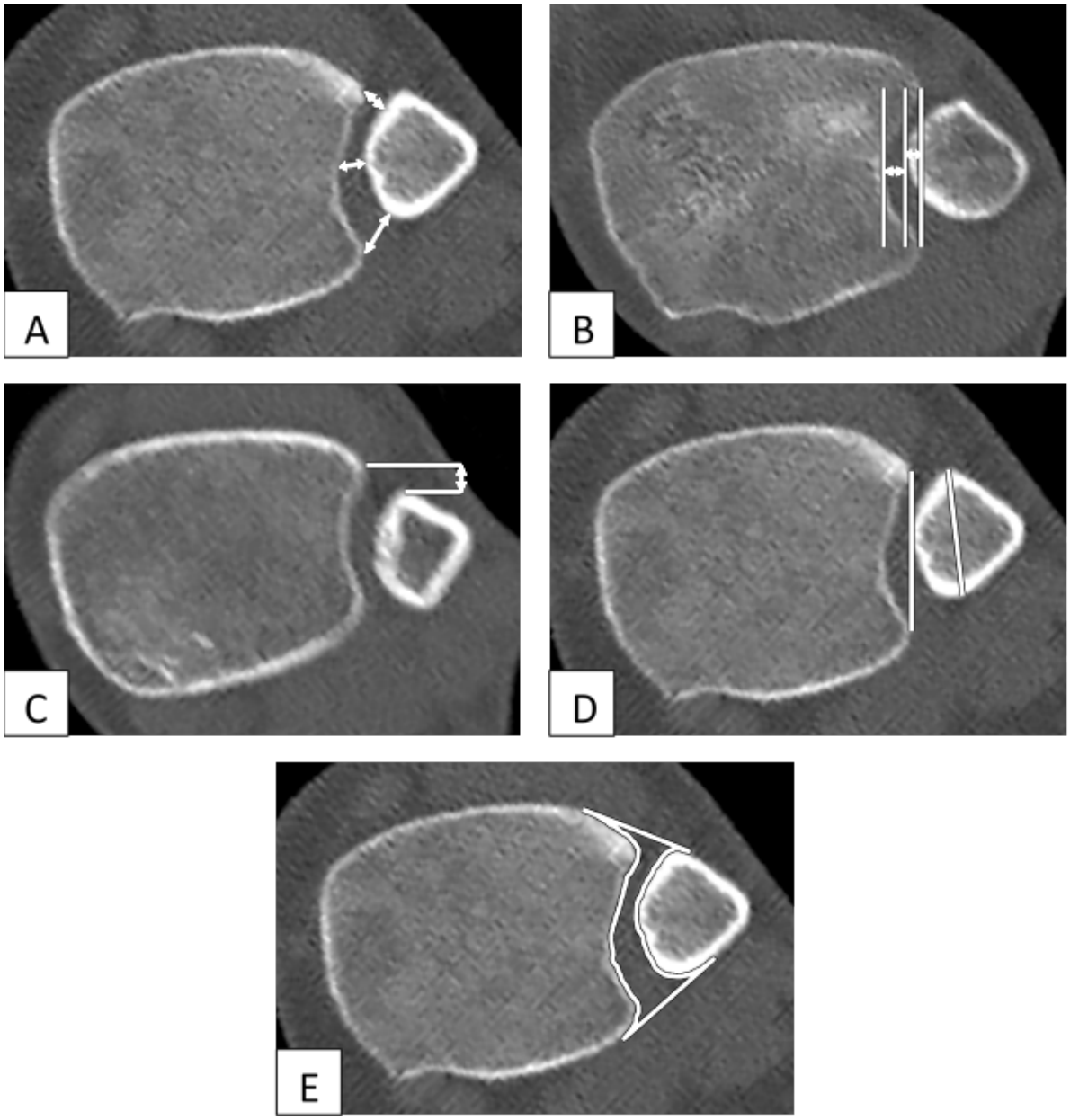

Figure 6.2: Syndesmotic measurements generated from 3D models overlain on 4DCT data. (A) Anterior, middle, and posterior syndesmosis distances, (B) tibiofibular clear space and tibiofibular overlap, (C) sagittal translation, (D) fibular rotation, and (E) syndesmotic area.

6.2.5. Statistical Analysis

Syndesmotic measurements were analyzed using linear mixed effects models, nested by patient and ankle, to investigate the impact of tibiotalar angle on each measurement. These models determined values of syndesmotic measurements in neutral (0° dorsiflexion) ankle position to ensure standardized syndesmotic position, as well as the change in these measurements across ankle ROM to evaluate syndesmotic motion. These results were stratified by fixation type (uninjured, rigid, and flexible). Adjusted marginal r-squared values were calculated to ensure the appropriateness of fitting a linear mixed effects model to the data. We performed Shapiro-Wilk tests to infer normally distributed data. P-values less than 0.05 were deemed significant.

6.3. Results

6.3.1. Demographics

Thirteen patients were included for analysis. Seven patients had rigid fixation and six had flexible fixation (Table 6.1). Of the patients with rigid fixation, none had intact syndesmotic fixation at the time of imaging. One patient had undergone syndesmotic screw removal for symptomatic stiffness, while the remainder of screws had either broken or loosened. ROM was not significantly different between the injured and contralateral, uninjured ankles ($p = 0.20$). Adjusted r-squared values for each model ranged from 0.93 to 0.98 demonstrating excellent model fit.

Table 6.1: Baseline demographics by fixation type.

Parameter	Rigid Fixation (range)	Flexible Fixation (range)	P-value
Sex (M:F)	7:0	3:3	0.03
Age (years)	37 (18 – 56)	46 (31 – 70)	0.29
ROM (degrees)	44 (37 – 65)	38 (19 – 51)	0.37

6.3.2. Syndesmotic Position

In all measures of medial-lateral translation, rigid fixation led to a wider syndesmosis than uninjured ankles (Table 6.2,Figure 6.3). However, only differences in MSD ($p = 0.039$), TFCS ($p = 0.032$), and syndesmotic area ($p < 0.001$) were significant compared to their contralateral ankles. There were no significant differences between ankles after rigid fixation and uninjured ankles for sagittal translation or fibular rotation. No significant differences between flexible fixation and the contralateral ankle were found for any measurement. Only syndesmotic area was able to detect a significant difference between rigid and flexible fixation showing greater areas after rigid fixation ($p = 0.011$).

Table 6.2: Syndesmotic position and change in syndesmotic position with ankle ROM (motion) stratified by fixation type.

		Position		Motion	
		Mean (SD)	95% CI	Mean (SD)	95% CI
ASD (mm)	Uninjured	3.4 (1.6)	2.7 – 4.1	-0.8 (0.8)	-1.2 – -0.4
	Rigid	4.2 (2.2)	3.3 – 5.0	-0.4 (1.1)	-0.9 – 0.1
	Flexible	4.5 (2.4)	3.5 – 5.4	-0.5 (1.4)	-1.0 – 0.1
MSD (mm)	Uninjured	3.3 (1.1)	2.8 – 3.8	-1.0 (0.6)	-1.3 – -0.7
	Rigid	4.1 (1.5)	3.4 – 4.7	-0.1 (0.8)	-0.4 – 0.3
	Flexible	4.0 (1.7)	3.3 – 4.7	-0.7 (0.9)	-1.1 – -0.3
PSD (mm)	Uninjured	5.9 (2.0)	5.0 – 6.9	-0.5 (0.6)	-0.7 – -0.2
	Rigid	6.9 (2.8)	5.8 – 8.1	0.1 (0.8)	-0.2 – 0.4
	Flexible	6.3 (3.0)	5.1 – 7.6	-0.3 (1.0)	-0.7 – 0.1
TFCS (mm)	Uninjured	3.7 (1.1)	3.2 – 4.3	-1.0 (0.6)	-1.3 – -0.7
	Rigid	4.6 (1.6)	3.9 – 5.2	-0.1 (0.9)	-0.4 – 0.3
	Flexible	4.2 (1.7)	3.5 – 4.9	-0.7 (1.1)	-1.2 – -0.3
TFO (mm)	Uninjured	-0.4 (1.2)	-0.9 – 0.2	1.0 (0.6)	0.7 – 1.3
	Rigid	-0.1 (1.7)	-0.8 – 0.6	0.1 (0.9)	-0.3 – 0.5
	Flexible	-0.6 (1.8)	-1.3 – 0.1	0.7 (1.1)	0.2 – 1.1
Sagittal Translation (mm)	Uninjured	1.0 (1.9)	0.0 – 1.9	-0.2 (0.7)	-0.5 – 0.1
	Rigid	1.0 (2.6)	-0.1 – 2.1	-0.4 (0.9)	-0.8 – -0.0
	Flexible	1.5 (2.8)	0.4 – 2.7	-0.5 (1.2)	-1.0 – -0.1
Fibular Rotation (degrees)	Uninjured	17.8 (10.1)	13.6 – 22.1	-1.2 (2.2)	-2.4 – 0.0
	Rigid	13.9 (13.9)	8.2 – 19.6	0.5 (2.9)	-1.2 – 2.1
	Flexible	11.8 (15.1)	5.6 – 18.0	-2.0 (4.9)	-4.1 – 0.1
Syndesmotic Area (mm^2)	Uninjured	124 (25)	112 – 135	-25 (13)	-32 – -18
	Rigid	164 (36)	150 – 179	-3 (19)	-11 – 5
	Flexible	136 (39)	120 – 152	-14 (25)	-23 – -5

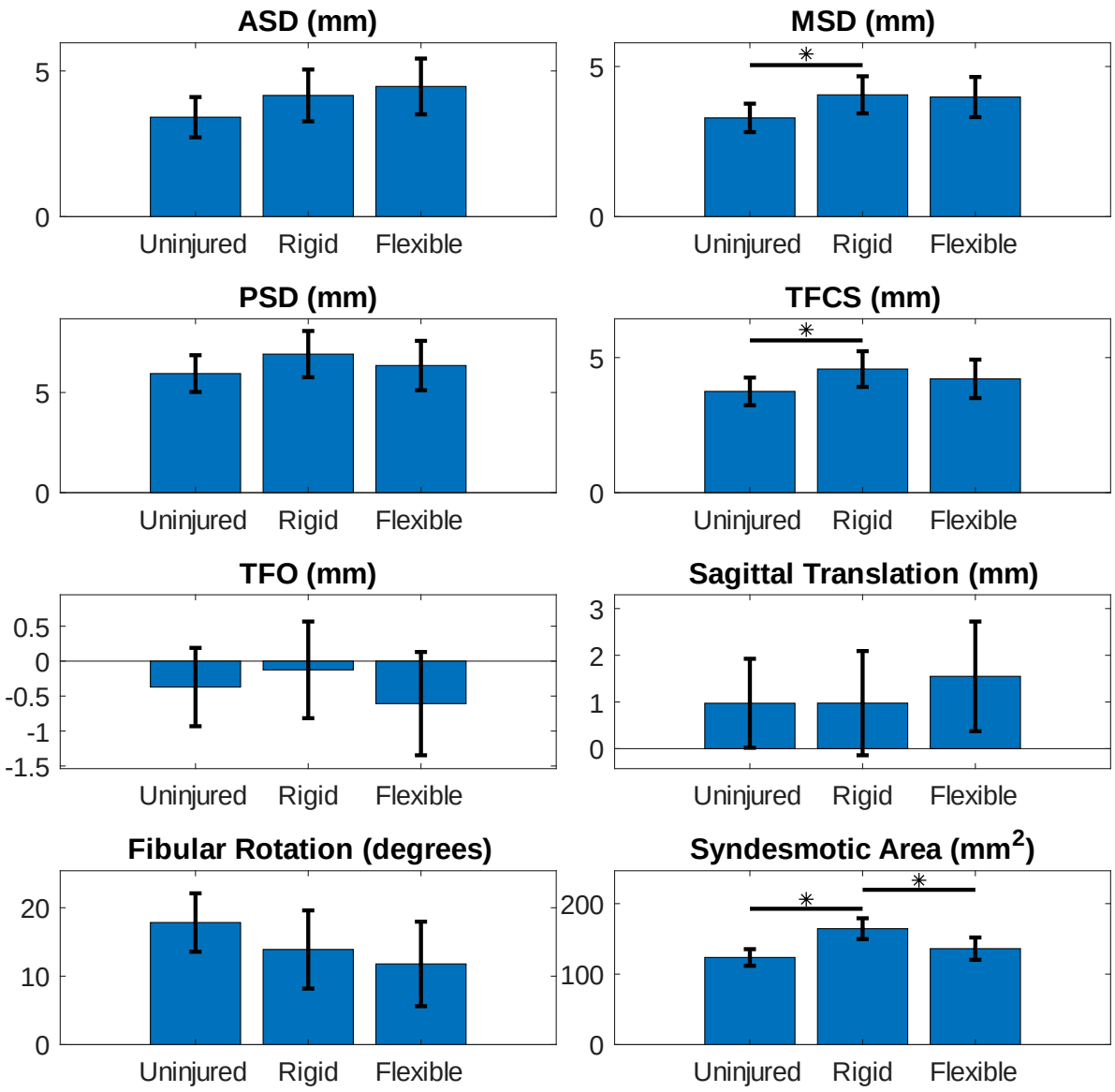

*Figure 6.3: Syndesmotic positions by fixation type. 95% Confidence intervals depicted. *p <0.05.*

6.3.3. Syndesmotic Motion

When investigating syndesmotic motion with changing ankle position, uninjured ankles demonstrated significant decreases in ASD, MSD, PSD, TFCS, and syndesmotic area, as well as increased TFO as ankles moved from dorsiflexion to plantarflexion ($p < 0.001$ for all measures) (Figure 6.4). There was no

significant sagittal translation or fibular rotation detected. When comparing motion after rigid fixation to the uninjured case, there was a significant decrease in motion for MSD ($p < 0.001$), PSD ($p = 0.008$), TFCS ($p < 0.001$), TFO ($p < 0.001$), and syndesmotic area ($p < 0.001$). While flexible fixation had reduced motion in the coronal plane and increased motion in sagittal translation and fibular rotation compared to uninjured ankles, none of these differences were statistically significant. There was significantly less motion in the rigid fixation group compared to motion in the flexible fixation group for MSD ($p = 0.017$), TFCS ($p = 0.021$), and TFO ($p = 0.041$).

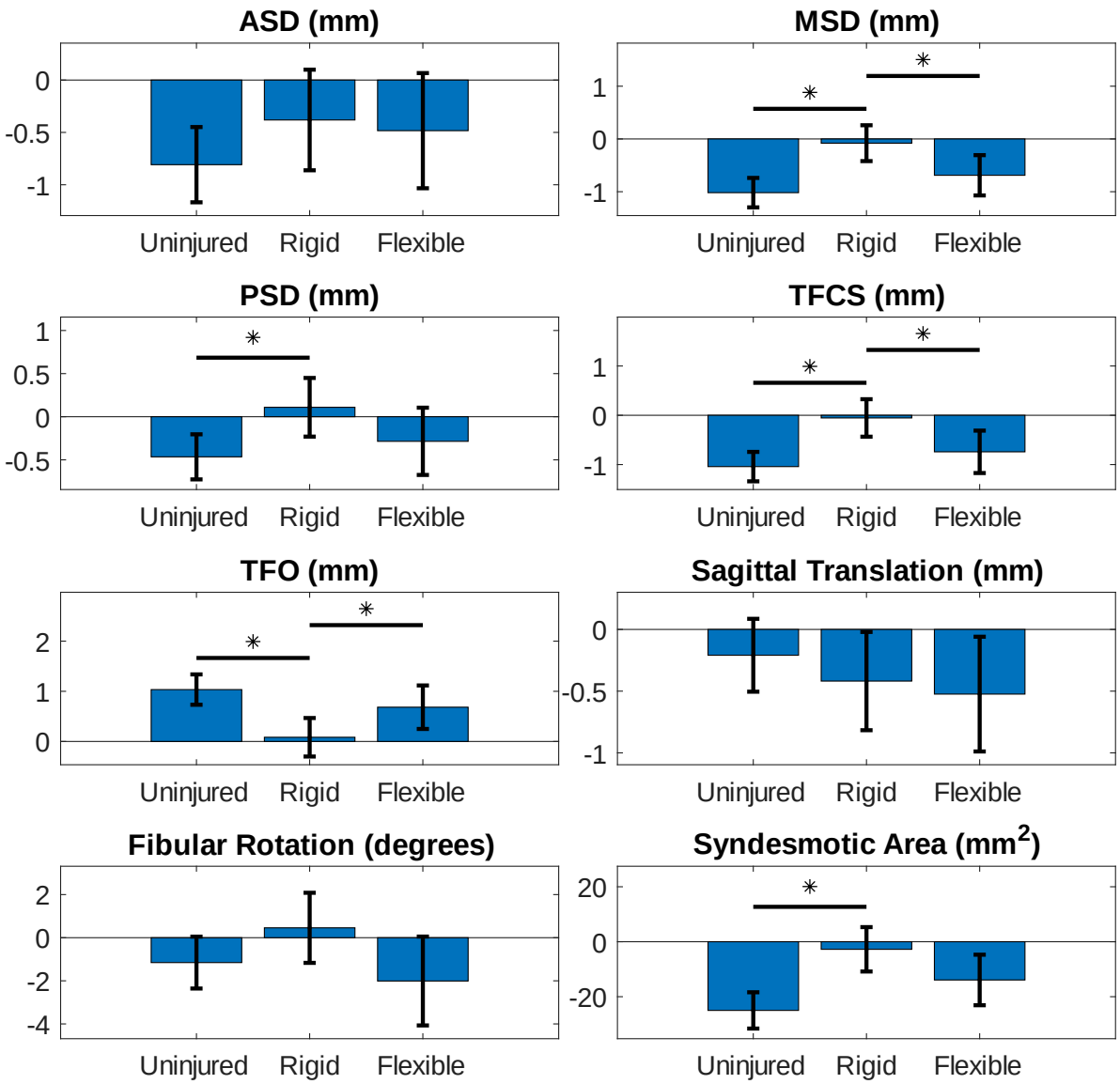

*Figure 6.4: Syndesmotic motion with tibiotalar motion by fixation type. 95% Confidence intervals depicted. *p <0.05.*

6.4. Discussion

Adequate reduction is the most important factor affecting outcomes after syndesmotic injury.[30,31] Given the demonstrated change in reduction parameters with ankle ROM, measuring the syndesmosis

throughout dorsiflexion and plantarflexion can generate a more accurate, complete assessment of syndesmotic reduction. Recreating physiologic syndesmotic motion after injury can help maintain reduction throughout ankle ROM and restore function to the distal tibiofibular joint.

6.4.1. Syndesmotic Position

The present study demonstrated greater MSD, TFCS, and syndesmotic area in rigid fixation compared to uninjured ankles when measured in dorsiflexion. These differences are further increased in plantarflexion. While prior studies have shown over-compression of the syndesmosis with either fixation method,[32–34] this study's protocol allowed for provisional syndesmotic reduction with either a clamp or direct manual pressure. Reduction method was not captured, but manual pressure or thumb reduction is favored by surgeons at our institution as it is less prone to over-compression than clamp reduction[35] and could explain why we saw greater syndesmotic widths after injury. Alternately, the loss of fixation in all patients with initial rigid fixation may have caused late diastasis as secondary loss of reduction has been shown in patients after implant removal or failure.[6,25,31,36] Andersen et al.[5] evaluated patients after flexible or rigid fixation and found that in patients who were over-compressed on initial post-operative imaging, screw removal at 10-12 weeks led to normalization of radiographic parameters by one year post-operatively.

There were no significant differences in syndesmotic position between flexible fixation and uninjured ankles. This finding supports previous work showing that over-compression can be minimized with appropriate suture button tensioning[27] and that flexible fixation provides better maintenance of reduction in the medium and long term.[17,25,31,36,37]

6.4.2. Syndesmotic Motion

Rigid fixation led to significantly sub-physiologic motion in MSD, PSD, TFCS, TFO, and syndesmotic area despite screw breakage or removal in all patients. Cadaveric studies have demonstrated reduced motion with rigid fixation compared to the uninjured case,[8,16,17] but this is the first study to demonstrate the effect *in vivo*. Interestingly, motion was still reduced with no remaining intact implants. Therefore, we hypothesize that initial rigid fixation can lead to healing of ligaments in a contracted state as well as increase the risk of heterotopic ossification or synostosis which would limit mobility of the syndesmosis, even after implant removal or failure. The duration of intact rigid fixation required to reduce motion is still unknown. When comparing motion after flexible fixation to uninjured ankles, we saw reduced motion in the coronal plane and increased sagittal translation and fibular rotation. However, none of these differences were statistically significant.

Flexible fixation resulted in significantly more motion compared to rigid fixation in MSD, TFCS, and TFO and was also more similar to physiologic syndesmotic motion. Cadaveric studies show increased motion after flexible fixation compared to physiologic motion, but this motion is in response to an applied external rotation stress rather than ankle ROM.[16,18,38] Reasons for an insignificant difference between motion after flexible fixation and physiologic motion could be due to the *in vivo* stability provided by intact soft-tissues and active muscular contraction, as well as the opportunity for ligamentous healing. In addition, the consistent 20 lb tension provided by the ACL graft tensioner may contribute to stability.[27] Allowing motion at the distal tibiofibular joint can also have a positive impact on ligamentous healing.[39] Despite concerns that flexible fixation does not adequately stabilize the syndesmosis,[18–20] this has not been shown in the current study. By restoring syndesmotic motion, ankle joint contact area is maintained and instability, cartilage degeneration, and impingement may be avoided.[15,16,40]

6.4.3. Limitations

We are aware of some limitations of the current study. In our rigid fixation cohort, no patients had intact syndesmotic screws at the time of imaging. Therefore, we are unable to determine the impact of intact rigid fixation on syndesmotic position and motion. We do feel that these results accurately capture medium to long term outcomes of rigid fixation, as up to 90% of rigid fixation fails due to loosening or breakage.[7,41] In addition, our study evaluated the impact of ankle ROM on syndesmotic measurements and not weightbearing or external rotation. Weightbearing may impart an additional stress on the syndesmosis leading to increased differences after fixation, though prior studies on the impact of weightbearing on syndesmotic measurements have conflicting results.[42–44] External rotation stress may also impact our findings. We chose to investigate changes with ankle ROM rather than external rotation as we believe that changes with ROM have more functional relevance to daily activities and gait than external rotation stress.

6.4.4. Strengths

To our knowledge, this study is the first to evaluate *in vivo* motion after treatment of syndesmotic injuries, thus capturing the impact of intact soft tissue, active motion, and biologic healing. Imaging patients one year after injury and surgery allowed us to capture motion and position once maximal recovery had been reached.[45] Additionally, a standardized image acquisition protocol, the use of 4DCT technology, and the automated measurement process allowed for accurate and repeatable measurement of bony relationships.

6.5. Conclusion

Restoring syndesmotic motion after injury can maintain syndesmotic reduction throughout ankle ROM and improve functional outcomes. Even with the loss of intact rigid fixation, initial rigid fixation leads to significantly less syndesmotic motion compared to the intact state. Flexible fixation adequately stabilized the distal tibiofibular joint during ankle ROM and provides more physiologic motion. This motion may contribute to the superior reduction and function reported with flexible fixation. This 4DCT application and analysis process can provide novel information regarding joint kinematics in both physiologic and pathologic cases.

6.6. References

1. Zalavras, C, Thordarson, D: Ankle syndesmotic injury. *J Am Acad Orthop Surg* 2007;15:330–339.

2. Carr, JC, Werner, BC, Yarboro, SR: An Update on Management of Syndesmosis Injury: A National US Database Study. *Am J Orthop (Belle Mead NJ)* 2016;45:E472–E477.

3. Sanders, D, Schneider, P, Taylor, M, Tieszer, C, Lawendy, A-R: Improved Reduction of the Tibiofibular Syndesmosis with Tightrope Compared to Screw Fixation: Results of a Randomized Controlled Study. *J Orthop Trauma* 2019;3:2473011418S0012.

4. Liu, G, Chen, L, Gong, M, Xing, F, Xiang, Z: Clinical Evidence for Treatment of Distal Tibiofibular Syndesmosis Injury: A Systematic Review of Clinical Studies. *J Foot Ankle Surg* 2019;58:1245–1250.

5. Andersen, MR, Diep, LM, Frihagen, F, Castberg Hellund, J, Madsen, JE, Figved, W: Importance of Syndesmotic Reduction on Clinical Outcome after Syndesmosis Injuries. *J Orthop Trauma* 2019;33:397–403.

6. Andersen, MR, Frihagen, F, Hellund, JC, Madsen, JE, Figved, W: Randomized trial comparing suture button with single syndesmotic screw for syndesmosis injury. *J Bone Jt Surg - Am Vol* 2018;100:2–12.

7. Rammelt, S, Obruba, P: An update on the evaluation and treatment of syndesmotic injuries. *Eur J Trauma Emerg Surg* 2015;41:601–614.

8. Huber, T, Schmoelz, W, Bölderl, A: Motion of the fibula relative to the tibia and its alterations with syndesmosis screws: A cadaver study. *Foot Ankle Surg* 2012;18:203–209.

9. Mousavian, A, Shakoor, D, Hafezi-Nejad, N, Haj-Mirzaian, A, de Cesar Netto, C, Orapin, J, Schon, LC, Demehri, S: Tibiofibular syndesmosis in asymptomatic ankles: initial kinematic analysis using four-dimensional CT. *Clin Radiol* 2019;74:571.e1-571.e8.

10. Qamar, F, Kadakia, A, Venkateswaran, B: An Anatomical Way of Treating Ankle Syndesmotic Injuries. *J Foot Ankle Surg* 2011;50:762–765.

11. Bartonicek, J: Anatomy of the tibiofibular syndesmosis and its clinical relevance. *Surg Radiol Anat* 2003;25:379–386.

12. Lepojärvi, S, Niinimäki, J, Pakarinen, H, Leskelä, HV: Rotational Dynamics of the Normal Distal Tibiofibular Joint With Weight-Bearing Computed Tomography. *Foot Ankle Int* 2016;37:627–635.

13. LaMothe, J, Baxter, JR, Gilbert, S, Murphy, CI, Karnovsky, SC, Drakos, MC: Effect of Complete Syndesmotic Disruption and Deltoid Injuries and Different Reduction Methods on Ankle Joint Contact Mechanics. *Foot Ankle Int* 2017;38:694–700.

14. Haraguchi, N, Armiger, RS, Myerson, MS, Campbell, JT, Chao, EYS: Prediction of three-dimensional contact stress and ligament tension in the ankle during stance determined from computational modeling. *Foot ankle Int* 2009;30:177–85.

15. Pereira, DS, Koval, KJ, Resnick, RB, Sheskier, SC, Kummer, F, Zuckerman, JD: Tibiotalar Contact Area and Pressure Distribution: The Effect of Mortise Widening and Syndesmosis Fixation. *Foot Ankle Int* 1996;17:269–274.

16. Lamothe, JM, Baxter, JR, Murphy, C, Gilbert, S, Desandis, B, Drakos, MC: Three-Dimensional Analysis of Fibular Motion after Fixation of Syndesmotic Injuries with a Screw or Suture-Button Construct. *Foot Ankle Int* 2016;37:1350–1356.

17. Klitzman, R, Zhao, H, Zhang, L-Q, Strohmeyer, G, Vora, A: Suture-Button Versus Screw Fixation of the Syndesmosis: A Biomechanical Analysis. *Foot Ankle Int* 2010;31:69–75.

18. Goetz, JE, Davidson, NP, Rudert, MJ, Szabo, N, Karam, MD, Phisitkul, P: Biomechanical Comparison of Syndesmotic Repair Techniques During External Rotation Stress. *Foot Ankle Int* 2018;39:1345–1354.

19. Lubberts, B, Vopat, BG, Wolf, JC, Longo, UG, DiGiovanni, CW, Guss, D: Arthroscopically measured syndesmotic stability after screw vs. suture button fixation in a cadaveric model. *Injury* 2017;48:2433–2437.

20. Forsythe, K, Freedman, KB, Stover, MD, Patwardhan, AG: Comparison of a Novel FiberWire-Button Construct versus Metallic Screw Fixation in a Syndesmotic Injury Model. *Foot Ankle Int* 2008;29:49–54.

21. Dikos, GD, Heisler, J, Choplin, RH, Weber, TG: Normal Tibiofibular Relationships at the Syndesmosis on Axial CT Imaging. *J Orthop Trauma* 2012;26:433–438.

22. Nault, M-LL, Hébert-Davies, J, Laflamme, G-YY, Leduc, S: CT scan assessment of the syndesmosis: A new reproducible method. *J Orthop Trauma* 2013;27:638–641.

23. Elgafy, H, Semaan, HB, Blessinger, B, Wassef, A, Ebraheim, NA: Computed tomography of normal distal tibiofibular syndesmosis. *Skeletal Radiol* 2010;39:559–564.

24. Nault, ML, Marien, M, Hébert-Davies, J, Laflamme, GY, Pelsser, V, Rouleau, DM, Gosselin-Papadopoulos, N, Leduc, S: MRI Quantification of the Impact of Ankle Position on Syndesmosis Anatomy. *Foot Ankle Int* 2017;38:215–219.

25. Kortekangas, T, Savola, O, Flinkkilä, T, Lepojärvi, S, Nortunen, S, Ohtonen, P, Katisko, J, Pakarinen, H: A prospective randomised study comparing TightRope and syndesmotic screw fixation for accuracy and

maintenance of syndesmotic reduction assessed with bilateral computed tomography. *Injury* 2015;46:1119–1126.

26. Kwong, Y, Mel, AO, Wheeler, G, Troupis, JM: Four-dimensional computed tomography (4DCT): A review of the current status and applications. *J Med Imaging Radiat Oncol* 2015;59:545–554.

27. Morellato, J, Louati, H, Bodrogi, A, Stewart, A, Papp, S, Liew, A, Gofton, W: The Effect of Varying Tension of a Suture Button Construct in Fixation of the Tibiofibular Syndesmosis - Evaluation Using Stress Computed Tomography. *J Orthop Trauma* 2017;31:103–110.

28. Gervaise, A, Teixeira, P, Villani, N, Lecocq, S, Louis, M, Blum, A: CT dose optimisation and reduction in osteoarticular disease. *Diagn Interv Imaging* 2013;94:371–388.

29. Malhotra, G, Cameron, J, Toolan, BC: Diagnosing chronic diastasis of the syndesmosis: A novel measurement using computed tomography. *Foot Ankle Int* 2014;35:483–488.

30. Weening, B, Bhandari, M: Predictors of functional outcome following transsyndesmotic screw fixation of ankle fractures. *J Orthop Trauma* 2005;19:102–108.

31. Naqvi, GA, Cunningham, P, Lynch, B, Galvin, R, Awan, N: Fixation of ankle syndesmotic injuries: Comparison of tightrope fixation and syndesmotic screw fixation for accuracy of syndesmotic reduction. *Am J Sports Med* 2012;40:2828–2835.

32. Mahapatra, P, Rudge, B, Whittingham-Jones, P: Is It Possible to Overcompress the Syndesmosis? *J Foot Ankle Surg* 2018;57:1005–1009.

33. Schon, JM, Mikula, JD, Backus, JD, Venderley, MB, Dornan, GJ, LaPrade, RF, Clanton, TO: 3D Model Analysis of Ankle Flexion on Anatomic Reduction of a Syndesmotic Injury. *Foot Ankle Int* 2017;38:436–442.

34. Phisitkul, P, Ebinger, T, Goetz, J, Vaseenon, T, Marsh, JL: Forceps reduction of the syndesmosis in rotational ankle fractures: A cadaveric study. *J Bone Jt Surg - Ser A* 2012;94:2256–2261.

35. Cosgrove, CT, Spraggs-Hughes, AG, Putnam, SM, Ricci, WM, Miller, AN, McAndrew, CM, Gardner, MJ: A novel indirect reduction technique in ankle syndesmotic injuries: A cadaveric study. *J Orthop Trauma* 2018;32:361–367.

36. Laflamme, M, Belzile, EL, Bedard, L, van den Bekerom, MPJ, Glazebrook, M, Pelet, S: A prospective randomized multicenter trial comparing clinical outcomes of patients treated surgically with a static or dynamic implant for acute ankle syndesmosis rupture. *J Orthop Trauma* 2015;29:216–223.

37. DeGroot, H, Al-Omari, AA, Ghazaly, SA El: Outcomes of Suture Button Repair of the Distal Tibiofibular Syndesmosis. *Foot Ankle Int* 2011;32:250–256.

38. Thornes, B, Walsh, A, Hislop, M, Murray, P, O'Brien, M: Suture-Endobutton Fixation of Ankle Tibio-Fibular Diastasis: A Cadaver Study. *Foot Ankle Int* 2003;24:142–146.

39. Hildebrand, KA, Frank, CB: Scar formation and ligament healing. *Can J Surg* 1998;41:425–429.

40. Vasarhelyi, A, Lubitz, J, Gierer, P, Gradl, G, Rosler, K, Hopfenmuller, W, Klaue, K, Mittlmeier, TWF: Detection of fibular torsional deformities after surgery for ankle fractures with a novel CT method. *Foot Ankle Int* 2006;27:1115–1121.

41. Dingemans, SA, Rammelt, S, White, TO, Goslings, JC, Schepers, T: Should syndesmotic screws be removed after surgical fixation of unstable ankle fractures? a systematic review. *Bone Jt J* 2016;98-B:1497–1504.

42. Beumer, A, Valstar, ER, Garling, EH, Niesing, R, Ranstam, J, Löfvenberg, R, Swierstra, BA: Kinematics of the distal tibiofibular syndesmosis: Radiostereometry in 11 normal ankles. *Acta Orthop Scand* 2003;74:337–343.

43. Clanton, TO, Williams, BT, Backus, JD, Dornan, GJ, Liechti, DJ, Whitlow, SR, Saroki, AJ, Turnbull, TL, Laprade, RF: Biomechanical Analysis of the Individual Ligament Contributions to Syndesmotic Stability. *Foot Ankle Int* 2017;38:66–75.

44. Hu, WK, Chen, DW, Li, B, Yang, YF, Yu, GR: Motion of the distal tibiofibular syndesmosis under different loading patterns: A biomechanical study. *J Orthop Surg* 2019;27:1–6.

45. Egol, KA, Tejwani, NC, Walsh, MG, Capla, EL, Koval, KJ: Predictors of Short-Term Functional Outcome Following Ankle Fracture Surgery. *J Bone Jt Surg* 2006;88:974–979.

7. General Discussion

7.1. Study Summary

The recognition and diagnosis of syndesmotic injuries is increasing, as is our understanding of the importance of an intact, anatomically reduced syndesmosis on ankle function. Over the past two decades, increasing attention has been paid to the syndesmosis complex and achieving a reduction following injury in orthopaedic literature. However, despite improved understanding of the importance of syndesmotic motion and its impact on joint congruity and ankle ROM, reduction is still viewed as a static parameter and *in vivo* motion is still poorly understood. This disconnect may contribute to the wide variability in treatment strategies, persistently high rates of post-operative malreduction, and resulting functional impairment. To address this knowledge gap, this thesis work aimed to achieve the following specific objectives.

1) To quantify normal syndesmotic kinematics through ankle ROM.
2) To quantify side-to-side variability in syndesmotic kinematics in healthy participants.
3) To compare syndesmotic kinematics following rigid and flexible syndesmotic fixation to normal, uninjured motion.

The studies presented in this thesis can be used to guide imaging protocols, surgical technique, and implant selection. When investigating normal syndesmotic motion, we demonstrated significant syndesmotic motion during ankle ROM, satisfying Objective 1. As such, we recommend standardizing ankle position during imaging and when performing fixation for syndesmotic injuries. Completing Objective 2 showed mild side-to-side variability in syndesmotic position and motion, confirming that imaging of the contralateral, uninjured ankle is an accurate template with which to measure reduction of the injured ankle. Our pilot study of post-fixation motion was performed to address Objective 3. In ankles

that have undergone rigid and flexible fixation, we showed that rigid fixation led to syndesmotic diastasis by some measures compared to normal position. Conversely, there were no differences between flexible fixation and normal position. When comparing motion, rigid fixation led to less than physiologic motion in the coronal plane, while there were no differences detected between motion after flexible fixation and physiologic motion. We therefore recommend that flexible fixation be performed over rigid fixation due to improvements in reduction and restoration of physiologic motion.

7.2. Data Acquisition and Processing

The developed imaging protocol uses 4DCT to accurately and non-invasively measure syndesmotic position and motion. The orthopaedic applications of 4DCT are expanding for both clinical practice and research. Such advances are due to improvements in image acquisition technology, reduction in ionizing radiation dose, and more widespread availability of 4DCT-capable scanners. Benefits of this technology are the ability to provide insight into dynamic phenomena such as joint instability, impingement, and kinematics with high accuracy and precision when compared to other dynamic measurement methods, such as radiostereometric analysis, surface marker optical tracking, or accelerometer analysis.[1,2] In addition, 4DCT does not require a dedicated scanner and can be accomplished using any multi-detector CT scanner with a large enough detector array. Low radiation doses have been accomplished through image reconstruction using partial gantry rotations, iterative reconstruction techniques, and through the peripheral nature of most musculoskeletal applications.[1,3] Consequently, our imaging protocol yielded an effective radiation dose of 0.06 mSv for static CT and 4DCT imaging combined, which is less than a routine chest x-ray or roughly equivalent to 10 days of background atmospheric radiation.[4,5]

After manual reference model creation once per specimen, the remainder of analysis was automated. The automated model registration process was highly successful, achieving a 99.8% success rate and a mean root mean square error of 0.3 mm. Automated registration success rates and error were improved in ankles without metal implants. Ankles with rigid syndesmosis screw fixation required more manual input when creating reference models to separate the tibia and fibula but the impact of rigid fixation was mitigated in the automated process through thresholding and custom screw blocking filters. The root mean square error accounts for voxel size, where our largest voxel dimension was 0.625 mm, as well as smoothing and rounding errors in the reference models, differences in CT data between reference and 4DCT datasets related to imaging parameters, metal and motion artifact, as well as imperfect segment selection. Therefore, the true error due to registration is likely substantially less than 0.3 mm. Ochia et al.[2] performed a phantom study using similar 4DCT analysis of motion and determined registration error was less than 0.1 mm and less than 0.2°.

When performing our measurements of syndesmotic position, parameters were selected for clinical relevance and prevalence of reporting, reproducibility, and sensitivity to detect malreduction. Numerous measurements have been described, contributing to varying rates of malreduction. Gardner's definition of malreduction has been most cited, as a 2 mm difference between the anterior and posterior syndesmotic distances.[6,7] However, there is no anatomic basis for this cutoff and subsequent authors have shown it to be a common finding in uninjured ankles.[8,9] We used the measurements described by Nault et al.[10] for ASD, MSD, PSD, and sagittal translation due to their demonstrated reproducibility as well as prevalence in syndesmotic literature to allow direct comparison of our results with those previously reported.[6] TFCS and TFO were selected as they are analogous to x-ray measurements used intraoperatively. These two measurements were made perpendicular to the incisura similar to Lepojärvi et al.[11] to minimize error related to tibial rotation. Because these measurements were exactly

perpendicular to the incisura, this may explain why we found less TFO than radiographic studies since any rotation of the x-ray beam away from the incisura axis would serve to increase this measurement. Our protocol for fibular rotation was modified from Nault et al.[10] as well. Their fibular axis was poorly defined and multiple authors have demonstrated difficulty reliably determining the fibular axis and measuring fibular rotation.[11–17] We therefore measured the fibular axis 5 mm distal to the plafond along the medial fibular articular border, where it is more reproducible, and translated this axis to the level of the syndesmosis.[13,18] While the goal of this adjustment was to more reliably define the fibular axis, anatomic variability may explain why we failed to find significant differences in rotational position and motion for some groups. Syndesmotic area is a two-dimensional measurement which has previously been shown to be the most repeatable measure of syndesmotic reduction and is highly sensitive to small changes in reduction.[17,19–22] Our studies confirmed that syndesmotic area was a sensitive measure of reduction.

Further complex measurements are possible such as 3D assessments of syndesmotic volume which is also highly sensitive, though often impractical to perform.[19] We elected not to perform 3D measurements of the syndesmosis due to the error introduced by metal artifact proximally. Each measurement was calculated on an axial plane 10 mm above the plafond, consistent with other authors, as these measurements can be correlated with x-ray findings and the anterior and posterior tubercles are most prominent at this level.[23]

7.3. Syndesmotic Position and Motion

The position of the uninjured syndesmosis in dorsiflexion was comparable to prior studies.[10,15,20] As the ankle moved from dorsiflexion to plantarflexion, measures of syndesmotic width decreased between 0.7-1.1 mm and the fibula externally rotated 1.2° on average within the incisura. No measure of syndesmotic

width demonstrated greater than 2 mm side-to-side variability, and the greatest fibular rotational difference was 9°.

Comparing post-fixation position to uninjured ankles, rigid fixation led to a wider syndesmosis on some measures, but not all. No differences were found between flexible fixation and the uninjured state. Rigid fixation led to less motion in all measures of syndesmotic width except ASD, whereas there was no difference between flexible motion and uninjured motion.

By demonstrating changes in radiographic syndesmotic parameters with ankle ROM, we confirm the findings of Nault et al.[24] and Kortekangas et al.[25] Therefore, we believe that ankle position should be considered when imaging ankles for diagnosis of syndesmotic injury and assessment of syndesmotic reduction. Mild variability in side-to-side measurements show that the contralateral ankle may be used to template reduction of the injured ankle, but assessment of bilateral ankles should be performed with both ankles in the same position. Failure to account for ankle position has led to some syndesmoses appearing malreduced initially but direct visualization and repeat imaging in dorsiflexion showed anatomic reduction.[25] This may also explain persistent malreduction when using intraoperative CT if ankle position is nonstandardized.[26]

When performing fixation of syndesmotic injuries, multiple influential studies have concluded that ankle position does not impact outcomes.[27–29] However, these were cadaveric studies and considered the impact of ankle position on post-operative ankle ROM, but they did not account for syndesmotic reduction.[27–29] Given the change in syndesmotic position with ankle ROM, reduction of the syndesmosis

with rigid fixation is a function of ankle position at the time of fixation. Despite the relatively small changes in syndesmotic position between dorsiflexion and plantarflexion, only small differences in syndesmotic width between 1.5 and 2.0 mm can lead to functional impairment.[30–32] Therefore the margin of error for reduction with rigid fixation is low. Surgeons should be cognisant that a syndesmosis rigidly fixed in dorsiflexion can become under-compressed and internally rotated in plantarflexion while fixation in plantarflexion can produce over-compression and external rotation of the syndesmosis in dorsiflexion. Possible *in vivo* consequences also depend on ankle position, such as instability in plantarflexion, but impingement or stiffness in dorsiflexion.

There were no patients in the rigid fixation group with intact syndesmotic screws at one year after surgery. Implant failure or removal may cause either loss of reduction or correction of malreduction, perhaps related to the time since fixation.[32–34] By removing implants or allowing them to fail, the common belief was that functional outcomes would improve through the restoration of normal motion.[35–37] This study demonstrates that even after loss of fixation, initial rigid fixation leads to reduced motion at the tibiofibular joint. Further investigation is required to determine the duration of rigid fixation required to cause abnormal motion. Even if implants are removed early in attempts to restore motion, removal is associated with high complication rates, risks loss of reduction if performed before three months, and has not demonstrated a functional benefit.[38,39]

Schon et al.[40] reported that reduction after flexible fixation is not impacted by ankle position at the time of fixation. With the anatomic reduction and physiologic motion demonstrated after flexible fixation, we conclude that flexible fixation can achieve self-centering within the syndesmosis as previously hypothesized, but also allows motion towards the physiologic position to maintain reduction throughout

ROM. Our results also show that appropriately tensioned flexible fixation adequately constrains the syndesmosis, allaying earlier concerns of excessive flexibility.[41–43]

In our limited sample, we found differences in syndesmotic position and motion between rigid fixation and uninjured ankles for measures of syndesmotic width only. Perhaps greater intra- and inter-subject variability may explain why we were unable to detect changes in the sagittal plane or in fibular rotation. While small alterations in syndesmotic width have significant functional consequences,[30–32] fibular rotation requires asymmetry of greater than 10-15° prior to impairment.[13,14] The functional impact of sagittal malreduction or appropriate thresholds are not well established.

7.4. Limitations

Both studies were performed in the supine position. We therefore only captured the impact of ankle ROM on syndesmotic kinematics and not the impact of weightbearing or external rotation stress. Studies produce conflicting results on whether weightbearing impacts syndesmotic position.[44–46] The impact of active ankle ROM was studied instead of external rotation stress due to the increased relevance of ankle ROM to gait and other common activities. We assumed linear change in syndesmotic measurements with ankle ROM, though this assumption was validated with adjusted r-squared values showing good model fit. In addition, the measurements investigated are surrogate measures for true position since a single measurement can be affected by translation or rotation in multiple planes. The benefits of these measurements over true translation or rotation about anatomic axes is their widespread clinical use and ease of measurement, as well as established relationships with functional outcomes.[13,30–32] Multiple measurements were investigated for completeness, though it does predispose our results to a type I error. In the pilot injury study, we are unable to determine the impact of intact rigid fixation on syndesmotic

kinematics, as all screws had failed or been removed at the time of image acquisition. We also risk type II error due to the small sample sizes in each treatment arm.

7.5. Strengths

The strengths of our studies include the use of 4DCT analysis which allows for highly accurate, non-invasive capture of *in vivo* motion. We present the largest study of uninjured syndesmotic kinematics and the first analysis of kinematics after syndesmotic fixation to our knowledge. Employing a generalized linear model to multiple datapoints per ankle per measurement provides accurate estimate of syndesmotic position and motion. As a result, we can confidently report the impact of ankle position and fixation methods on syndesmotic kinematics and make recommendations on a previously poorly understood, yet common injury pattern.

7.6. Future Directions

A larger prospective cohort study, informed by the pilot study on post-fixation motion, is ongoing. Forty total patients will be recruited with 20 patients after rigid fixation and 20 after flexible fixation. Functional outcomes will be collected at two weeks, six weeks, three months, six months, and 12 months post-operatively. Patients will undergo bilateral ankle 4DCT scans at three months and six months. An increased sample size will allow greater power in detecting differences between post-injury and uninjured position and motion. Additionally, by imaging patients at three months and six months we will be able to capture ankles with intact rigid fixation and determine longitudinal changes to the syndesmosis to assess healing and implant failure. Relating syndesmotic position and motion to functional outcomes will allow us to determine the functional impact of multiple measures of malreduction and abnormal motion. A larger

cohort will also permit subgroup analyses of syndesmotic morphology, relating bony morphology of the incisura to normal and post-operative syndesmotic motion and position, as well as functional outcomes.

Furthermore, future work will study patients who have undergone posterior malleolus fixation as a method of syndesmotic stabilization. Posterior malleolus fixation provides equivalent repair strength to rigid fixation due to an intact PITFL,[47,48] but our study will determine whether anatomic reduction and motion is achieved. Traumatic attenuation of the PITFL or lack of intact anterior ligaments may predispose these ankles to altered syndesmotic kinematics.

Finally, the developed image acquisition and analysis protocol has been highly successful and can be applied to additional orthopaedic applications. The protocol lends itself well to larger joints with thicker cartilage separation due to the ease in automated segmentation. Applying advances in imaging technologies and processing with half gantry rotation and iterative image reconstruction can ensure that 4DCT remains safe with minimal radiation in more proximal joints.

7.7. Conclusion

The studies presented in this thesis determined syndesmotic position and motion in uninjured ankles, as well as in participants with syndesmotic injuries who underwent surgical fixation. We demonstrated that plantarflexion leads to decreased syndesmotic width and subtle fibular external rotation, supporting that ankle position should be considered when imaging the syndesmosis, when performing fixation, and when comparing images with the contralateral ankle. Side-to-side variability within patients is low enough that a contralateral, uninjured ankle may be used to assess syndesmotic reduction, provided that the same

ankle position is used. Flexible fixation better restores normal syndesmotic position and motion compared with rigid fixation. By applying these findings to clinical practice, we aim to decrease the rate of syndesmotic malreduction and improve patient outcomes after injury.

7.8. References

1. Gondim Teixeira, PA, Formery, AS, Hossu, G, Winninger, D, Batch, T, Gervaise, A, Blum, A: Evidence-based recommendations for musculoskeletal kinematic 4D-CT studies using wide area-detector scanners: a phantom study with cadaveric correlation. *Eur Radiol* 2017;27:437–446.

2. Ochia, RS, Inoue, N, Renner, SM, Lorenz, EP, Lim, T-H, Andersson, GBJ, An, HS: Three-Dimensional In Vivo Measurement of Lumbar Spine Segmental Motion. *Spine* 2006;31:2073–2078.

3. Lombard, C, Gervaise, A, Villani, N, Louis, M, Raymond, A, Blum, A, Teixeira, PAG: The Impact of Dose Reduction in Quantitative Kinematic CT of Ankle Joints Using a Full Model-Based Iterative Reconstruction Algorithm: A Cadaveric Study. *Am J Roentgenol* 2018;210:396–403.

4. Gervaise, A, Teixeira, P, Villani, N, Lecocq, S, Louis, M, Blum, A: CT dose optimisation and reduction in osteoarticular disease. *Diagn Interv Imaging* 2013;94:371–388.

5. Biswas, D, Bible, JE, Bohan, M, Simpson, AK, Whang, PG, Grauer, JN: Radiation exposure from musculoskeletal computerized tomographic scans. *J Bone Jt Surg - Ser A* 2009;91:1882–1889.

6. van den Heuvel, SB, Dingemans, SA, Gardenbroek, TJ, Schepers, T: Assessing Quality of Syndesmotic Reduction in Surgically Treated Acute Syndesmotic Injuries: A Systematic Review. *J Foot Ankle Surg* 2019;58:144–150.

7. Gardner, MJ, Demetrakopoulos, D, Briggs, SM, Helfet, DL, Lorich, DG: Malreduction of the Tibiofibular Syndesmosis in Ankle Fractures. *Foot Ankle Int* 2006;27:788–792.

8. Lepojärvi, S, Pakarinen, H, Savola, O, Haapea, M, Sequeiros, RB, Niinimäki, J: Posterior translation of the fibula may indicate malreduction: CT study of normal variation in uninjured ankles. *J Orthop Trauma* 2014;28:205–209.

9. Elgafy, H, Semaan, HB, Blessinger, B, Wassef, A, Ebraheim, NA: Computed tomography of normal distal tibiofibular syndesmosis. *Skeletal Radiol* 2010;39:559–564.

10. Nault, M-LL, Hébert-Davies, J, Laflamme, G-YY, Leduc, S: CT scan assessment of the syndesmosis: A new reproducible method. *J Orthop Trauma* 2013;27:638–641.

11. Lepojärvi, S, Niinimäki, J, Pakarinen, H, Leskelä, HV: Rotational Dynamics of the Normal Distal Tibiofibular Joint With Weight-Bearing Computed Tomography. *Foot Ankle Int* 2016;37:627–635.

12. Yeung, TW, Chan, CYG, Chan, WCS, Yeung, YN, Yuen, MK: Can pre-operative axial CT imaging predict syndesmosis instability in patients sustaining ankle fractures? Seven years' experience in a tertiary trauma center. *Skeletal Radiol* 2015;44:

13. Vasarhelyi, A, Lubitz, J, Gierer, P, Gradl, G, Rosler, K, Hopfenmuller, W, Klaue, K, Mittlmeier, TWF: Detection of fibular torsional deformities after surgery for ankle fractures with a novel CT method. *Foot Ankle Int* 2006;27:1115–1121.

14. Warner, SJ, Fabricant, PD, Garner, MR, Schottel, PC, Helfet, DL, Lorich, DG: The Measurement and Clinical Importance of Syndesmotic Reduction After Operative Fixation of Rotational Ankle Fractures. *J Bone Jt Surg* 2015;97:1935–1944.

15. Dikos, GD, Heisler, J, Choplin, RH, Weber, TG: Normal Tibiofibular Relationships at the Syndesmosis on Axial CT Imaging. *J Orthop Trauma* 2012;26:433–438.

16. Knops, SP, Kohn, MA, Hansen, EN, Matityahu, A, Marmor, M: Rotational malreduction of the syndesmosis: Reliability and accuracy of computed tomography measurement methods. *Foot Ankle Int* 2013;34:1403–1410.

17. Hagemeijer, NC, Chang, SH, Abdelaziz, ME, Casey, JC, Waryasz, GR, Guss, D, DiGiovanni, CW: Range of Normal and Abnormal Syndesmotic Measurements Using Weightbearing CT. *Foot Ankle Int* 2019;40:

18. Morellato, J, Louati, H, Bodrogi, A, Stewart, A, Papp, S, Liew, A, Gofton, W: The Effect of Varying Tension of a Suture Button Construct in Fixation of the Tibiofibular Syndesmosis - Evaluation Using Stress Computed Tomography. *J Orthop Trauma* 2017;31:103–110.

19. Taser, F, Shafiq, Q, Ebraheim, NA: Three-dimensional volume rendering of tibiofibular joint space and quantitative analysis of change in volume due to tibiofibular syndesmosis diastases. *Skeletal Radiol* 2006;35:935–941.

20. Malhotra, G, Cameron, J, Toolan, BC: Diagnosing chronic diastasis of the syndesmosis: A novel measurement using computed tomography. *Foot Ankle Int* 2014;35:483–488.

21. Kocadal, O, Yucel, M, Pepe, M, Aksahin, E, Aktekin, CN: Evaluation of Reduction Accuracy of Suture-Button and Screw Fixation Techniques for Syndesmotic Injuries. *Foot Ankle Int* 2016;37:1317–1325.

22. Abdelaziz, ME, Hagemeijer, N, Guss, D, El-Hawary, A, El-Mowafi, H, DiGiovanni, CW: Evaluation of Syndesmosis Reduction on CT Scan. *Foot Ankle Int* 2019;40:

23. Chen, Y, Qiang, M, Zhang, K, Li, H, Dai, H: A reliable radiographic measurement for evaluation of normal distal tibiofibular syndesmosis: a multi-detector computed tomography study in adults. *J Foot Ankle Res* 2015;8:32.

24. Nault, ML, Marien, M, Hébert-Davies, J, Laflamme, GY, Pelsser, V, Rouleau, DM, Gosselin-Papadopoulos, N, Leduc, S: MRI Quantification of the Impact of Ankle Position on Syndesmosis Anatomy. *Foot Ankle Int* 2017;38:215–219.

25. Kortekangas, T, Savola, O, Flinkkilä, T, Lepojärvi, S, Nortunen, S, Ohtonen, P, Katisko, J, Pakarinen, H: A prospective randomised study comparing TightRope and syndesmotic screw fixation for accuracy and maintenance of syndesmotic reduction assessed with bilateral computed tomography. *Injury* 2015;46:1119–1126.

26. Davidovitch, RI, Weil, Y, Karia, R, Forman, J, Looze, C, Liebergall, M, Egol, K: Intraoperative syndesmotic reduction: Three-dimensional versus standard fluoroscopic imaging. *J Bone Jt Surg* 2013;95:1838–1843.

27. Gonzalez, T, Egan, J, Ghorbanhoseini, M, Blais, M, Lechtig, A, Velasco, B, Nazarian, A, Kwon, JY: Overtightening of the syndesmosis revisited and the effect of syndesmotic malreduction on ankle dorsiflexion. *Injury* 2017;48:1253–1257.

28. Pallis, MP, Pressman, DN, Heida, K, Nicholson, T, Ishikawa, S: Effect of Ankle Position on Tibiotalar Motion With Screw Fixation of the Distal Tibiofibular Syndesmosis in a Fracture Model. *Foot Ankle Int* 2018;39:746–750.

29. Tornetta, P, Spoo, JE, Reynolds, FA, Lee, C: Overtightening of the ankle syndesmosis: Is it really possible? *J Bone Jt Surg - Ser A* 2001;83:489–492.

30. Wikerøy, AKB, Høiness, PR, Andreassen, GS, Hellund, JC, Madsen, JE: No Difference in Functional and Radiographic Results 8.4 years after quad vs tricortical syndesmosis fixation in ankle fractures. *J Orthop Trauma* 2010;24:17–23.

31. Andersen, MR, Diep, LM, Frihagen, F, Castberg Hellund, J, Madsen, JE, Figved, W: Importance of Syndesmotic Reduction on Clinical Outcome after Syndesmosis Injuries. *J Orthop Trauma* 2019;33:397–403.

32. Naqvi, GA, Cunningham, P, Lynch, B, Galvin, R, Awan, N: Fixation of ankle syndesmotic injuries: Comparison of tightrope fixation and syndesmotic screw fixation for accuracy of syndesmotic reduction. *Am J Sports Med* 2012;40:2828–2835.

33. Laflamme, M, Belzile, EL, Bedard, L, van den Bekerom, MPJ, Glazebrook, M, Pelet, S: A prospective randomized multicenter trial comparing clinical outcomes of patients treated surgically with a static or dynamic implant for acute ankle syndesmosis rupture. *J Orthop Trauma* 2015;29:216–223.

34. Song, DJ, Lanzi, JT, Groth, AT, Drake, M, Orchowski, JR, Shaha, SH, Lindell, KK: The effect of syndesmosis screw removal on the reduction of the distal tibiofibular joint: A prospective radiographic study. *Foot Ankle Int* 2014;35:543–548.

35. Hamid, N, Loeffler, BJ, Braddy, W, Kellam, JF, Cohen, BE, Bosse, MJ: Outcome after fixation of ankle fractures with an injury to the syndesmosis. *J Bone Joint Surg Br* 2009;91-B:1069–1073.

36. Needleman, RL, Skrade, DA, Stiehl, JB: Effect of the Syndesmotic Screw on Ankle Motion. *Foot Ankle* 1989;10:17–24.

37. Pereira, DS, Koval, KJ, Resnick, RB, Sheskier, SC, Kummer, F, Zuckerman, JD: Tibiotalar Contact Area and Pressure Distribution: The Effect of Mortise Widening and Syndesmosis Fixation. *Foot Ankle Int* 1996;17:269–274.

38. Hsu, Y-T, Wu, C-C, Lee, W-C, Fan, K-F, Tseng, I-C, Lee, P-C: Surgical treatment of syndesmotic diastasis: emphasis on effect of syndesmotic screw on ankle function. *Int Orthop* 2011;35:359–64.

39. Schepers, T, Van Lieshout, EMM, de Vries, MR, Van der Elst, M: Complications of Syndesmotic Screw Removal. *Foot Ankle Int* 2011;32:1040–1044.

40. Schon, JM, Mikula, JD, Backus, JD, Venderley, MB, Dornan, GJ, LaPrade, RF, Clanton, TO: 3D Model Analysis of Ankle Flexion on Anatomic Reduction of a Syndesmotic Injury. *Foot Ankle Int* 2017;38:436–442.

41. Goetz, JE, Davidson, NP, Rudert, MJ, Szabo, N, Karam, MD, Phisitkul, P: Biomechanical Comparison of Syndesmotic Repair Techniques During External Rotation Stress. *Foot Ankle Int* 2018;39:1345–1354.

42. Lubberts, B, Vopat, BG, Wolf, JC, Longo, UG, DiGiovanni, CW, Guss, D: Arthroscopically measured syndesmotic stability after screw vs. suture button fixation in a cadaveric model. *Injury* 2017;48:2433–2437.

43. Forsythe, K, Freedman, KB, Stover, MD, Patwardhan, AG: Comparison of a Novel FiberWire-Button Construct versus Metallic Screw Fixation in a Syndesmotic Injury Model. *Foot Ankle Int* 2008;29:49–54.

44. Beumer, A, Valstar, ER, Garling, EH, Niesing, R, Ranstam, J, Löfvenberg, R, Swierstra, BA: Kinematics of the distal tibiofibular syndesmosis: Radiostereometry in 11 normal ankles. *Acta Orthop Scand* 2003;74:337–343.

45. Clanton, TO, Williams, BT, Backus, JD, Dornan, GJ, Liechti, DJ, Whitlow, SR, Saroki, AJ, Turnbull, TL, Laprade, RF: Biomechanical Analysis of the Individual Ligament Contributions to Syndesmotic Stability. *Foot Ankle Int* 2017;38:66–75.

46. Hu, WK, Chen, DW, Li, B, Yang, YF, Yu, GR: Motion of the distal tibiofibular syndesmosis under different loading patterns: A biomechanical study. *J Orthop Surg* 2019;27:1–6.

47. Miller, AN, Carroll, EA, Parker, RJ, Helfet, DL, Lorich, DG: Posterior Malleolar Stabilization of Syndesmotic Injuries is Equivalent to Screw Fixation. *Clin Orthop Relat Res* 2010;468:1129–1135.

48. Gardner, MJ, Brodsky, A, Briggs, SM, Nielson, JH, Lorich, DG: Fixation of posterior malleolar fractures provides greater syndesmotic stability. *Clin Orthop Relat Res* 2006;165–171.